ADVANCES IN INORGANIC CHEMISTRY, VOL. 38

TRINUCLEAR CUBOIDAL AND HETEROMETALLIC CUBANE-TYPE IRON–SULFUR CLUSTERS: NEW STRUCTURAL AND REACTIVITY THEMES IN CHEMISTRY AND BIOLOGY

R. H. HOLM

Department of Chemistry, Harvard University, Cambridge, Massachusetts 02138

I. Introduction

More than ever, it is now apparent that protein-bound Fe_4S_4 clusters must be accorded significance as prosthetic groups at a level that has historically been reserved for hemes and flavins. Although we have observed that iron–sulfur proteins, "having passed from scientific near-obscurity to prosperity in the last 15 [now ~20] years, represent one of the major stories in contemporary metallobiochemistry" (*1*), knowledge of their structure and function certainly has not reached maturity. This contention is well supported by consideration of just four of the major

discoveries in the field in the last decade: (1) not all reduced ($[Fe_4S_4]^{1+}$) clusters have the classical "$g = 1.94$-type" $S = \frac{1}{2}$ ground state with otherwise standard electronic properties; (2) an Fe_4S_4 cluster is covalently bound to a catalytic site (in sulfite reductase), to which it electronically couples and functions as an electron donor; (3) Fe_4S_4 and (probably) Fe_2S_2 clusters are implicated in the catalysis of nonredox enzymatic reactions (as in aconitase); (4) protein-bound Fe_4S_4 clusters may be converted adventitiously or deliberately by oxidation to the previously unknown and unanticipated cuboidal cluster Fe_3S_4, which has an unprecedented electronic structure and supports reconstitution with metal ions to afford the heterometal cubane-type clusters MFe_3S_4.

It may be noted that the foregoing developments involve nearly exclusively Fe_4S_4 clusters, indicating that these species (with occasionally modified terminal ligation) possess the more diverse structural and functional roles. In this article, some of the most significant recent findings and unusual properties of native and synthetic Fe_4S_4 clusters are first examined. Certain of these properties lead to newer types of clusters, viz., the cuboidal and heterometal cubane-type species mentioned above. As will be shown, these afford new structural and reactivity themes in both inorganic chemistry and biology.

II. Homometallic Cubane-Type Clusters

The cluster **1** is one of the most pervasive electron transfer centers in biology. Accessible Fe_4S_4 core oxidation states, presented in vertical alignment with isoelectronic protein and synthetic analog clusters, are set out in Eq. (1). The indicated potential ranges are approximate. The cubane-type structure and tetracysteinate ligation of **1** have been demonstrated most directly by the protein crystallography of *Peptococcus aerogenes* ferredoxin (Fd) (*2*), *Chromatium* "high-potential" (HP) protein (*3, 4*), trimethylamine dehydrogenase (*5*), *Azotobacter vinelandii* Fd I (*6, 7*), *Bacillus thermoproteolyticus* Fd (*8, 9*), the active form of pig heart aconitase (*10*), and a mutated form of *A. vinelandii* Fd I (*11*). In addition, the structures of over 35 synthetic clusters containing the

core ox. state:	$[Fe_4S_4]^{0}$	$[Fe_4S_4]^{1+}$		$[Fe_4S_4]^{2+}$		$[Fe_4S_4]^{3+}$
spin state	?	S = 1/2, 3/2		S = 0		S = 1/2
proteins:	--	Fd_{red}	$\overset{-0.3\text{ to }-0.7\text{ V}}{\rightleftharpoons}$	Fd_{ox}/HP_{red}	$\overset{+0.1\text{ to }+0.3\text{ V}}{\rightleftharpoons}$	HP_{ox}
analogs:	$[Fe_4S_4(SR)_4]^{4-}$	$\rightleftharpoons$ $[Fe_4S_4(SR)_4]^{3-}$	$\rightleftharpoons$	$[Fe_4S_4(SR)_4]^{2-}$	$\rightleftharpoons$	$[Fe_4S_4(SR)_4]^{1-}$

(1)

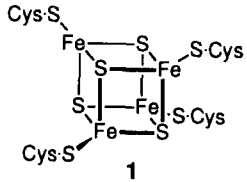

1

Fe_4Q_4 core (Q = S, Se, or Te) in different oxidation states have been determined by X-ray analysis. The great majority of these contain the $[Fe_4S_4]^{2+/1+}$ cores, usually with four terminal thiolate ligands (*1, 12–14*). A smaller body of structural data is available for $[Fe_4Se_4]^{2+/1+}$ clusters (*1, 13, 15*), and the structures of two $[Fe_4Te_4]^{1+}$ clusters have been determined (*16, 17*). Consequently, native and synthetic Fe_4Q_4 cubane-type species constitute the most extensive structurally defined cluster type. With the former clusters, structural definition has advanced to the point where the relative stabilities of oxidation states of conventional Fd versus HP proteins can be sensibly interpreted in terms of the influence of the immediate protein environment; viz., the different numbers of protein–cluster N—H . . . S hydrogen bonds (*18*). As will become evident, however, considerably more is known about structure than about structure/property relationships and the reactivity of terminal and core ligands. Many of the recent developments in the chemistry and biology of Fe_4S_4 clusters have been summarized (*19–23*). The majority of topics presented here have not been comparably treated in these sources.

A. Protein-Bound Clusters with Unconventional Terminal Ligation

The tetracysteinate binding of cluster **1** is the conventional terminal ligation mode of protein-bound Fe_4S_4 clusters. It has been established by protein crystallography in some cases, which serve as points of reference for the many other proteins in which terminal coordination has been deduced from spectroscopic and amino acid sequence data. Proved and probable cluster binding patterns for representative proteins of interest are illustrated schematically in Table I.

In the case of *B. thermoproteolyticus* Fd (*8, 9*), three of the residues that bind the cluster occur in the prototypical Cys-triplet run Cys-X-X-Cys-X-X-Cys near the N terminus of the polypeptide chain. The fourth Cys residue occurs near the C terminus and is often part of a Cys-Pro-Val fragment. In the 8Fe protein *P. aerogenes* Fd (*2, 18*), there are two triplet runs and two "distant" Cys residues that bind the two

TABLE I

CLUSTER BINDING PATTERNS IN PROTEINS WITH $[Fe_4S_4]$ AND $[Fe_3S_4]$ CLUSTERS

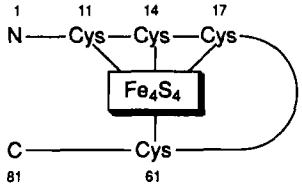

B. thermoproteolyticus Fd

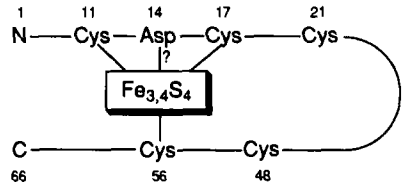

P. furiosus Fd

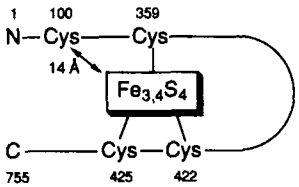

Pig Heart Aconitase (11-12 Cys)

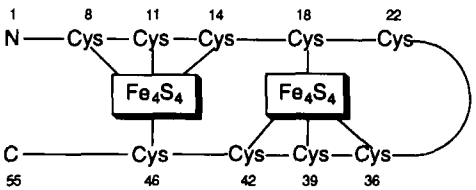

P. aerogenes Fd

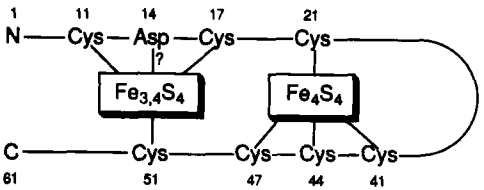

D. vulgaris Fd I
D. africanus Fd III
S. acidocaldarius Fd (7 Cys, 103 residues)
T. acidophilum Fd (9 Cys, 142 residues)

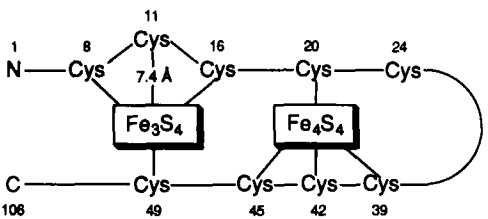

A. vinelandii Fd I

TABLE I (*Continued*)

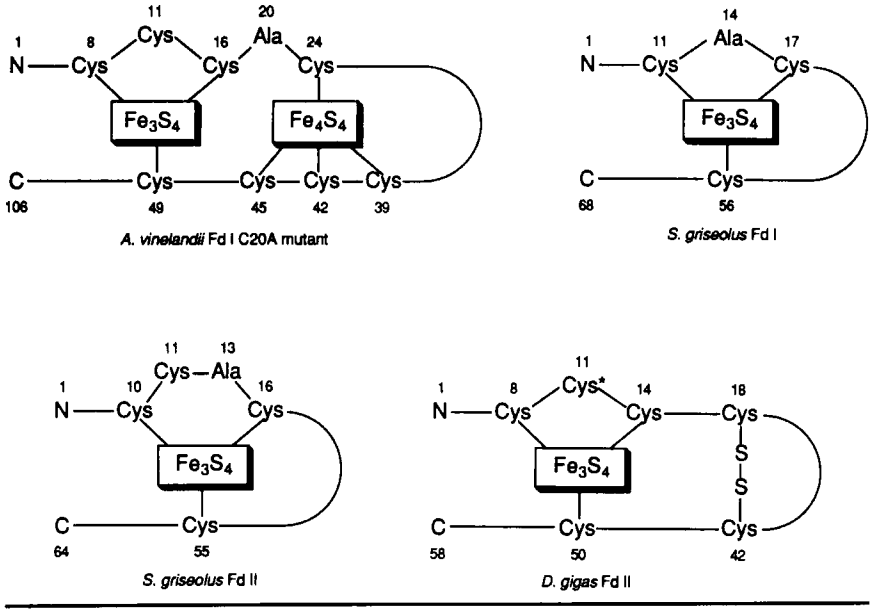

clusters. Consequently, the protein is disposed in a cross-threaded structure of near twofold symmetry. [Note that the original X-ray structure has recently been amended to include Cys 22 and increase the number of residues by one (*18*).] In the 7Fe protein *A. vinelandii* Fd (*6, 7*), the fold of the N-terminal half of the polypeptide chain is very similar to that of *P. aerogenes* Fd, and Fe_4S_4 cluster binding also occurs by means of a Cys triplet and a distant residue. In the C20A mutant protein, Cys 20 has been replaced by Ala using site-directed mutagenesis. The tendency to achieve the binding pattern of **1** results in a "cluster-driven protein rearrangement" (*11*) whereby Cys 24, uncoordinated in the native form, is positioned to bind to the cluster.

Proteins of comparable sizes that observe these sequence patterns (*24*) are expected to bind Fe_4S_4 clusters similarly. The HP proteins represent an exception. They contain a single cluster **1** that is not bound to residues in a Cys-triplet run. Because these proteins exhibit only electron transfer reactivity thus far, they are not directly pertinent to this report.

Sequence departures from the patterns in the foregoing proteins signal potentially unconventional terminal binding modes. Thus, *Pyro-*

coccus furiosus Fd (*25*) carries Asp 14 in the central Cys position in the triplet run of other proteins. Similarly, one of the triplets in the sequences of the 8Fe proteins *Desulfovibrio vulgaris* Fd I (*26, 27*) and *Desulfovibrio africanus* Fd III (*28–30*) is broken by a central Cys/Asp replacement. Similar situations are found with the ferredoxins from *Sulfolobus acidocaldarius* (7 Cys, 103 residues) (*31, 32*) and *Thermoplasma acidophilum* (9 Cys, 142 residues) (*31, 33*). Two 3Fe ferredoxins have been isolated from *Streptomyces griseolus* (*34*). Both contain an Ala residue at the central position of what would be a Cys triplet near the N terminus. Fd I has only three Cys residues, whereas Fd II has four Cys, but one of these (Cys 11) is located in a nonstandard position for cluster binding. *Desulfovibrio gigas* Fd II, whose structure has been crystallographically determined (*35, 36*), has six Cys residues, three of which are involved in a triplet near the N terminus, and an Fe_3S_4 cluster. However, the side chain of Cys 11 is rotated away from the Fe_3S_4 cluster and the sulfur atom appears to be substituted, possibly with a thiomethyl group, leading to a modified (Cys*) residue that may be incapable of cluster binding. The binding pattern of the 3Fe cluster of *A. vinelandii* Fd I is somewhat different, owing to the presence of a Cys-X_4-Cys run involving one of the cluster ligands (Cys 16). The sulfur atom of uncoordinated Cys 11 is placed 7.37 Å from the nearest Fe atom, possibly due to interactions with other residues.

The information in Table I presents three circumstances leading to unconventional Fe_4S_4 cluster binding patterns: (1) occurrence of fewer than four Cys residues per cluster; (2) displacement of Cys residues from, or their replacement in, conventional sequence positions in chain segments where they are known to bind in other proteins; and, correlatively, (3) placement of Cys residues outside of binding distances as dictated by the exigencies of protein structure. In these events, proteins contain clusters whose Fe subsites are differentiated in a 3 : 1 ratio by the terminal ligands, and the binding modes of clusters **2** and **3** become

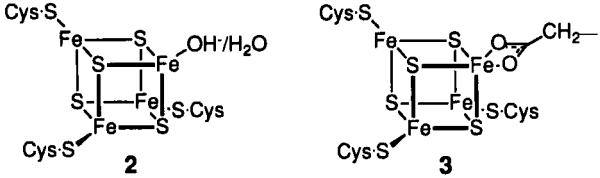

possible. Some evidence has been adduced for binding of the carboxylate group of Asp (shown arbitrarily in a chelate form in **3**) in *D. africanus* Fd III (*30*). Among other observations is the small or nil pH dependence of redox potentials, a behavior inconsistent with a coordinated H_2O/OH^- equilibrium. Alternatively, only hydroxide may be ligated over

the pH range investigated. Cluster **2** has been crystallographically established in the active form of pig heart aconitase, in which the unique subsite of **2** is coordinated by water or hydroxide and the sulfur atom of the nearest Cys residue is 14.3 Å from the center of the cluster (*10*). Inasmuch as the homology of the Cys sequence of the beef heart enzyme (*37*) with the DNA-derived pig heart enzyme sequence is greater than 98% (*10*), it is likely that all properties associated with the clusters in the two enzymes will be nearly identical. Indeed, electron–nuclear double-resonance (ENDOR) studies of active, substrate-free beef heart aconitase reveal the presence of H_2O/OH^- ligation (*38*). In view of the large size of these molecules ($M_r \approx 80{,}000$), it is unlikely that circumstance (2) given above is pertinent to cluster binding patterns in these enzymes.

The foregoing circumstances could conceivably destabilize Fe_4S_4 clusters to the extent that they cannot be readily maintained, or formed at all, in a protein structure. In this event, with three Cys ligands available, the only known alternative is the cuboidal Fe_3S_4 cluster **4** (RS = Cys · S), which is considered in some detail later. In addition to the foregoing cases, this cluster has been crystallographically demonstrated in the inactive form of aconitase (*10*). On the basis of an electron paramagnetic resonance (EPR) criterion (a broad asymmetric signal centered at $g \approx 2.01$ and observable below ~15 K), it is present in the *S. griseolus* proteins wherein Fd I has only three Cys residues and Fd II lacks the standard Cys-triplet binding sequence (Table I). The Fe_3S_4 cluster in *A. vinelandii* Fd I is not readily converted to an Fe_4S_4 cluster, presumably because of the unfavorable location of Cys 11 as a fourth ligand. There is a further structural alternative, the linear cluster **5**, which requires four Cys ligands. It has been detected thus far only in an unfolded form of inactive aconitase (*39*), where ligands in the Cys-X-X-Cys segment apparently are retained (*40*). Linear cluster **5** has been synthesized and fully characterized (*41*), but cuboidal cluster **4** has not been obtained in isolable form.

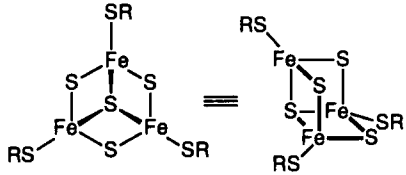

4

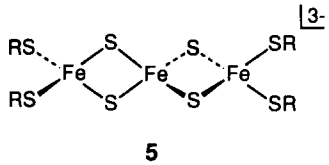

5

Having established the existence of unconventional ligation in protein-bound clusters, we shall examine the consequences of the resultant

subsite differentiation and its relation to Fe_3S_4 cluster formation and reactivity. As will be seen, protein-bound **4** and synthetic **5**, although of much interest in their own right, are precursors to new clusters.

B. Subsite-Differentiated Synthetic Clusters

1. 3:1 Subsite Differentiation

Stimulated by the recognition of such clusters in proteins, research was undertaken in this laboratory to prepare clusters whose subsites are differentiated in a 3:1 ratio. We have obtained two solutions to this problem by use of trithiol ligands **6** and **7**. These are shown in Fig. 1 together with their subsite-differentiated clusters **8** and **9**. The design aspects of **6** [$L(SH)_3$] and its successful use in the binding of cubane-type clusters have been summarized (*22*). Molecular mechanics and dynamics analysis of this ligand reveals majority conformations in which central ring substituents alternate in position above and below the central ring (*42*). The coordinating "arms" with their thiol groups are buttressed in positions on the same side of the ring by the *p*-tolylthio "legs" on the opposite side. Further, the 6Me substituents on the arms tend to direct rotation of the phenyl rings such that their thiol groups are pointed inward over the central ring. This arrangement is sterically preferred to one that places one or more methyl groups over this ring. The existence of configurations of this type is experimentally recognized by the substantial nuclear magnetic resonance (NMR) shielding of the 2H protons. Thus, ligand **6** is largely predisposed to capture a cubane cluster in ligand substitution reactions such as Eq. (2) [R = alkyl and LS_3 = 1,3,5-tris((4,6-dimethyl-3-mercaptophenyl)thio)-2,4,6-tris(*p*-tolylthio)benzene(3 −), or triply deprotonated **6**] and to suppress polymer formation. *In situ* cluster capture is quantitative in this reaction and isolated yields of product cluster **8** (L′ = SR) are high (*42–44*). When 6H rather than 6Me is present, the directing influence on the rotation of the arms is lost, and the amount of insoluble oligomeric product in Eq. (2) substantially increases (*42*). Cyclic ligand **7** [*c*-$L(SH)_3$] is of a different design, with the 3-3-2 pattern of methylene groups selected in order that the ligand bind snugly to three subsites of the cluster. The substitution reaction given by Eq. (3) proceeds smoothly to afford the subsite-differentiated cluster **9** (L′ = SR) (*45*).

$$[Fe_4S_4(SR)_4]^{2-} + L(SH)_3 \rightarrow [Fe_4S_4(LS_3)(SR)]^{2-} + 3RSH \quad (2)$$

$$[Fe_4S_4(SR)_4]^{2-} + c\text{-}L(SH)_3 \rightarrow [Fe_4S_4(c\text{-}LS_3)(SR)]^{2-} + 3RSH \quad (3)$$

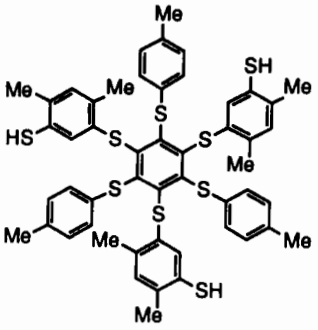

6

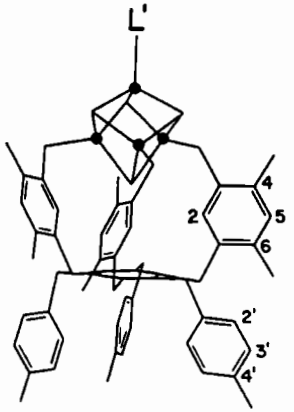

8 (• = Fe)

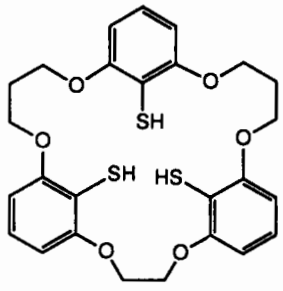

7

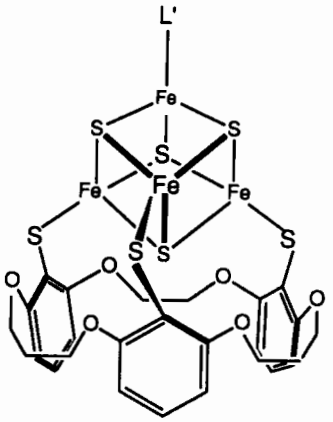

9

FIG. 1. Formulas of the trithiol ligand $L(SH)_3$ (**6**) and cyclic trithiol ligand $c\text{-}L(SH)_3$ (**7**) and schematic depictions of their 3 : 1 subsite-differentiated clusters $[Fe_4S_4(LS_3)L']^{z-}$ (**8**) and $[Fe_4S_4(c\text{-}LS_3)L']^{z-}$ (**9**), respectively.

The cluster binding mode of **8** has been verified by X-ray structure determinations (*42, 43*) and the trigonally symmetric configuration is consistent with the ^1H NMR spectra of over 40 clusters. The ligand resembles a cavitand whose floor is the central benzene ring and whose "walls" are the closest edge regions of the three coordinating phenyl

rings. The $[Fe_4S_4]^{2+}$ core partially occupies this cavity, the perpendicular distance from the unique sulfur atom of the core to the central ring being 3.74 Å in $[Fe_4S_4(LS_3)Cl]^{2-}$ (*43*). The ligand is sufficiently flexible that it binds the $[Fe_4Se_4]^{2+}$ core, whose van der Waals volume is ~25% larger than that of $[Fe_4S_4]^{2+}$. In the Ph_4P^+ salt of $[Fe_4Se_4(LS_3)Cl]^{2-}$, there are three inequivalent clusters, each with crystallographically imposed trigonal symmetry and different extents of cavity occupancy (*42*). The corresponding distances from the unique selenium atom to the ring centroid are 3.68, 3.69, and 4.09 Å. These observations afford the description of the deprotonated form of **6** as a semirigid cavitand ligand. Diffraction-quality crystals of salts of **9** have not been obtained, but the indicated structure with mirror symmetry is fully supported by ^1H NMR spectra (*45*). The ligand in this cluster is not of the cavitand type.

The principal advantage of subsite-differentiated clusters **8** and **9**—indeed, the reason they were prepared—is that they undergo subsite-specific substitution reactions at the unique subsite, thereby opening a new dimension in the chemistry of Fe_4S_4 clusters. Although clusters of the general type $[Fe_4S_4L_4]^{z-}$ ($L = RS^-$, halide) readily undergo substitution reactions, any mixed ligand products that are formed occur in near-statistical mixtures and are in labile equilibrium in solutions of polar solvents (*22*). This is not the case with **8** and **9** and their derivatives, most importantly the chloride clusters ($L' = Cl^-$). These clusters are obtained as exemplified with **8** ($L' = RS^-$) in the reaction given by Eq. (4) (*43*).

$$[Fe_4S_4(LS_3)(SR)]^{2-} + t\text{-BuCOCl} \rightarrow [Fe_4S_4(LS_3)Cl]^{2-} + t\text{-BuCOSR} \qquad (4)$$

As anticipated by earlier work (*46*), chloride is an excellent leaving group. Thus the reactions of cluster **10**, represented generally by Eq. (5) and illustrated in Fig. 2, lead to a diverse set of products (*47, 48*). Most of these species were not isolated but were generated in solution

$$[Fe_4S_4(LS_3)Cl]^{2-}\ (\mathbf{10}) + L' \rightarrow [Fe_4S_4(LS_3)L']^{z-} + Cl^- \qquad (5)$$

and unambiguously detected by ^1H NMR. The isotropically shifted resonances of the 4Me, 5H, and 6Me substituents of the phenyl rings in the coordinating arms of the ligand are exquisitely sensitive to the nature of ligand(s) L′ at the unique subsite. In most cases, substitution could also be detected by potential shifts of the $[Fe_4S_4]^{2+/1+}$ couple of Eq. (1). The reactions of **9** ($L' = Cl^-$) have been less thoroughly examined, but reactivity, where tested with the same ligand, is analogous (*45*). The ligand structural features of **8** do not appear to have any special effects on reactivity at the unique subsite.

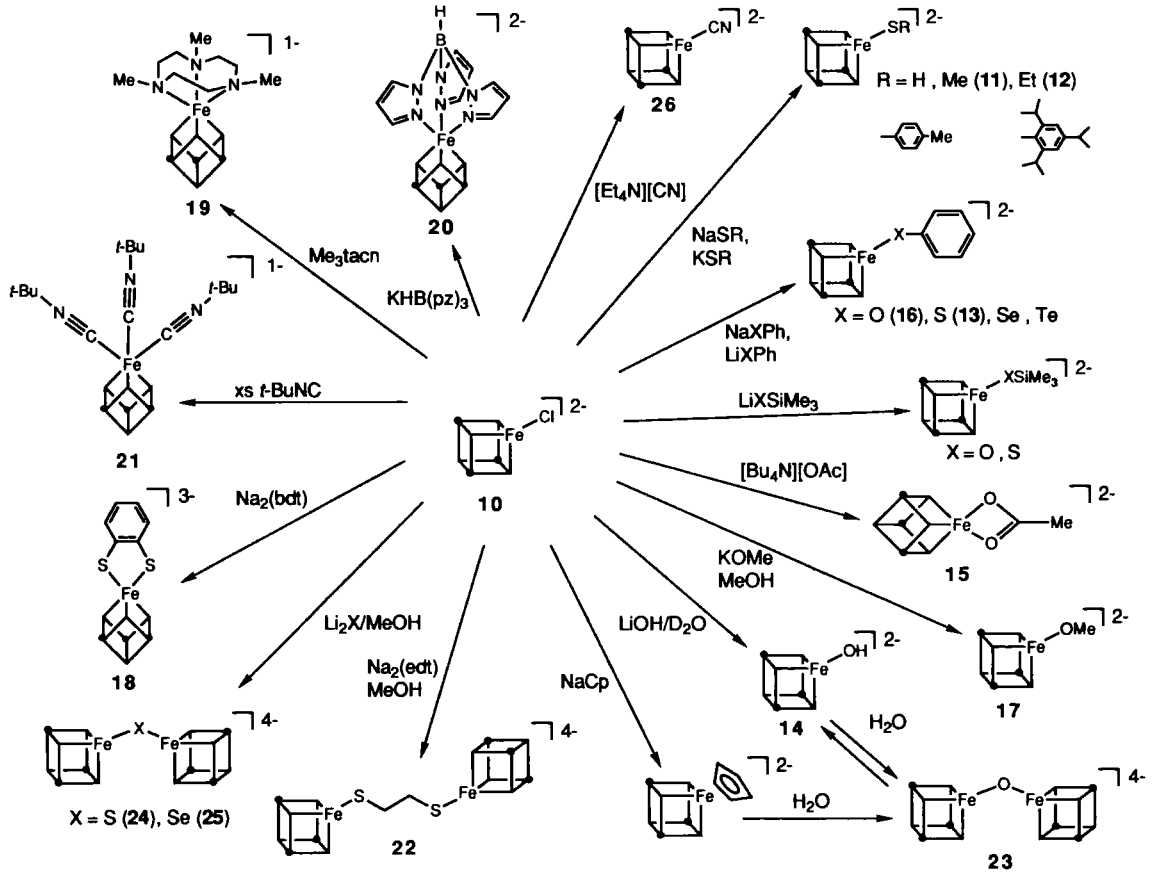

FIG. 2. Summary of subsite-specific substitution reactions of $[Fe_4S_4(LS_3)Cl]^{2-}$ (**10**) in Me_2SO solution (*47*). The cube symbol represents the $Fe_4S_4(LS_3)$ portion of generalized cluster **8**. A related summary involving other ligands is given elsewhere (*48*).

In the event that displacement of chloride from **10** is not successful, Eq. (6) offers an alternative means of substitution. Advantage is taken

$$[Fe_4S_4(LS_3)(OC_6H_4\text{-}p\text{-}Br)]^{2-} + Me_3SiL' \rightarrow [Fe_4S_4(LS_3)L']^{z-} + Me_3SiOC_6H_4\text{-}p\text{-}Br \quad (6)$$

of the higher strength of a Si—O versus a Si—L′ bond. The *p*-bromophenolate ligand has been utilized because it facilitates isolation of the initial cluster. In this way, clusters with $L = N_3^-$ and $MeSO_3^-$, ligands that do not displace chloride, were obtained as well as certain other clusters that have also been prepared by the reaction given in Eq. (5) (*47*).

Among the clusters obtained are those whose ligands L′ simulate known or potential cysteinate (**11–13**, as in **1**), hydroxide (**14**, as in **2**), and carboxylate (**15**, as in **3**) ligation of protein-bound clusters. Note also phenolate binding (**16**), which had been established earlier with $[Fe_4S_4(OPh)_4]^{2-}$ (*49*) and indicates the feasibility of Tyr as a cluster ligand. Cluster **17** simulates alkoxide binding; however, no deprotonated Ser residue has been detected as a ligand in any metalloprotein. Somewhat less exactly, **18** presents the possibility of a five-coordinate subsite with two Cys ligands, and **19** and **20** that of six-coordinate subsites with neutral weak-field ligands. At the same time, **20** and $[Fe_4S_4(LS_3)(H_2B(pz)_2)]^{2-}$ [not shown; $H_2B(pz)_2$ is dihydrobis(pyrazolyl)-borate(1 −)] suggest that imidazole groups of His residues may have cluster binding affinity.

Subsite-differentiated synthetic clusters lend themselves to many applications, which have been summarized (*22*). These include modulations of redox potentials, electron distributions, and interactions between subclusters in bridged double cubanes, all dependent on the ligand at the unique subsite. Although detailed consideration of these matters is beyond the purview of this article, certain leading results are noted. Introduction of a dianionic electron-rich ligand such as benzene-1,2-dithiolate in **18** causes very large (~500–600 mV) negative shifts of the $[Fe_4S_4]^{3+/2+}$ potential (*48*), thereby stabilizing the +3 core to reduction. Alteration of core electron distribution reaches an extreme upon the binding of three strong-field isonitrile ligands, as in **21**. The unique subsite becomes low-spin Fe(II), thereby generating the $[Fe_3S_4]^0$ cluster fragment with the same ground state spin ($S = 2$) and electronic structure as protein-bound cuboidal cluster **4** in the same oxidation state (*50, 51*). Clusters may be covalently linked by dithiolate bridges, as in **22**, or by oxide (**23**), sulfide (**24**), or selenide (**25**). When centroids of subclusters bridged by dithiolates are separated by less than ~11 Å, the two redox steps of the double cubanes are detectably coupled when examined by differential pulse polarography (*52*). The largest coupling,

in terms of a potential difference (220–230 mV), is found with oxide and sulfide bridges, which reduce subcluster separation to a minimum. The sulfide bridge has been structurally demonstrated in $[(Fe_4S_4Cl_3)_2S]^{4-}$ (Fe–S–Fe $= 102°$, $\Delta E_{1/2} = 300$ mV), which was prepared without using a subsite-differentiated cluster (*53*). In a further application, sulfur-bound pyridine-3/4-thiolate groups have been placed at the unique site. These bind Fe(II) complexes in covalently bridged assemblies, which provide an initial approach to the bridged Fe_4S_4–siroheme active site of *Escherichia coli* sulfite reductase (*54*).

The reactions of cluster **10**, which were conducted in Me_2SO solutions, represent the first extensive examination of the reactivity of an Fe_4S_4 cluster toward terminal ligand substitution.[1] Nearly all reactions are stoichiometric and, under the constant conditions employed, demonstrate that an iron subsite has an intrinsic affinity for a large range of ligands. Inasmuch as no nonthiolate ligand is known to displace alkylthiolate, it is improbable that other protein ligands can compete with cysteinate when four Cys residues are within bonding distance of a single-cubane core. However, it is now clear that, if not blocked by cysteinate, a subsite may accept other terminal ligands, including those in clusters **2** and **3**.

The reactions in Fig. 2 provide a guide to possible reactions of subsite-differentiated native clusters with exogenous ligands, at least in the $[Fe_4S_4]^{2+}$ oxidation state. In the only detailed study thus far, certain spectroscopic evidence has been interpreted in terms of cyanide binding to the cluster of *P. furiosus* Fd_{red} (*56*). ENDOR results indicate the presence of a type **2** cluster, which, from EPR spectra, exists as a ground spin state mixture of 20% $S = \frac{1}{2}$ and 80% $S = \frac{3}{2}$. Incubation of the protein with a 250-fold excess of cyanide resulted in conversion to a single EPR species with $S = \frac{1}{2}$ and a magnetic circular dichroism (MCD) spectrum consistent with the $[Fe_4S_4]^{1+}$ state but different from that of the initial cluster. Removal of cyanide by gel filtration restored the original EPR spectrum. Cyanide-induced perturbations of the EPR and MCD spectra were not observed with *Clostridium pasteurianum* Fd_{red}, which contains two standard clusters **1**, or with the 3Fe form of *P. furiosus* Fd. These results are consistent with reversible cyanide binding to the unique subsite of the cluster, similar to formation of oxidized cluster **26** (Fig. 2). The number of cyanide ligands bound to the protein cluster has not been established. Experience with synthetic clusters

[1] Core ligand substitution in the form of chalcogenide atom (Q) exchange reactions in the clusters $[Fe_4Q_4(SR)_4]^{2-}$ and $[Fe_4Q_4(SR)_4]^{3-}$ (Q = S, Se) had been demonstrated earlier (*55*).

such as **8** indicates that only one anionic monodentate ligand binds at a given subsite, a behavior that derives in part from ligand–ligand repulsion; two such ligands have been bound in a stable cluster only by chelation as, e.g., in **18**. In these experiments, bound cyanide has not been directly detected. It is unclear whether the observed spectral perturbations could arise from cyanide interactions with the protein but without specific cluster binding. Despite this uncertainty, it appears likely that a substantial reaction chemistry of protein-bound clusters having one labile subsite will be developed with *P. furiosus* Fd or other proteins, provided that protein structure allows access to the cluster by a variety of potential ligands.

2. 2:2 Subsite Differentiation

Although no protein-bound clusters with two non-Cys ligands have been recognized, we note, in the context of subsite differentiation, the existence of synthetic clusters with two different ligands. Anionic clusters of the general type $[Fe_4S_4L_2L'_2]^{2-}$ in polar solvents tend to exist in disproportion equilibria with other clusters. Several such clusters, among them $[Fe_4S_4Cl_2(OPh)_2]^{2-}$ and $[Fe_4S_4Cl_2(SPh)_2]^{2-}$, have been crystallized and their structures established by X-ray analysis (*57, 58*).

Somewhat more interesting are the neutral clusters $[Fe_4S_4L_2L'_n]$, examples of which have only recently been prepared. These species contain anionic (L) and neutral (L′) ligands. Cluster **27** has been obtained from the reaction of $[Fe(THF)_6][Fe_4S_4I_4]$, Ph_3PS, and sulfur in toluene/dichloromethane (*59*). The related cluster **28** was synthesized in the cluster assembly system, Eq. (7) (*60*). Cluster **29** was prepared by ligand substitution reaction, Eq. (8) (*51*), similar to the method for **21**, and **30** was readily produced by the subsequent substitution reaction, Eq. (9), in the presence of excess *t*-BuNC to suppress ligand dissociation (*61*). Under these conditions in the indicated solvents, neutral rather than charged products are formed.

$$3Fe(CO)_5 + [FeI_2((t\text{-}BuNH)_2CS)_2] + 4S \xrightarrow{THF} [Fe_4S_4I_2((t\text{-}BuNH)_2CS)_2] + 15CO \quad (7)$$

$$[Fe_4S_4Cl_4]^{2-} + 6t\text{-}BuNC \xrightarrow{THF} [Fe_4S_4Cl_2(t\text{-}BuNC)_6] + 2Cl^- \quad (8)$$

$$\xrightarrow[PhMe]{Na(OC_6H_4\text{-}p\text{-}Me)} [Fe_4S_4(OC_6H_4\text{-}p\text{-}Me)_2(t\text{-}BuNC)_6] + 2Cl^- \quad (9)$$

The structures of **27** and **28** contain the familiar $[Fe_4S_4]^{2+}$ cubane-type cores with unexceptional dimensions except for the relatively short Fe–Fe distance [2.687(4) Å] between atoms bound to the thiourea ligands of **28**. The structures of **29** and **30** are nearly isodimensional and

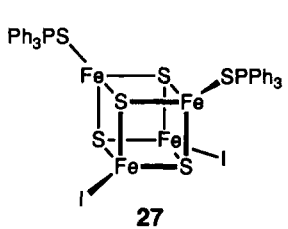

27

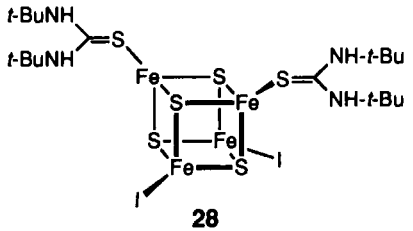

28

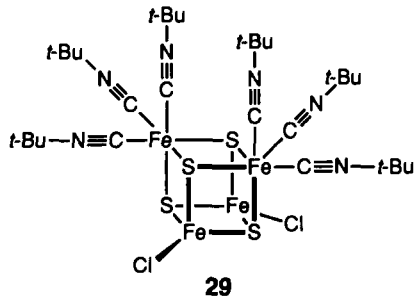

29

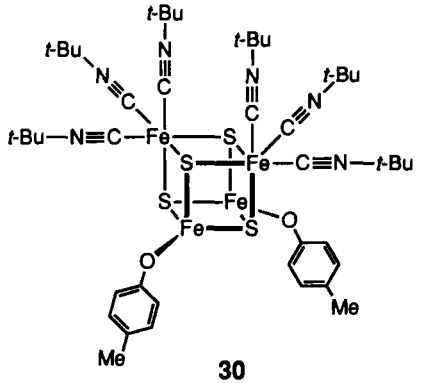

30

are conspicuously different from those of any other $[Fe_4S_4]^{2+}$ species. The cores exhibit six long and six short Fe–S distances. In **30** the mean values are 2.38(2) and 2.26(1) Å. The short distances are normal and involve the four-coordinate subsites, which are separated by 2.74–2.77 Å. The long distances are found at the six-coordinate subsites, and, together with the long Fe . . . Fe separation of 3.45 Å, demonstrate the presence of two low-spin Fe(II) subsites and their effective electronic isolation from each other and from the Fe_2S_2 cluster portion with tetrahedral subsites. The structures at the six-coordinate subsites undoubtedly represent that of the corresponding subsite in cluster **21**, whose electronic structure has been elucidated (*50, 51*).

In low-polarity solvents such as toluene, tetrahydrofuran (THF), and dichloromethane, neutral clusters should prove stable to disproportionation inasmuch as the reaction given by Eq. (10) generates ionic prod-

$$2[Fe_4S_4L_2L_2'] \rightleftharpoons [Fe_4S_4L_3L']^{1-} + [Fe_4S_4LL_3']^{1+} \qquad (10)$$

ucts. The occurrence of these reactions, Eqs. (7)–(9), in such media is an obvious reflection of stability of the product clusters.[2] The solution

[2] There is no implication that only neutral clusters will be formed in low-polarity solvents; for example, $[Fe_4S_4I_3((Me_2N)_2CS)]^{1-}$ [as the $[FeI((Me_2N)_2CS)_3]^{1+}$ salt] is formed by two different reactions in THF (*60*).

properties of **27** and **28** have not been reported other than the note that the former decomposes (to unspecified products) in THF and acetonitrile (*59*). Clusters **29** and **30** are stable in toluene, THF, and dichloromethane; the occurrence of the (heterogeneous) reaction, Eq. (9), demonstrates the feasibility of anion/anion ligand substitution in toluene to generate another neutral cluster. Neutral ligands, especially those at tetrahedral high-spin subsites, are potentially susceptible to replacement by other neutral ligands. Neutral/anion substitution appears most likely when the other two subsites carry strongly bound thiolate ligands, but the formation of charged clusters implies the possibility of disproportionation even in a low-polarity medium. Among Fe_4S_4 clusters, the unique potential reactivity of $[Fe_4S_4L_2L'_n]$ is that of neutral/neutral ligand substitution in low-polarity media to afford stable 2:2 subsite-differentiated products. At present, there is practically no information on the affinity of Fe_4S_4 clusters in any oxidation state for neutral ligands. Clusters **19–21** and **27–30**, $[Fe_4S_4(LS_3)(tacn)]^{1-}$ (*48*), and $[Fe_4S_4(CO)_{12}]$ (*62*), with the fully reduced $[Fe_4S_4]^0$ core, are the only examples with neutral ligand donors (tacn is 1,4,7-triazacyclononane).

III. Trinuclear Cuboidal Clusters

A. Protein-Bound Fe_3S_4 Clusters

Whereas the synthesis of new clusters is an everyday occurrence in chemistry, the discovery of a new metal cluster in biology is a signal event. The pleasure of watching the chemistry and biochemistry of the cuboidal Fe_3S_4 cluster **4** and its derivatives unfold is enhanced by the realization that its occurrence was totally unpredicted. Although not a new structural motif (*vide infra*), it joins Fe_4S_4 and Fe_2S_2 (*63–66*) units in the set of structurally defined biological iron–sulfur clusters and is among the very few structurally characterized (*67*) polynuclear metal units in proteins. An account of the discovery of Fe_3S_4 clusters has been provided by Beinert and Thomson (*68*). In brief, aerobically purified ferredoxins often show a nearly isotropic EPR signal at $g \approx 2.01$, which was first thought by some investigators in the 1970s to arise from a minor impurity of "superoxidized" ($[Fe_4S_4]^{3+}$) clusters. Subsequent spectroscopic and crystallographic studies of *D. gigas* Fd II and *A. vinelandii* Fd I, originally believed to be an 8Fe protein, led to the conclusion that both proteins accommodated the same cluster that contained *three* iron atoms. This conflicted with the orthodox view at the time that low-molecular-weight ferredoxins contained only two cluster

types, Fe_2S_2 and Fe_4S_4. The definitive identification of the cluster as cuboidal Fe_3S_4 was forthcoming from protein crystallography in 1988 (*6, 7, 35*).

1. Formation, Oxidation States, and Spin States

Consideration of the occurrence and formation of Fe_3S_4 clusters in proteins necessarily involves those factors that destabilize, or prevent the formation of, the far more widely distributed Fe_4S_4 clusters. Two factors are of prime importance: protein compositional and structural features that lead to unconventional terminal ligation, and cluster oxidation level. Except for the standard cases of *B. thermoproteolyticus* Fd and *P. aerogenes* Fd, the cluster binding patterns in Table I reveal that known or putative Fe_4S_4 clusters in these proteins display the unconventional terminal ligation in **2** and, perhaps, **3**. The lack of a strongly bound Cys ligand promotes lability at the unique subsite. For at least aconitase (*38*) and *P. furiosus* Fd (*69*), the ligand at that subsite is OH^-/H_2O. In those cases wherein an iron atom has been removed from a tetranuclear cluster, the atom is released from the $[Fe_4S_4]^{3+}$ oxidation level in reaction (a) of the scheme given by Eq. (11). Spontaneous iron atom uptake to rebuild an Fe_4S_4 cluster occurs with $[Fe_3S_4]^0$ in reaction (b). Neither reaction is known to be reversible.

$$\begin{array}{ccc} [Fe_4S_4]^{3+} & \xrightarrow[(a)]{} & [Fe_3S_4]^{1+}\ (S = 1/2) + Fe^{2+} \\ \uparrow\downarrow \pm e^- & & \uparrow\downarrow \pm e^- \\ [Fe_4S_4]^{2+} & \xleftarrow[(b)]{Fe^{2+}} & [Fe_3S_4]^{0}\ (S = 2) \\ & & \uparrow\downarrow \pm e^- \\ & & [Fe_3S_4]^{1-}\ (S = 5/2) \\ & & (c) \end{array} \qquad (11)$$

Protein cluster conversion reactions are summarized in Table II (*70–84*). Those of aconitase and *D. gigas* Fd II have been the most carefully studied, and afford different results. With use of Mössbauer spectroscopy and ^{57}Fe-enriched samples, it has been demonstrated that the subsite voided in reaction (a) of aconitase is that occupied in reaction (b) (*70*). In the case of *D. gigas* Fd II, the addition of external $^{57}Fe^{2+}$ to the $[Fe_3S_4]^0$ form of the protein results in the occupation of one of three subsites that are indistinguishable by Mössbauer spectroscopy (*76*). It was also shown that exchange between the two Mössbauer-detectable subsites of the Fe_4S_4 cluster, present in a 3 : 1 ratio, does not occur over a time sufficient for cluster conversion. This indicates that the (final)

TABLE II

CLUSTER CONVERSION REACTIONS

Reaction	Protein	Ref.
$[Fe_3S_4] \rightleftharpoons [Fe_4S_4]$	Aconitase (beef heart)	*70–74*
	Desulfovibrio gigas Fd II	*75–77*
	Pyrococcus furiosus Fd	*25*
$[Fe_3S_4] \rightarrow [Fe_4S_4]$	*Desulfovibrio africanus* Fd III	*30*
	Thermodesulfobacterium commune Fd	*78*
$[Fe_4S_4] \rightarrow [Fe_3S_4]$	*Azotobacter chroococcum* Fd	*79*
	Bacillus stearothermophilus Fd	*80, 81*
	Clostridium pasteurianum Fd	*82, 83*
	Mycobacterium smegmatis Fd	*84*
	Pseudomonas ovalis Fd	*84*
	Thermus thermophilus Fd	*84*

subsite assumed is one of the three that are Cys ligated rather than the initially vacant subsite, in contrast to the behavior of aconitase. In proteins such as *B. stearothermophilus* Fd and *C. pasteurianum* Fd, which contain only type 1 clusters, conversion to the Fe_3S_4 form has been accomplished by treatment with an excess of a chemical oxidant such as ferricyanide. Assuming that the iron atoms retain four coordination, one or more Cys ligands must be removed from the cluster in the process, either by displacement and protonation or by oxidation, possibly to the sulfonate. Treatment of *A. vinelandii* Fd I with excess ferricyanide results in selective destruction of the Fe_4S_4 cluster, leaving the Fe_3S_4 cluster intact (*85*).

Although few details of reactions (a) and (b) of Eq. (11) are known, it is now quite clear that the electrophilic demands of the three Fe(III) atoms in $[Fe_3S_4]^{1+}$ render the sulfur atoms insufficiently nucleophilic to bind relatively hard (divalent) metal ions. Reduction by one electron redresses this problem. We shall return to the concept of the cuboidal Fe_3S_4 cluster as a ligand.

Also shown in Eq. (11) is the electron transfer series (c) of Fe_3S_4 clusters and the ground spin state of each oxidation level. The latter has been established for $[Fe_3S_4]^{1+/0}$ by analysis of low-temperature MCD spectra (*25, 82, 86–90*) and by direct measurement of magnetization (*91*). In the oxidized state $[Fe_3S_4]^{1+}$, the three $S = \frac{5}{2}$ Fe(III) atoms, indistinguishable by Mössbauer spectroscopy, are antiferromagnetically coupled to give an $S = \frac{1}{2}$ ground state with a nearly isotropic EPR

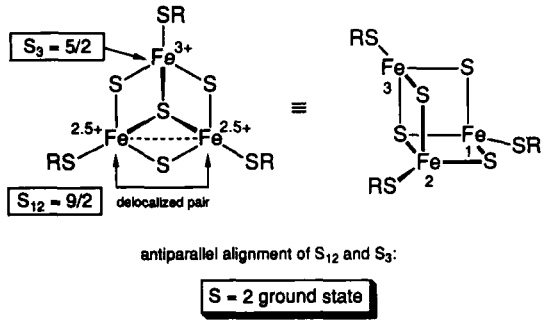

FIG. 3. Schematic representation of the geometric and electronic structure of the $[Fe_3S_4]^0$ oxidation level showing the high-spin Fe^{3+} site and the $Fe^{3+/2+}$ delocalized pair, which account for doublets A and B,B′, respectively, in the Mössbauer spectra (Table III).

signal near $g \approx 2.01$ (*68*). Potentials for the $[Fe_3S_4]^{1+/0}$ couple span the range -130 to -420 mV (*29, 92–95*).[3]

The most unusual electronic structure of $[Fe_3S_4]^0$ is schematically represented in Fig. 3; isomer shifts (δ) and quadrupole splittings (ΔE_Q) of representative proteins are listed in Table III. The cluster contains a high-spin Fe(III) subsite with normal Mössbauer parameters (doublet A), which are nearly the same as those for $[Fe_3S_4]^{1+}$. Also present is an electronically delocalized pair of Fe(II,III) atoms (doublets B,B′) that are effectively identical on the Mössbauer time scale; a small inequivalence has been detected in aconitase. The average isomer shift is in the range of $[Fe_4S_4]^{2+}$ clusters, indicating the mean oxidation state $Fe^{2.5+}$. The spins at these subsites ($S = 2, \frac{5}{2}$) are ferromagnetically coupled to afford the resultant $S = \frac{9}{2}$. This spin is in turn antiferromagnetically coupled to the Fe(III) spin to yield the system spin $S = 2$. A spin-coupling mechanism with electron delocalization over two subsites has been proposed to account for the observed electronic structure (*99, 100*), which shall be of subsequent interest in connection with the ligand properties of $[Fe_3S_4]^0$. In selenide-reconstituted aconitase, the $[Fe_4Se_4]^{2+}$ cluster can be converted with ferricyanide to $[Fe_3Se_4]^{1+}$. This cluster is reducible to $[Fe_3Se_4]^0$, which has the same electronic structure as its sulfide congener (*96*).

[3] In accordance with the way in which they are typically reported, protein potentials are referenced to the normal hydrogen electrode (NHE) and those of synthetic compounds (usually in nonaqueous solvents) are versus the SCE ($E_{NHE} = E_{SCE} + 0.24$ V). When applied to redox reactions, the term "reversible" refers to chemical reversibility ($i_{pa}/i_{pc} \approx 1$ in cyclic voltammetry).

TABLE III

MÖSSBAUER PARAMETERS AND OXIDATION AND SPIN STATES FOR CUBOIDAL $[Fe_3S_4]$ AND HETEROMETAL CUBANE $[MFe_3S_4]$ CLUSTERS

Cluster/protein	Oxidation state	$\delta^{a,b}$ (mm/sec)	$\Delta E_Q{}^b$ (mm/sec)	Spin state (S)	Fragments	Ref.
$[Fe_3S_4]$						
Aconitase (beef heart)	$[Fe_3S_4]^{1+}$	0.27	0.71	$\frac{1}{2}$	—	*70*
A. vinelandii Fd I	$[Fe_3S_4]^{1+}$	0.27	0.63	$\frac{1}{2}$	—	*97*
D. gigas Fd II	$[Fe_3S_4]^{1+}$	0.27	0.54	$\frac{1}{2}$	—	*98*
Aconitase (beef heart)	$[Fe_3S_4]^{0}$	A 0.31	0.56	2	—	*96*
		B 0.46	1.15		—	
		B′ 0.49	1.46		—	
A. vinelandii Fd I	$[Fe_3S_4]^{0}$	A 0.29	0.40	2	—	*97*
		B 0.47	1.45		—	
D. gigas Fd II	$[Fe_3S_4]^{0}$	A 0.30	0.47	2	—	*98*
		B 0.46	1.47		—	
Mean (three proteins)		0.42	—			
$[MFe_3S_4]$						
M = Fe, Co, Ni, Zn, Cd (Set I)						
$[Fe_4S_4(LS_3)(t\text{-BuNC})_3]^{1-}$ (**21**)	$[Fe_4S_4]^{2+}$	A 0.34	0.59	2	$[Fe_3S_4]^0 + Fe^{2+}$ ($S = 0$)	*50, 51*
		B 0.46	1.21			
		B′ 0.47	1.49			
D. gigas Fd II/Co	$[CoFe_3S_4]^{2+}$	A 0.35	1.1	$\frac{1}{2}$		*199*
		B 0.44	1.35			
$[CoFe_3S_4(tibt)_4]^{2-}$ (**70**)	$[CoFe_3S_4]^{2+}$	A 0.33	0.78	$\frac{1}{2}$	$[Fe_3S_4]^0 + Co^{2+}$ ($S = \frac{3}{2}$)	*197*
		B 0.43	1.32			
		B′ 0.46	0.93			

TABLE III (*continued*)

Cluster/protein	Oxidation state	δ[a,b] (mm/sec)	ΔE_Q[b] (mm/sec)	Spin state (S)	Fragments	Ref.
D. gigas Fd II/Co	$[CoFe_3S_4]^{1+}$	0.53	1.28	>0 (1)[d]	$[Fe_3S_4]^{1-}$ + Co^{2+} (S = ½)	*199*
P. furiosus Fd/Ni	$[NiFe_3S_4]^{1+}$	—[c]	—[c]	½	$[Fe_3S_4]^{1-}$ + Ni^{2+} (S = 1)	*201*
$[NiFe_3S_4(SEt)_3(PPh_3)]^{2-}$ (**68**)	$[NiFe_3S_4]^{1+}$	0.47	0.90	½		*195*
D. gigas Fd II/Cd	$[CdFe_3S_4]^{1+}$	—[c]	—[c]	½	$[Fe_3S_4]^{1-}$ + Cd^{2+}	*200*
D. gigas Fd II/Zn	$[ZnFe_3S_4]^{1+}$	A 0.62	2.7	½	$[Fe_3S_4]^{1-}$ + Zn^{2+}	*102*
		B 0.51	1.6			
		B′ 0.54	1.6			
Mean		0.56	—			
M = V, Mo, W, Re (Set II)						
$[VFe_3S_4(S\text{-}p\text{-}tol)_3(DMF)_3]^{1-}$ (**56**)	$[VFe_3S_4]^{2+}$	0.46	1.08	½	$[Fe_3S_4]^{0/1-}$ + $V^{2+/3+}$	*189*
$[Mo_2Fe_6S_8(SPh)_9]^{3-}$ (**43**)	$[MoFe_3S_4]^{3+}$	0.40	1.01	½	$[Fe_3S_4]^{0}$ + Mo^{3+}	*176*
		0.44	1.41			
$[MoFe_3S_4(S\text{-}p\text{-}C_6H_4Cl)_4(cat)]^{3-}$ (**48**)	$[MoFe_3S_4]^{3+}$	0.40	1.76	½		*202*
		0.43	1.14			
$[Mo_2Fe_6S_8(SPh)_9]^{5-}$ (**45**)	$[MoFe_3S_4]^{2+}$	0.53	2.21	2	$[Fe_3S_4]^{1-}$ + Mo^{3+}	*176*
		0.54	0.84			
$[MoFe_3S_4(S\text{-}p\text{-}C_6H_4Cl)_4(EtCN)]^{3-}$ (**48**)	$[MoFe_3S_4]^{2+}$	0.52	2.25	2	$[Fe_3S_4]^{1-}$ + Mo^{3+}	*202*
		0.54	0.91			
$[W_2Fe_6S_8(SEt)_9]^{3-}$	$[WFe_3S_4]^{3+}$	0.45[e]	1.41[e]	½	$[Fe_3S_4]^{0}$ + W^{3+}	*203*
$[Re_2Fe_7S_8(SEt)_{12}]^{2-}$ (**66**)	$[ReFe_3S_4]^{4+}$	0.37	0.86	½	$[Fe_3S_4]^{0}$ + Re^{4+}	*191*
$[Re_2Fe_6S_8(SEt)_9]^{3-}$ (**63**)	$[ReFe_3S_4]^{3+}$	0.44	0.87	2	$[Fe_3S_4]^{0/1-}$ + $Re^{3+/4+}$	*204*
		0.46	1.17			
$[ReFe_3S_4(SEt)_4(dmpe)]^{1-}$ (**67**)	$[ReFe_3S_4]^{3+}$	0.49[e]	1.37[e]	2		*193*

[a] Referenced to Fe metal at room temperature.
[b] Measured at 4.2 or 80 K.
[c] Not reported.
[d] Predicted value.
[e] Average values.

The terminal reduced member of series (c) has not yet been detected in the unmodified $[Fe_3S_4]^{1-}$ form. However, this oxidation level has been stabilized as $[ZnFe_3S_4]^{1+}$ (*101*), from which the $S = \frac{3}{2}$ ground state has been determined. This cluster will be considered later in connection with heterometallic MFe_3S_4 clusters. An electrochemical study of *D. africanus* Fd III has shown that a reduction step at near −720 mV is coupled to the $[Fe_3S_4]^{1+/0}$ reaction at −140 mV (*95*). The pH dependence of the potential together with the approximately twofold greater current passed than in the −140-mV process implies the proton-coupled reaction $[Fe_3S_4]^0 + 2e^- + 2H^+ \rightarrow [Fe_3S_4H_2]^0$. The product, which without protonation would be a dianionic 3Fe(II) cluster, could conceivably be sufficiently basic to be stabilized by sulfide protonation in the 6.2–7.8 pH range studied. The reason why the potentials of two successive one-electron reductions are not resolved is unclear, and it has been suggested that a chemical step of structural rearrangement may intervene (*95*).

2. Structures

Similarities in the MCD and Mössbauer spectra of $[Fe_3S_4]^{1+/0}$ clusters in various proteins make it virtually certain that all such clusters have the cuboidal structure **4**. This structure has been crystallographically established for the $[Fe_3S_4]^{1+}$ clusters in inactive aconitase (*10*), *A. vinelandii* Fd I (*6, 7*), the C20A mutant of this protein (*11*), and *D. gigas* Fd II (*35, 36*). The most detailed metric data have been reported for *D. gigas* Fd II, whose cluster structure at 1.7 Å resolution is presented in Fig. 4. Two principal points emerge from the structural results, although exact comparisons among structures are not possible owing to different states of refinement.

First, clusters are dimensionally similar and bond distances and angles are unexceptional in relation to those of protein-bound and synthetic Fe_4S_4 clusters. For example, when the clusters of aconitase (2.1 Å refinement) and *A. vinelandii* Fd I (1.9 Å refinement) are compared, the positions of the seven iron and sulfur atoms agree on average to 0.09 Å (*10*). Second, Fe_3S_4 portions of trinuclear and tetranuclear clusters are structurally nearly the same. To demonstrate this point, Kissinger *et al.* (*35*) have provided a comparative tabulation of cluster bond distances and angles of *D. gigas* Fd II, *P. aerogenes* Fd_{ox}, and *Chromatium vinosum* HP_{red}. Consider the case of inactive and active aconitase, which are isomorphous and whose cluster structures are shown in Fig. 4. The seven iron and sulfur atoms common to the two clusters differ in position on average by only 0.11 Å, and the three common Cys sulfur atoms vary by 0.25 Å (*10*). It seems highly probable

D. gigas Fd II

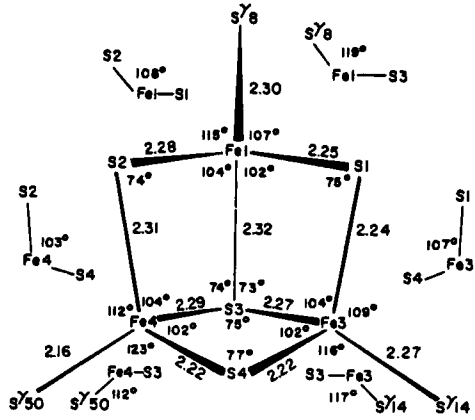

Aconitase (pig heart)

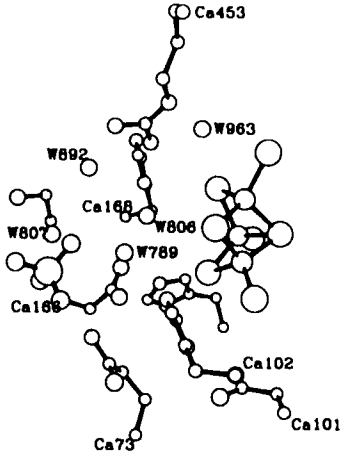

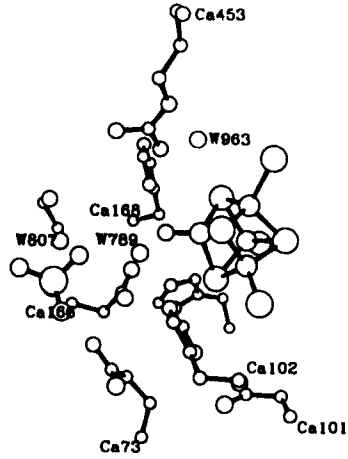

inactive: $[Fe_3S_4]^{1+}$ **active: $[Fe_4S_4]^{2+}$**

FIG. 4. Structures of the $[Fe_3S_4]^{1+}$ cluster in *D. gigas* Fd II (*35*) and the $[Fe_3S_4]^{1+}$ and $[Fe_4S_4]^{2+}$ clusters in inactive and active aconitase (*10*), respectively.

that such a condition would hold also for the $[Fe_3S_4]^0$ oxidation state, which in *D. gigas* Fd II is fully delocalized at ambient temperature (*99*). It remains to be learned whether the lack of structural relaxation, say to a more open or flattened structure along the (idealized) threefold axis of **4**, upon removal of an iron atom is an intrinsic cluster property or is enforced by protein structure. In any event, the Fe_3S_4 cluster is effectively configured to bind a metal atom with very little structural rearrangement required of the product cluster core.

B. Clusters of Related Structure

Cluster **4** is one member of a larger series of molecules containing the generalized cuboidal core **31**. While such a structure might appear

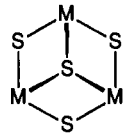

31

relatively ordinary, there was, in fact, only a single proved molecular example in metal–chalcogenide chemistry prior to 1980 (*102*). In 1971, Dahl and co-workers (*103*) prepared and determined the structure of $[Cp_3Mo_3S_4]^{1+}$ [Cp is cyclopentadienide(1 −)]. They noted about this molecule, somewhat prophetically in a biological context (despite the difference in metals), that it "can be visualized as arising from a cubane-like $[Cp_4Mo_4S_4]$ architecture by formal removal of one [MoCp] group." The compound $[Cp_3Mo_3S_4]$ was prepared in 1973 (*104*), but its structure was not determined. No further activity on cuboidal M_3S_4 compounds was evident until the report in 1980 of $[Mo_3S_4(CN)_9]^{5-}$ (*105*). In that same year, Müller *et al.* (*106*) reviewed the state of trinuclear clusters and noted the existence of "incomplete cube" structures in oxo- and halide-bridged compounds of niobium, molybdenum, and tungsten. An explosive growth of the chemistry of synthetic cuboidal clusters occurred in the 1980s, somewhat coincidentally with the recognition of the related cluster **4** in proteins. The accomplishments of Cotton, Shibahara, Sykes, and their co-workers, in particular, have done much to open and define this area of cluster chemistry.

There are now over 30 synthetic cuboidal clusters **31** whose structures have been demonstrated by X-ray analysis. These are of the types $M_3S_4L_n$, with $n = 6$, 8, or 9, examples of which are collected in Table IV. There is a notably large group $[Mo_3S_4(dtp)_4L]$, in which L is a loosely

held neutral ligand (*129*) [dtp is *O,O*-diethyldithiophosphate(1 −)]. All molybdenum and tungsten compounds contain the metal in the IV oxidation state. Differences in coordination numbers and ligand types notwithstanding, the core structures of the molybdenum and tungsten clusters are very similar, as illustrated for cationic six-coordinate $[Mo_3S_4(OH_2)_{12}]^{4+}$ (**32**) (*110*) and anionic five-coordinate $[Mo_3S_4(edt)_3]^{2-}$ (**33**) (*120*), whose dimensions are typical [edt is ethane-1,2-dithio-

TABLE IV

SYNTHETIC CLUSTERS WITH THE CUBOIDAL M_3S_4 CORE (**31**)

Cluster	Ref.
$[V_3S_4(edt)_3]^{3-}$	*112*
$[Mo_3S_4(OH_2)_9]^{4+}$	*107–111, 250*
$[Mo_3S_4(CN)_9]^{5-}$	*105, 113*
$[Mo_3S_4(C_2O_4)_3(OH_2)_3]^{2-}$	*107*
$[Mo_3S_4(tacn)_3]^{4+}$	*114*
$[Cp_3Mo_3S_4]^{1+}$	*103*
$[Mo_3S_4(ida)_3]^{2}$	*115*
$[Mo_3S_4(Hnta)_3]^{2-}$	*250*
$[Mo_3S_4(nta)(Hnta)_2]^{3-}$	*116*
$[Mo_3S_4(S_2PEt_2)_4]$	*117–119*
$[Mo_3S_4(edt)_3]^{2-}$	*120*
$[Mo_3S_4Cl_3(dmpe)_3]^{1+}$	*121–123*
$[Mo_3S_4Cl_4(PEt_3)_3(MeOH)_2]$	*124*
$[Mo_3S_4Cl_4(PEt_3)_4(MeOH)]$	*124*
$[Mo_3S_4Cl_4(PPh_3)_3(OH_2)_2]$	*122, 128*
$[Mo_3S_4Cl_4(PEt_3)_3(OH_2)_2]$	*252*
$[Mo_3S_4Br_4(PEt_3)_3(OPEt_2H)(OH_2)]$	*252*
$[Mo_3S_4(dtp)_4(OH_2)]$	*125, 129*
$[Mo_3S_4(dtp)_4(PhCH_2CN)]$	*126*
$[Mo_3S_4(dtp)_3(OAc)(MeCN)]$	*127*
$[Mo_2WS_4(OH_2)_9]^{4+}$	*134*
$[MoW_2S_4(OH_2)_9]^{4+}$	*134*
$[W_3S_4(OH_2)_9]^{4+}$	*130, 131, 250, 251*
$[W_3S_4(S_4)_3(OH_2)_3]^{2-}$	*135*
$[W_3S_4(S_4)_3(NH_3)_3]^{2-}$	*251*
$[W_3S_4(NCS)_9]^{5-}$	*132, 250, 251*
$[W_3S_4(Hnta)_3]^{2-}$	*250*
$[W_3S_4Cl_3(dmpe)_3]^{1+}$	*123, 133*
$[W_3S_4Cl_3(depe)_3]^{1+}$	*123*
$[W_3S_4H_3(dmpe)_3]^{1+}$	*123*
$[W_3S_4Br_4(PEt_3)_3(OPEt_2H)(OH_2)]$	*252*
$[W_3S_4(dtp)_3(OAc)(py)]$	*136, 137, 253*

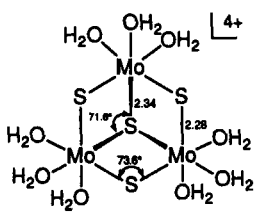

32 (Mo-Mo, 2.74)

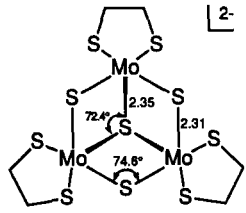

33 (Mo-Mo, 2.78)

late(2−)]. The clusters are electron precise inasmuch as they contain the six electrons necessary for M—M single bonds. In addition, there are subsets of cuboidal clusters $M_3O_{4-n}S_n$ displaying permutations of oxygen and sulfur atoms in the μ_2 and μ_3 positions. The complete set of eight molybdenum clusters (n = 0–4) has been obtained, primarily by the chemical ($NaBH_4$) or electrochemical reduction of $[Mo_2O_{4-n}S_n(S \cdot Cys)_2]^{2-}$ in aqueous solution followed by aerial oxidation (*108, 109, 138–144*).

Reduction of $Mo_2^VO_{4-n}S_n$ complexes affords both trinuclear and tetranuclear clusters, and has been the most frequently utilized method for the preparation of Mo_4S_4 clusters (*108, 109, 111, 115, 145–148*). It was recognized in the early work on these species that exposure to air resulted in the formation of some trinuclear clusters (*107, 108, 114, 145*). Under the usual workup conditions, the acidic aqueous reaction mixture after reduction is handled in the air and the cluster products are separated by ion-exchange chromatography. With controlled exposure to oxidizing conditions, the green +5 cubane-type aqua ion can be obtained, which is part of the three-membered electron transfer series of Eq. (12) (*144*). An analogous series [Eq. (13)] of ethylenediaminetetraacetate(4−) (EDTA) complexes has been prepared (*149, 150*). Both series

$$[Mo_4S_4(OH_2)_{12}]^{4+} \xleftrightarrow{-0.03\ V} [Mo_4S_4(OH_2)_{12}]^{5+} \xleftrightarrow{0.52\ V} [Mo_4S_4(OH_2)_{12}]^{6+} \qquad (12)$$

$$[Mo_4S_4]^{5+} + 5VO_2^{1+} + 10H^+ \rightarrow [Mo_3S_4]^{4+} + Mo^{VI} + 5VO^{2+} + 5H_2O \qquad (13)$$

can be traversed chemically and electrochemically. When stored under dinitrogen, acid solutions of the +5 aqua ion are stable indefinitely. For this ion in air, $t_{1/2} \approx 4$ days at 50°C (1 *M* HCl); heating at 95°C for 2–3 hr gives $[Mo_3S_4(OH_2)_9]^{4+}$ in essentially quantitative yield (*148*). Further, the reaction given by Eq. (13) with excess oxidant has been demonstrated; with a restricted amount of V(V) oxidant, the +6 cubane cluster is obtained (*148*).

These observations, summarized in the scheme shown in Eq. (14), show that when sufficiently oxidized, the aqua cubane cluster will

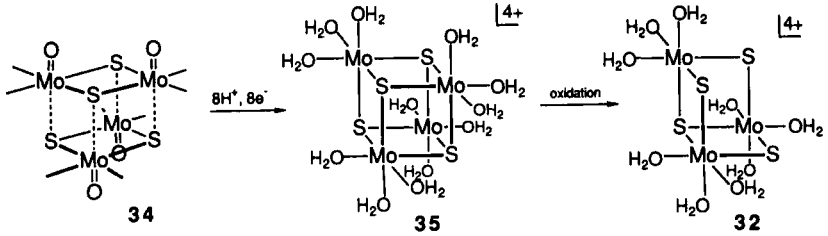

34 35 32

(14)

release a molybdenum atom. The initial cluster is likely formed by the interaction of two $Mo_2O_2S_2$ fragments (**34**). Essentially concomitant reduction and protonation would transform oxo to aqua ligands, thereby removing an oxo trans effect unfavorable to dimerization. Under reducing conditions the +4 aqua cubane **35** is first generated, but is subsequently oxidized to a level, presumably past the +6 aqua ion, where the affinity for one molybdenum atom has decreased to the point of spontaneous release of that atom. The reaction shown in Eq. (15), with $NaBH_4$ as the reductant, occurs to a limited extent (*111*). It suggests

$$[Mo_3S_4]^{4+} + Mo^{3+} + 2e^- \rightarrow [Mo_4S_4]^{5+} \quad (15)$$

that the cuboidal cluster requires reduction by two electrons to bind a (tripositive) cation. In the preparation of $[Mo_4S_4(EDTA)_2]^{3-}$, a solution was maintained at 90°C for 24 hr in the air just prior to chromatographic separation of the ion (*150*). The chelating ligand does not stabilize the cluster against oxidation because the potentials are ~0.2 V more negative than those in Eq. (12). Apparently, the ligand impedes spontaneous loss of a molybdenum atom, which would require the rupture of three terminal Mo—O/N bonds. An unforeseen parallel behavior of Fe_4S_4 and Mo_4S_4 clusters is evident. When sufficiently oxidized, the M_3S_4 fragment of each loses binding affinity for the remaining M atom of the cluster, which then dissociates. Protein cysteinate and edta ligands may perhaps be likened in the sense that their strong coordination slows or altogether prevents M atom loss. As will be seen, cuboidal Mo_3S_4 binds metal ions. The formation of heterometal cubanes MMo_3S_4 often requires the use of reducing conditions, and the nature of the product is such as to suggest a two-electron reduction of the cuboidal cluster in most cases.

Certain preparative routes to M_3S_4 clusters either do not, or are not known to require, the intermediacy of a cubane cluster. No such cluster intervenes in the desulfurization of coordinated persulfide in the trinuclear core $[M_3(\eta^4\text{-}\mu_2\text{-}S_2)_3(\mu_3\text{-}S)]^{4+}$ (M = Mo, W) by thiophilic reagents

such as cyanide (*105, 113*) and tertiary phosphines (*118, 122, 135*). The reaction of $MoCl_3$ or WCl_4 with NaSH in the presence of chelating diphosphines (*121, 123*) and the reduction of $[WS_4]^{2-}$ with $NaBH_4$ (*130–132*) are other cases in which tetranuclear species are evidently not necessary to product formation. Reduction of a mixture of $[WS_4]^{2-}$ and $[Mo_2O_2S_2(S \cdot Cys)_2]^{2-}$ affords mixed-metal aqua ions, which were separated by cation exchange (*134*). Their identification completes the series of cuboidal nonaqua ions.

$$[Mo_3S_4]^{4+} \quad [Mo_2WS_4]^{4+} \quad [MoW_2S_4]^{4+} \quad [W_3S_4]^{4+}$$

Before leaving the subject of trinuclear cuboidal clusters, we observe that cuboidal units occur in clusters of higher nuclearity. In the context of iron–sulfur chemistry, several examples may be cited. The clusters $[Fe_6S_9(SR)_2]^{4-}$ (**36**) contain two $[Fe_3(\mu_2\text{-}S)_2(\mu_3\text{-}S)(\mu_4\text{-}S)]$ units (*41, 151,*

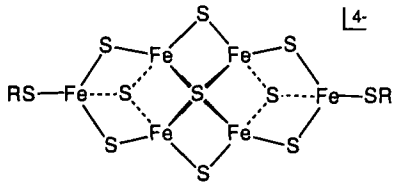

36

152); these also occur in the cyclic cluster $[Na_2Fe_{18}S_{30}]^{8-}$ (*153*). In the discrete double cluster $[Na_2(Fe_6S_9(SMe)_2)_2]^{6-}$, crystallized as its Et_4N^+ salt (*152*), the two Fe_6S_9 clusters are bridged by two sodium ions, each of which forms six Na–S interactions to two Fe_3S_4 units. In an approximate sense, the sodium ions occupy the voids in these incomplete cubes, but the long bond lengths (2.88–3.11 Å) suggest that the interactions are mainly ionic in character. No transition element ion has been placed in these voids, where it may be expected that interactions with the μ_4-S atoms in the intact cluster will be weak.

C. Inverted (M_4S_3) Clusters

Although tetranuclear rather than trinuclear, these clusters are considered briefly here in the context of cuboidal structures. In relation to **31**, cuboidal core $M_4(\mu_3\text{-}S)_3$ (**37**) has an inverted population of metal and sulfur subsites; it is represented by very few compounds. Cluster **38** is the classical black Roussin monoanion. It may be conceived as a derivative of the cubane $Fe_4S_4(NO)_4$ by removal of one sulfur atom and the addition of three nitrosyl ligands and one electron. The structures of two salts (*154, 155*) establish that the Fe_4S_3 core is a virtually congruent

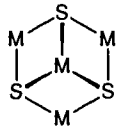

37

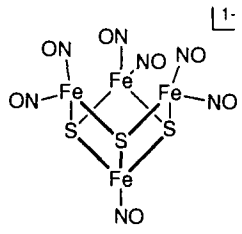

38

fragment of the cubane core. The cluster has been obtained by reduction (Na/Hg) of $Fe_4S_4(NO)_4$ in THF (*154*). The course of this reaction is unknown. One might speculate that the process is the inverse of Fe_3S_4 cluster formation; viz., a sufficiently reduced cluster releases sulfide (to a suitable acceptor). The clusters $[MCu_3OS_3Cl_3]^{2-}$ (**39**, M = Mo, W) also have a voided core ligand position (*156–158*). Occupation of this subsite, as by chloride in $[MCu_3OS_3Cl(PPh_3)_3]$ (**40**, M = Mo, W) (*159*),

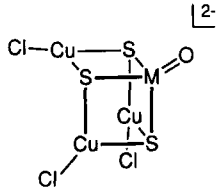

39

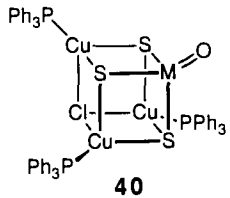

40

completes a distorted cubane framework. The Fe_4S_3 cluster core, with the fourth ligand subsite occupied by an element other than sulfur or selenium (*55*), has not been encountered.

IV. Heterometallic MFe_3S_4 Cubane-Type Clusters

A. Clusters of Synthetic Origin

The first clusters containing the cubane-type MFe_3S_4 core unit **41** were prepared in 1978. Double cubanes composed of two $MoFe_3S_4$ groups bridged through the molybdenum atoms by a sulfide atom and two thiolates, and by three thiolates, were obtained by my group (*160*) and by Christou *et al.* (*161, 162*), respectively. An extensive research

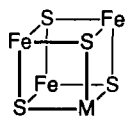

41

effort followed, which in this laboratory has resulted in the synthesis of bridged double cubanes and single cubanes with M = Mo, W, V, and Re, and, most recently, Co, Ni, and Nb. In the early development of the chemistry of these clusters, all examples contained either molybdenum or tungsten as the heterometal. The motivation for much of this work remains unchanged: clarification of the structure and other properties of the Fe–Mo cofactor of nitrogenase by the synthesis and characterization of suitable model clusters or, in the limit of unqualified success, the cofactor itself. With the recent demonstrations of vanadium-containing nitrogenases, pursuit of the Fe–V cofactor has become an equivalent challenge. Much of the extensive research through 1985 has been reviewed (*163–165*), at which time only the M = Mo and W clusters had been prepared. In the sections that follow, attention is restricted to recent developments, especially as related to synthesis, reactivity, and biological relevance. The considerable scope of the chemistry of synthetic MFe_3S_4 clusters is evident from Table V, which reveals that seven heterometals have thus far been incorporated in the cubane-type core units, each of which may exist in several oxidation levels.

1. Tetrathiometalates

The intensely colored tetrahedral d^0 species $[MS_4]^{z-}$ (*166*) are obligatory precursors to all heterometal cubanes with M = V, Nb, Mo, W, and Re synthesized by cluster self-assembly. Of these, $[VS_4]^{3-}$, $[MoS_4]^{2-}$, and $[WS_4]^{2-}$ were prepared before 1900 by the reaction of hydrogen sulfide with oxoanions in strongly alkaline solutions and were isolated as alkali metal or ammonium salts. $[ReS_4]^{1-}$ has been obtained similarly (*167*). Known tetrathiometalates and the dates of their initial preparations are summarized in Fig. 5. The foregoing salts of $[MoS_4]^{2-}$ and $[WS_4]^{2-}$ are water soluble; quaternary ammonium salts soluble in organic solvents are also available (*168*). The recently prepared compound $Li_3[VS_4] \cdot 2DMF$ (DMF is *N,N*-dimethylformamide) has the advantage in reaction chemistry of solubility in water and in dry anaerobic polar solvents such as DMF and Me_2SO (*169*).

The newest additions to the set of soluble tetrathiometalates are $[NbS_4]^{3-}$ and $[TaS_4]^{3-}$. These ions had been earlier recognized as components of certain intractable solids prepared by high-temperature methods (*170*). Low-temperature preparations have been hampered by the lack of suitable oxometalate precursors. Recently, the reaction given by Eq. (16) (M = Nb, Ta) in acetonitrile has been devised in this laboratory (*171*).

$$M(OEt)_5 + 4(Me_3Si)_2S + 3LiOMe \rightarrow Li_3[MS_4] + 5Me_3SiOEt + 3Me_3SiOMe \quad (16)$$

TABLE V

SCOPE OF $[MFe_3S_4]$ CLUSTER FORMATION[a]

Electron number[b]/spin S	Cluster
49 e^-/S = ?	**$[MoFe_3S_4]^{5+}$**
	$[WFe_3S_4]^{5+}$
50 e^-/S = ?	$[VFe_3S_4]^{3+}$
	$[NbFe_3S_4]^{3+}$
	$[MoFe_3S_4]^{4+}$
	$[WFe_3S_4]^{4+}$
51 e^-/S = $\frac{3}{2}$	**$[VFe_3S_4]^{2+}$**
	$[NbFe_3S_4]^{2+}$
	$[MoFe_3S_4]^{3+}$
	$[WFe_3S_4]^{3+}$
	$[ReFe_3S_4]^{4+}$
52 e^-/S = 2	$[VFe_3S_4]^{1+}$
	$[Fe_4S_4]^{4+}$
	$[MoFe_3S_4]^{2+}$
	$[WFe_3S_4]^{2+}$
	$[ReFe_3S_4]^{3+}$
53 e^-/S = $\frac{1}{2}$	**$^p[Fe_4S_4]^{3+}$**
	$[ReFe_3S_4]^{2+}$
54 e^-/S = 0	**$^p[Fe_4S_4]^{2+}$**
55 e^-/S = $\frac{1}{2}$, $\frac{3}{2}$	**$^p[Fe_4S_4]^{1+}$**
	$^p[CoFe_3S_4]^{2+}$
56 e^-/S = ?	$[Fe_4S_4]^0$
	$^p[CoFe_3S_4]^{1+}$
	$[NiFe_3S_4]^{2+}$
57 e^-/S = $\frac{3}{2}$	**$^p[NiFe_3S_4]^{1+}$**
58 e^-/S = ?	
59 e^-/S = $\frac{5}{2}$	$^p[ZnFe_3S_4]^{1+}$
	$^p[CdFe_3S_4]^{1+}$

[a] Boldface denotes an isolated cluster; p, protein-bound cluster; other clusters have been detected electrochemically.

[b] S, Six-electron donor.

After workup, the compounds $Li_3[MS_4] \cdot 2TMEDA$ (TMEDA is *N,N,N,'N'*-tetramethylethylenediamine) were isolated in ~60% yield. The compounds are isostructural and contain discrete tetrahedral $[MS_4]^{3-}$ ions. They are soluble and stable in polar solvents; the light yellow color of these solutions results from the occurrence of ligand to metal charge transfer (LMCT) bands below 400 nm rather than in the visible region as for the other tetrathiometalates. With the likely exceptions of chromium and manganese, it is possible that tetrathio-

SOLUBLE TETRATHIOMETALATES: $[M^zS_4]^{(8-z)-}$

Ti^{IV}	V^{V} 1890	Cr^{z}	Mn^{z}	
Zr^{IV}	Nb^{V} 1990	Mo^{VI} 1884	Tc^{VII}	Ru^{z}
Hf^{IV}	Ta^{V} 1990	W^{VI} 1886	Re^{VII} 1970	Os^{z}

FIG. 5. Elements of Groups IV–VIII that form tetrathiometalates and the dates of their original syntheses (white boxes); nearby elements, some of which might form $[MS_4]^{z-}$ species, are shown in shaded boxes. The case of Fe(III) is discussed in the text.

metalates of the other elements in Fig. 5 may be obtainable as soluble salts. Of these, $[TcS_4]^{2-/1-}$ appear to be the most readily achievable. Last, we take note of the compound Na_5FeS_4, synthesized from Na_2S, Fe, and S at 970 K (*172*). It contains discrete tetrahedral $[FeS_4]^{5-}$ ions, each of which is immersed in an environment of sodium ions, effectively reducing anion–anion repulsion and stabilizing the small, very highly charged anions. Although a tetrathiometalate by definition, $[FeS_4]^{5-}$ lacks the short bond distances associated with multiple bonding in d^0 $[MS_4]^{z-}$ species. It is too intensely nucleophilic to have any solution stability unless this property is modulated by association with cations such as Li^+ or Mg^{2+}. Li^+–anion interactions occur in the structures of $Li_3[MS_4] \cdot 2TMEDA$ and very probably in solutions of these compounds. Interactions of this sort would presumably be necessary to obtain stable solution species of the Group IV anions $[MS_4]^{4-}$. Any new $[MS_4]^{z-}$ species is a potential cluster precursor in the types of self-assembly systems to be considered next.

2. *[$MoFe_3S_4$] and [WFe_3S_4] Clusters*

Because the preparations and properties of these two cluster types are in general similar, with the main differences being more negative redox potentials and somewhat stronger terminal ligand binding of the tungsten clusters, we shall deal only with the molybdenum clusters.

In the original cluster self-assembly system in methanol shown in Fig. 6, three double-cubane clusters **42–44** were obtained (*163, 165, 173–175*). Cluster **42** is our original contribution to this field; because it is not easy to purify, its chemistry has been little developed. Triply thiolate-bridged cluster **43** can be readily obtained in high yield. It has been converted to the doubly reduced species **45**, which has been isolated and exists in the $[MoFe_3S_4]^{2+}$ state (*176*). The easily accessible

Fe(II,III)-bridged clusters **44** are principally important as forerunners of single cubanes. Reaction of the Fe(III) form with catecholates affords the doubly thiolate-bridged clusters **46** whose Mo–S–Fe links are readily cleaved in coordinating solvents to produce the solvated single

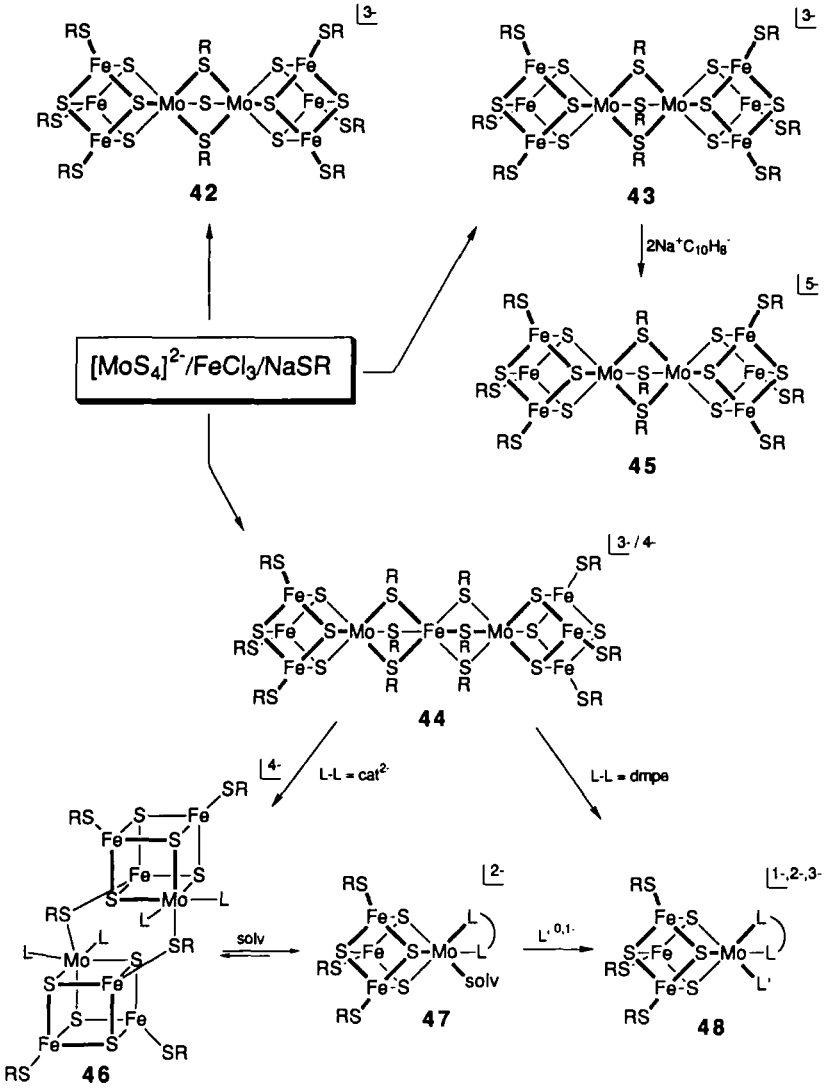

FIG. 6. The original $MoFe_3S_4$ cluster *self-assembly system yielding* triply bridged double cubanes **42** and **43** and the Fe(II,III)-bridged clusters **44** (*160, 173–175*). Also shown is the two-electron reduction of **43** to yield **45** and the reactions of **44** to give the doubly bridged double cubane **46** and the single cubanes **47** and **48** (*165*).

cubanes **47**. These react with neutral or anionic monodentate ligands to afford **48**, examples of which have been isolated (*165*). Single cubanes are also obtainable by cleavage of **44** with 1,2-bis(dimethylphosphino)-ethane (dmpe); product clusters **48** retain one thiolate ligand (L′ = RS^-) at the molybdenum site (*177*). Inclusion of Na_2S_2 in the assembly system results in the reaction given by Eq. (17), which produces the

$$2[MoS_4]^{2-} + 6FeCl_3 + 14RS^- + 2S_2^{2-} \rightarrow [Mo_2Fe_6S_8(S_2)_2(SR)_6]^{4-} + 4RSSR + 18Cl^- \quad (17)$$

persulfide-bridged double cubane **49** (R = p-C_6H_5Cl) in low yield together with an appreciable quantity of $[Fe_4S_4(S\text{-}p\text{-}C_6H_4Cl)_4]^{2-}$, which is separated by fractional crystallization (*178*).[4] The unsymmetrical $Mo_2(\eta^4\text{-}\mu_2\text{-}S_2)_2$ bridge structure is precedented. Cluster **49** offers a num-

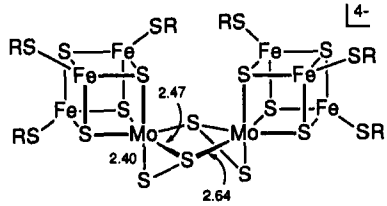

49

ber of intriguing reaction possibilities, including reductive cleavage of the persulfide bridges with low-valent metal compounds to afford modified single cubanes with external metal bridges $Mo(\mu_2\text{-}S)_2M$. These cluster assembly systems are conducted with exact stoichiometries (or with nonstoichiometric mole ratios constituting a redox buffer) that afford the $[MoFe_3S_4]^{3+}$ oxidation state. Bridged clusters and single cubanes can be reduced [usually at <1 V versus a saturated calomel electrode (SCE)] and several have been oxidized, thereby encompassing the $[MoFe_3S_4]^{4+/3+/2+}$ oxidation levels in Table V.

Since the foregoing developments, several other valuable results in cluster synthesis have been reported. One double cubane (**43**) has been assembled in aqueous solution by means of the reaction given by Eq. (18); the *in situ* yield exceeds 80% (*179*). The same cluster can also be

$$2[MoS_4]^{2-} + 6Fe^{2+} + 11HOCH_2CH_2S^- \rightarrow [Mo_2Fe_6S_8(SCH_2CH_2OH)_9]^{3-} + (SCH_2CH_2OH)_2 \quad (18)$$

[4] In more recent work in this laboratory, the yield of $(Et_4N)_4$ [**49**] in Eq. (17) has been increased from 11 to 35%.

formed from $[MoO_4]^{2-}$ and $FeCl_2$ in the presence of a dithiol, $S_2O_3^{2-}$, and the enzyme rhodanese. The latter three components separately generate hydrosulfide, which may react with molybdate to produce thiomolybdates prior to cluster formation; however, the immediate source of the sulfide incorporated into the cluster has not been identified.

The anaerobic reaction system given by Eq. (19) in DMF affords in one operation the single cubanes **50** (M = Mo, W) in moderate yields

$$[MS_4]^{2-} + 3FeCl_2 + 6\text{–}9Na(R_2dtc) \rightarrow [MFe_3S_4(R_2dtc)_5]^{0/1-} \qquad (19)$$

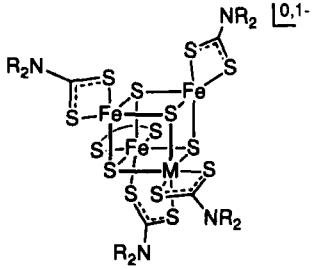

50

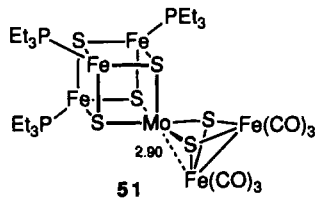

51

(*180–183*). Although the system subsumes the stoichiometry required for formation of $[MFe_3S_4(R_2dtc)_5]^{1-}$ (dtc is dithiocarbamate), this is not the case for the neutral cluster, whose $[MFe_3S_4]^{5+}$ state is one electron more oxidized than the apparent stoichiometry permits. The source of the additional oxidizing equivalent is unclear. Owing to very similar six-coordinate geometries at the iron and heterometal subsites on the same core face, clusters exhibit a twofold disorder in the crystalline state. Consequently, a precise metric comparison in the two oxidation states is lacking. However, it is clear that the reduced cluster has slightly increased dimensions and, from Mössbauer spectroscopic data, the larger ^{57}Fe isomer shift indicates that the added electron is associated mainly with the iron atoms (*183*). The clusters **50** have several notable properties. Their single-cubane structure is assembled directly, without the necessity of prior cleavage of a double cubane. The tendency of dithiocarbamates to stabilize higher oxidation states is reflected in the occurrence of the $[MFe_3S_4]^{4+/5+}$ states in isolated compounds. These have not been stabilized in isolated MFe_3S_4 clusters (M = Mo, W) with any other terminal ligands; their ground state spins have not been reported and would be of much interest. A cluster formulated as $[MoFe_3S_4(Me_2dtc)_6]$ has been claimed (*183*). Because its structure has not been demonstrated, its apparent core oxidation state is not included

in Table V. The ease of synthesis of these single cubanes may be offset, in reactivity studies at the heterometal subsite, by the potential difficulty of removing dithiocarbamate ligands with retention of the core structure.

Cluster **51** contains the features, unique to $MoFe_3S_4$ clusters, of terminal phosphine ligands at the iron subsites and bidentate coordination of $[Fe_2S_2(CO)_6]^{2-}$ at the molybdenum subsite with an accompanying weak Mo–Fe interaction at 2.90 Å (*184*). It was prepared by the reaction of $[MoFe_5S_6(CO)_6I_3]^{2-}$ with three equivalents of triethyl phosphine (PEt_3) in acetonitrile solution. The structure of the precursor may be inferred from that of **51**, but in the process of ligand substitution its $[MoFe_3S_4]^{3+}$ oxidation state was reduced by one electron. These species are members of a set of Mo–Fe–S–CO clusters prepared by Averill and co-workers as "potential precursors to models for the FeMo-cofactor of nitrogenase" (*185*).

Last, we note the occurrence of the reaction given by Eq. (20) (*186*). Here, linear trinuclear **5** is caused to rearrange to cuboidal **4**, ligating the $Mo(CO)_3$ fragment to form the product **52**, whose average bond

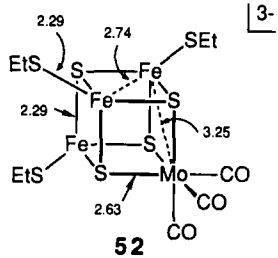

52

lengths are indicated. Although disulfide formation was not proved,

$$[Fe_3S_4(SEt)_4]^{3-} + Mo(CO)_3(MeCN)_3 \rightarrow [MoFe_3S_4(SEt)_3(CO)_3]^{3-} + \tfrac{1}{2}EtSSEt \qquad (20)$$

isomer shifts and the terminal Fe—SR bond distance are entirely consistent with a one-electron reduction of the Fe_3S_4 fragment. Compared to $[Fe_4S_4(SR)_4]^{2-}$ clusters (*1*), bond distances within this fragment are normal. However, the cluster displays a trigonal elongation that is evident in the very long Mo—S and Mo—Fe distances; in the $[MoFe_3S_4]^{3+}$ clusters of Fig. 6, these occur in the ranges 2.3–2.4 and 2.7–2.8 Å, respectively (*165*). These ranges largely apply to more oxidized and reduced clusters as well. Consequently, the molybdenum atom is not tightly integrated into the $MoFe_3S_4$ "core," and **52** is appropriately considered as a complex between the cuboidal $[Fe_3S_4]^0$ fragment and the Lewis acidic $Mo(CO)_3$ group. As will be seen, Eq. (20) is

representative of a transformation of more general consequence wherein **5** is induced to rearrange to cuboidal **4**, which captures a heterometal. The first indication of this rearrangement was found with the homometallic reaction given by Eq. (21), which resulted in a 63% isolated yield of the tetranuclear product (*41*). Although rupture

$$[Fe_3S_4(SEt)_4]^{3-} + FeCl_2 + EtS^- \rightarrow [Fe_4S_4(SEt)_4]^{2-} + \tfrac{1}{2}EtSSEt + 2Cl^- \quad (21)$$

of the Fe_3S_4 fragment of **5** has not been eliminated, the implication of both reactions is that fragment reduction in the presence of a suitable metal drives the rearrangement to the cuboidal form, which is immediately stabilized by metal binding.

3. *[VFe_3S_4] and [$NbFe_3S_4$] Clusters*

The first vanadium-containing cluster, $[VFe_3S_4Cl_3(DMF)_3]^{1-}$ (**55**), was reported in 1986 (*187*). It and related clusters are set out in Fig. 7. The cluster formation reaction given by Eq. (22) in DMF solution proceeds in two detectable stages. In the first, the linear trinuclear cluster **53** is formed; this has been isolated (*188*). This species then reacts with an additional equivalent of $FeCl_2$ to produce an as-yet undetected intermediate with the proposed structure **54** [Eq. (22)]. The second stage likely involves intermolecular electron transfer, causing reduction below the V(V) state and electron redistribution within the core. Core conversion steps are summarized in the sequence given in Eq. (23). The six-coordinate stereochemical preference of reduced vanadium is considered to drive the rearrangement of **54** to the cubane-type structure **55**. This is an exceptional means of closing a metal cluster polyhedron. Isomer shifts and structural results for **55** imply that the hetero-

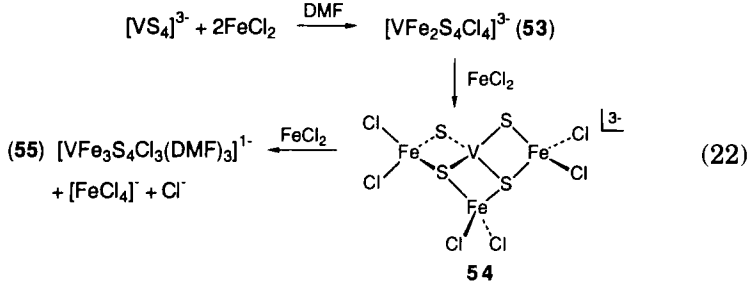

(22)

$$[VFe_2S_4]^{1+} + Fe^{2+} \longrightarrow [VFe_3S_4]^{3+} \xrightarrow{e^-} [VFe_3S_4]^{2+} \quad (23)$$

metal oxidation state does not exceed V^{3+} and that the iron oxidation state is near $Fe^{2.5+}$ (*189*). The latter allows the formalisms V^{3+} +

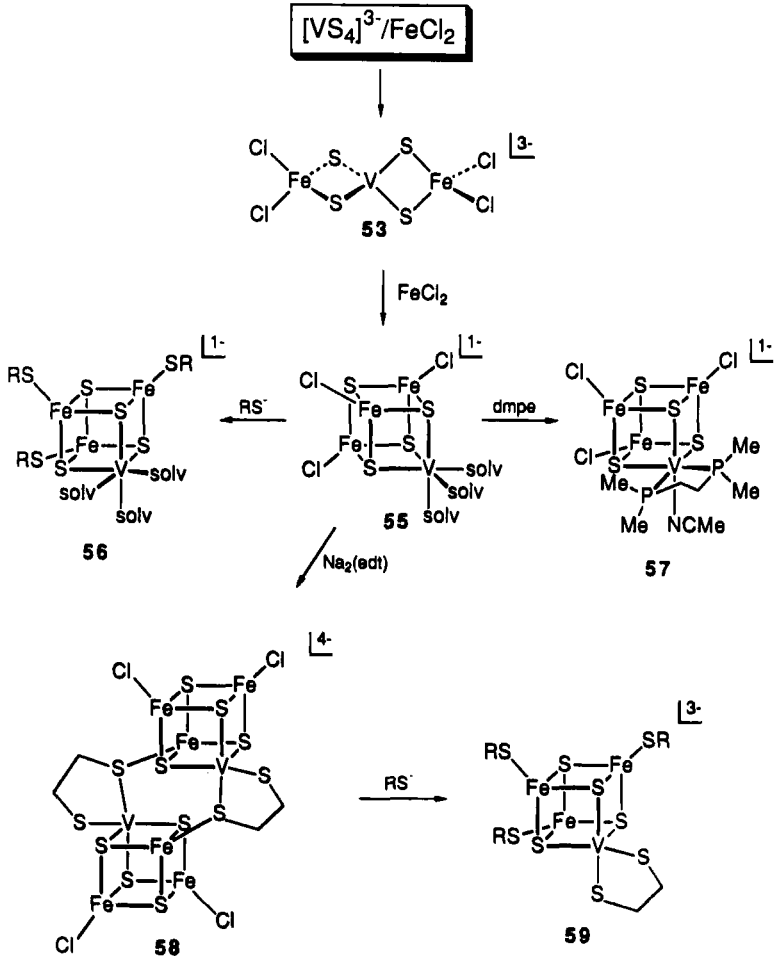

FIG. 7. The VFe_3S_4 cluster self-assembly system showing the trinuclear intermediate **53**, its conversion to cubane cluster **55**, and ligand substitution reactions of **55** at the vanadium and iron subsites (*190*).

$[Fe_3S_4]^{1-}$ and V^{2+} + $[Fe_3S_4]^0$. In the reactivity studies summarized next, a variety of clusters in the $[VFe_3S_4]^{2+}$ oxidation state have been prepared. There is only one example of a chemically reversible reduction to the $[VFe_3S_4]^{1+}$ state, but several clusters are reversibly oxidized to the $[VFe_3S_4]^{3+}$ state. Clusters in these two oxidation states have not been isolated. The three states are included in Table V, but the cluster spin state has been proved only for $[VFe_3S_4]^{2+}$ (*189*).

The key species in the reaction chemistry of VFe_3S_4 clusters is **55**. The original preparation of the Me_4N^+ salt (*190*) has been improved, and the compound is readily obtainable in ~60% yield (*44*). It is stable in the coordinating solvents DMF and Me_2SO, and acetonitrile, although in Me_2SO a very slow conversion to **53** has been observed (*190*). The order of binding affinity at the vanadium subsite is MeCN < DMF < Me_2SO. Owing to labile ligands at both the vanadium and iron subsites, the cluster undergoes a variety of substitution reactions and offers an opportunity to examine relative reactivities at the two subsites. Some of these reactions (*190*) are summarized in Fig. 7. Thiolate reacts preferentially at the iron subsites to afford **56**; an excess causes core breakdown. *p*-Cresolate also binds preferentially at the iron subsites. Phosphines, including dmpe (**57**), react at the vanadium subsite; 2,2-bipyridyl (bpy) behaves similarly. In acetonitrile solution, edt binds at both the vanadium and iron subsites to yield the double cubane **58**, whose V–S–Fe doubly bridged structure is analogous to **46** (Fig. 6). Unlike the latter, **58** is not cleaved by solvent in Me_2SO solution, but chloride substitution by *p*-tolylthiolate results in the generation of **59**. Similarly, reaction with *p*-tolylthiol in Me_2SO gave the solvated cluster with mixed chloride/thiolate terminal ligation. The structures of **53**, **55**, **57**, **58**, and $[VFe_3S_4Cl_3(bpy)(DMF)]^{1-}$ have been proved by X-ray diffraction (*190*).

Competitive reactivity at the two types of subsites can be altered by cluster insertion into the semirigid cavitand ligand **6** (Fig. 1). The reaction given by Eq. (24) affords cluster **60** in 87% isolated yield (*44*).

$$[VFe_3S_4Cl_3(DMF)_3]^{1-} + L(SH)_3 + 3NaSEt \rightarrow [VFe_3S_4(LS_3)(DMF)_3]^{1-} + 3EtSH + 3NaCl \quad (24)$$

The intrinsic subsite differentiation by the heterometal is reinforced by the ligand, which directs substrate reactivity to the vanadium subsite. One cluster prepared in this way is $[VFe_3S_4(LS_3)(HB(pz)_3)]^{2-}$ [$HB(pz)_3$ is hydrotris(pyrazolyl)borate(1−)], which undergoes chemically reversible oxidation and reduction at $E_{1/2} = -0.37$ and -1.52 V, respectively, thereby demonstrating the existence of the three oxidation levels in Table V with a single cluster. In another application, **60** in Me_2SO solution reacts with cyanide in stepwise equilibria, forming as the final product the stable cluster $[VFe_3S_4(LS_3)(CN)_3]^{4-}$. In contrast, **55** and **56** are decomposed by three equivalents of cyanide.

Despite its trisolvated condition, the vanadium subsites in **55** and **60** are not especially reactive. Of other ligands tested, cresolate and azide bind weakly and incompletely when present in excess. A variety of

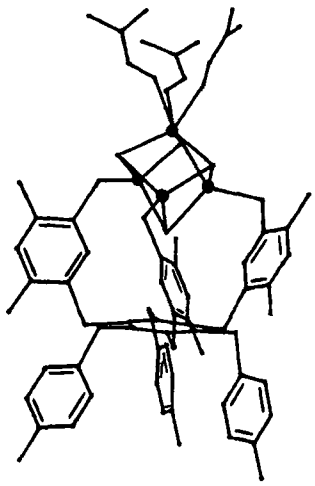

60

anionic and neutral ligands such as halide, SCN^-, pyridine, imidazole, aliphatic amines, and NH_3, when present in large excess, are bound slightly or not at all. In comparison, the monosolvated molybdenum site in cluster **47** binds a much wider variety of ligands, including R_3P, RS^-, RO^-, CN^-, N_3^-, hydrazines, amines, and ammonia (*165*). The corresponding tungsten cluster behaves similarly. None of these clusters has been shown to bind dinitrogen. However, as seen later, they are meaningful structural models of the vanadium and molybdenum sites in nitrogenases.

With the recent access to $[NbS_4]^{3-}$ and $[TaS_4]^{3-}$, the chemistry of the corresponding MFe_3S_4 clusters can now be explored. At this writing, experimentation is in an early stage. Several results are summarized in Fig. 8. Cluster **61** and $[TaFe_2S_4Cl_4]^{3-}$ have been prepared from $[MS_4]^{3-}$ and $FeCl_2$ in acetonitrile and were shown to be isostructural with the vanadium cluster **53** by X-ray analysis (*171*). In a self-assembly system, **61** and the strong reductant $[Fe(SEt)_4]^{2-}$ yield the triply thiolate-bridged double cubane **62**, which is isostructural with the $MoFe_3S_4$ cluster **43** (R = Et). Cluster **62** is reducible in two chemically reversible one-electron steps, thereby demonstrating the existence of the two oxidation levels in Table V. It remains to be seen if $[TaS_4]^{3-}$ is reducible and analogously reactive in a cluster self-assembly system.

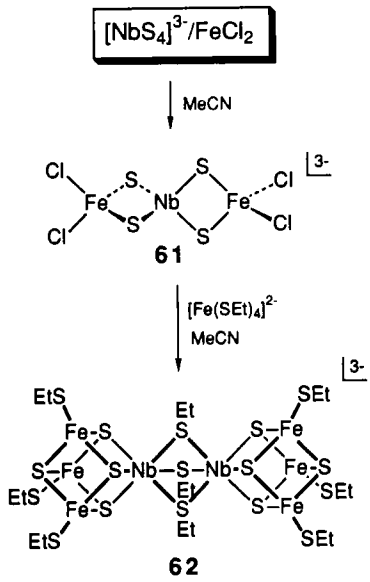

FIG. 8. The $NbFe_3S_4$ cluster self-assembly system showing the trinuclear cluster **61** (*171*) and the formation of the triply bridged double cubane **62**.

4. *[$ReFe_3S_4$] Clusters*

The self-assembly system in Fig. 9 produces the triply thiolate-bridged double-cubane trianion **63** and a mixture of the Fe(II)-bridged double cubanes **65** and **66** (*191, 192*). The outcome of the assembly reaction is sensitive to temperature and reactant mole ratios. Manipulation of these factors has led to the preparation of the individual clusters in yields in excess of ~70%. Cluster **63**, containing two $[ReFe_3S_4]^{3+}$ cores, undergoes a two-electron oxidation to **64**, with two $[ReFe_3S_4]^{4+}$ cores. Structural, magnetic, and spectroscopic evidence establishes the presence of Fe(II) in the bridge units of **65** and **66**, which therefore contain the +3 and +4 cores, respectively. Reaction of **66** with dmpe effects bridge cleavage and apparent core reduction by thiolate to form the single cubane **67** with the $[ReFe_3S_4]^{3+}$ oxidation state (*193*). This cluster undergoes reversible one-electron oxidation and reduction at −0.31 and −1.18 V, respectively. This result and the redox reactions of the double cubanes demonstrate the three oxidation states

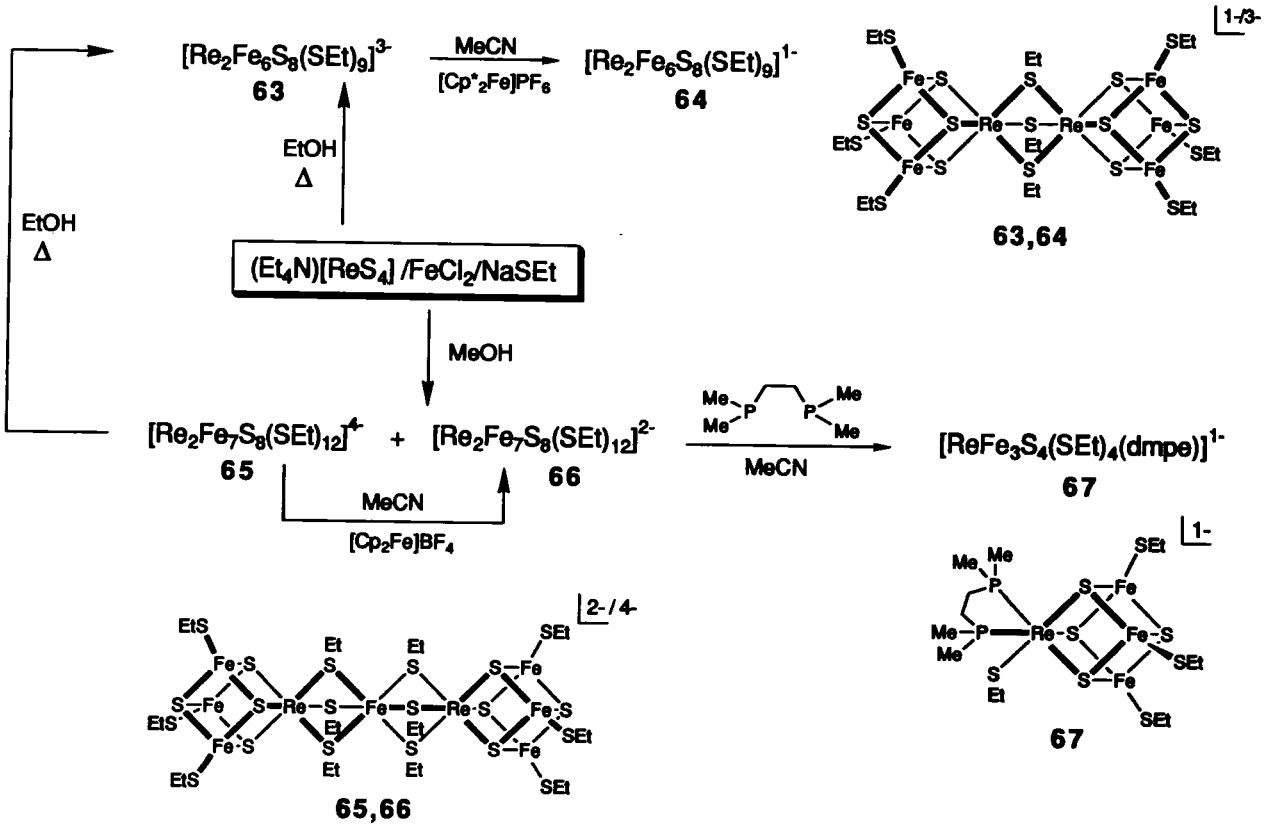

FIG. 9. The $ReFe_3S_4$ cluster self-assembly system showing the triply bridged double cubane **63** and the Fe(II)-bridged double cubanes **65** and **66**. Also shown is the two-electron oxidation of **63** to **64** and cleavage of **66** to give the single cubane **67** (*191–193*).

entered in Table V; the ground state spin has not been demonstrated for $[ReFe_3S_4]^{2+}$.

Cluster **63** exhibits the five-member electron transfer series, Eq. (25), with overall charge $z = -1$ to -5 and the indicated $E_{1/2}$ values. It encompasses the $[ReFe_3S_4]^{4+/3+/2+}$ oxidation levels with 51–53 e^-. Species of intermediate charge can be generated by comproportion reactions (26). With attainment of the 52-e^- level in [3−], the individual cubanes become much more difficult to reduce and the potentials are shifted in the negative direction by 1 V or more. Clusters **65** and **66** are part of the four-member series [Eq. (27)]. These series are analogous to

$$\mathbf{63}:\ z = [1-] \overset{-0.29}{\rightleftharpoons} [2-] \overset{-0.44}{\rightleftharpoons} [3-] \overset{-1.40}{\rightleftharpoons} [4-] \overset{-1.65}{\rightleftharpoons} [5-] \quad (25)$$

$$[1-] + [3-] \rightleftharpoons 2[2-] \qquad [3-] + [5-] \rightleftharpoons 2[4-] \quad (26)$$
$$K_{com} = 10^{3.4} \qquad K_{com} = 10^{4.1}$$

$$\mathbf{65}:\ z = [1-] \overset{-0.09}{\rightleftharpoons} [2-] \overset{-0.58}{\rightleftharpoons} [3-] \overset{-0.72}{\rightleftharpoons} [4-] \quad (27)$$

those for $[M_2Fe_6S_8(SEt)_9]^{3-}$ and $[M_2Fe_7S_8(SEt)_{12}]^{3-}$ (M = Mo, W) (*163, 165, 174*). Potential differences of successive steps are essentially independent of M, and are relatively large (200–250 mV), showing that electron transfer reactions of individual cubanes are coupled. Potentials for the reduction of isoelectronic clusters with M = Mo and W generally differ by ≲100 mV, but those for the reductions of the 51-e^- cores in $[Mo_2Fe_6S_8(SEt)_9]^{3-/4-}$ are ~1 V more negative than those for $[Re_2Fe_6S_8(SEt)_9]^{1-/2-}$, primarily because of the larger negative charge of the molybdenum clusters. In the series given by Eq. (27), the first step, at −0.09 V, is reduction of bridge Fe(III) to Fe(II). However, the potential for this step is sufficiently close to that of an irreversible multielectron process near 0 V that it is doubtful if the Fe(III)-bridged cluster can be prepared. Succeeding steps result in subcluster reductions, for which the potential difference (140 mV) is smaller than in the series given by Eq. (25) because of the greater separation of subclusters. However, this difference is considerably larger than that (<100 mV) in the $[M^{III}_2Fe_7S_8(SEt)_{12}]^{4-/5-/6-}$ (M = Mo, W) series, presumably because of the larger incremental increase in cluster negative charge upon reduction.

5. *Stability Patterns*

Because all other MFe_3S_4 clusters are not prepared by assembly methods based on $[MS_4]^{z-}$ and involve the later transition metals, it

is useful at this point to summarize the scope of cluster formation and stability thus far. From the results of four self-assembly systems containing $[MS_4]^{z-}$, $FeCl_3$ or $FeCl_2$, and RS^-, the pattern of stable heterometal cubanes has emerged. Systems with M = Nb, Mo, W, and Re form the triply thiolate-bridged double cubanes $[M_2Fe_6S_8(SR)_9]^{3-}$ (**42**, **62**, and **63**), the most widely distributed cluster structural type. Systems with M = Mo, W, and Re form the Fe(II)-bridged double cubanes $[M_2Fe_7S_8(SR)_{12}]^{4-}$ (**44** and **65**) and the Fe(III)-bridged species $[M_2Fe_7S_8(SR)_{12}]^{3-}$ (**44**). The latter has not been isolated with M = Re. The lack of vanadium double cubanes of these types may simply be a consequence of the absence of thiolate in the assembly system (Fig. 7). However, solvated clusters such as **56** have shown little affinity for binding monofunctional thiolates at the vanadium subsite. Double cubanes with two M–S(R)–Fe bridges have been obtained with M = V, Mo, and W (**46** and **58**) and may be cleaved to single cubanes (**47**, **48**, and **59**). Similarly, Fe(II,III) bridges of double cubanes may be severed with dmpe to afford single cubanes in which the metal retains a thiolate ligand (**48** and **67**). Single cubanes (MFe_3S_4) can be assembled directly with M = V (**55**), but thus far with M = Mo and W only in the presence of dithiocarbamates (**50**).

Clusters with the foregoing heterometals exhibit a stability plateau at 49–53 e^-, especially at 51 e^- (Table V). Based on the broken symmetry MS-Xα calculation of $[MoFe_3S_4(SH)_6]^{3-}$ by Cook and Karplus (*194*), the highest occupied orbitals, at least for $[MoFe_3S_4]^{3+/2+}$ species, are mainly antibonding core Fe–S in character. It may be anticipated that the cluster types encountered with M = Mo, W, and Re can be prepared with M = Nb and, possibly, Ta. The present results certainly imply stability of $TcFe_3S_4$ clusters. In view of the unlikely existence of tetrathiometalates of chromium and manganese, their heterometal clusters will have to be obtained by different routes. For the same reason, this is the case for the synthetic nickel and cobalt clusters, which are considered next. Research on these cluster types is at an early stage.

6. *[$NiFe_3S_4$] Clusters*

The reaction given by Eq. (28) in Fig. 10 affords in the same system the two clusters **68** and **69** in ~40% yield each as Et_4N^+ salts (*195*). The corresponding clusters $[NiFe_3Se_4(SEt)_3(PPh_3)]^{2-}$ and $[NiFe_3Se_4(SEt)_4]^{3-}$ have been prepared in an analogous manner. The reactions involve reductive rearrangement of the linear cluster precursors by interaction with Ni(0), which may be considered to form a persistent inner sphere complex concomitant with the formal electron transfer $[Fe_3S_4]^{1+} + Ni(0) \rightarrow [Fe_3S_4]^{1-}$ and Ni^{2+}. Thus these processes bear a relation to Eq. (20), but there the apparent reducing equivalent derives

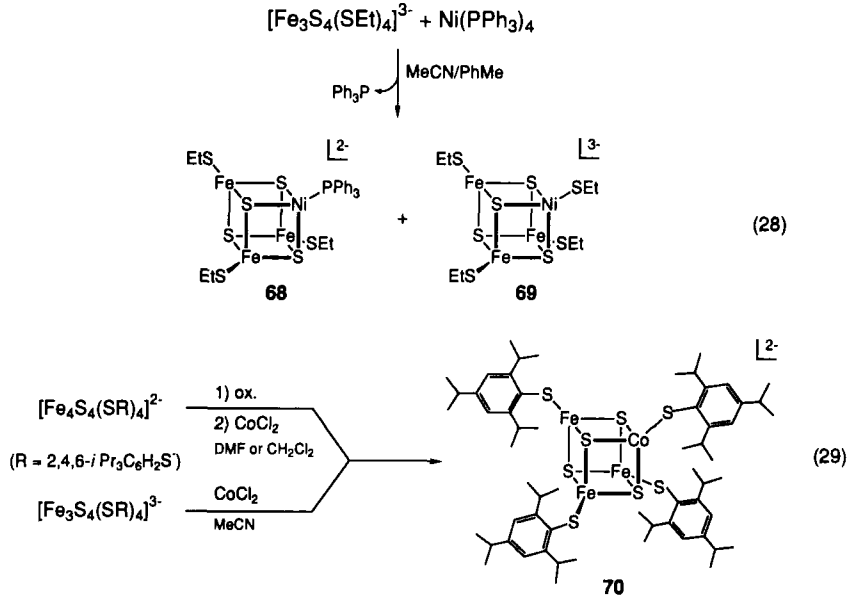

FIG. 10. Reactions [Eqs. (28) and (29)] resulting in the formation of the $[NiFe_3S_4]$ clusters **68** and **69** (*195*) and the $[CoFe_3S_4]$ cluster **70** (*197*).

from a coordinated ligand and not a low-valent metal. In the reaction workup, **69** is obtained as an inseparable mixture with $[Fe_4S_4(SEt)_4]^{3-}$. The cubane-type structure of **68** has been demonstrated by X-ray diffraction, as has that of **69** in a disordered single crystal also containing $[Fe_4S_4(SEt)_4]^{3-}$. Pure cluster **69** may be prepared by treatment of **68** with excess thiolate, and is likely formed in the reaction mixture by the same process.

The core unit in **68** and **69** is $[NiFe_3S_4]^{1+}$, whose $S = \frac{3}{2}$ ground state has been demonstrated from its low-temperature Curie paramagnetism and EPR spectrum. Magnetically perturbed Mössbauer spectra can be satisfactorily fit with this spin (*195*). Access to **69** permits the first comparison of redox potentials of (nonisoelectronic) Fe_4S_4 and MFe_3S_4 clusters with identical overall charges and terminal ligands. The effect of nickel as a heterometal is considerable, and provides a relative stability to the reduced form; thus, for the $[NiFe_3S_4]^{2+/1+}$ couple of **69**, $E_{1/2} = -0.95$ V, whereas $E_{1/2} = -1.26$ V for the $[Fe_4S_4]^{2+/1+}$ couple of $[Fe_4S_4(SEt)_4]^{2-/3-}$. These oxidation states are included in Table V. The phosphine ligand in **68** is replaceable in substitution reactions that usually afford some $[Fe_4S_4(SEt)_4]^{2-/3-}$ by-product, which is readily detected when reactions are monitored by ^1H NMR. Clusters containing CN^-, RNC, and RS^- ligands at the unique site have been detected

in this way. The reaction chemistry of **68** and **69** is currently under investigation in this laboratory.

7. *[$CoFe_3S_4$] Clusters*

The first indication that cobalt could be integrated into a cubane cluster of the Fe_4S_4 type was obtained when a small amount of $CoCl_2$ was added to the cluster assembly reaction mixture that forms $[Fe_4S_4(SPh)_4]^{2-}$ (*196*). This resulted in a cobalt-doped preparation of $(Bu_4N)_2[Fe_4S_4(SPh)_4]$, whose EPR spectrum is indicative of the $[CoFe_3S_4]^{2+}$ core with $S = \frac{1}{2}$. More recently, this cluster type has been directly prepared by Jordanov and co-workers (*197*) using the two reactions of Eq. (29) in Fig. 10. One method is based on controlled aerobic oxidation of $[Fe_4S_4(tibt)_4]^{2-}$ [tibt is 2,4,6-tris(isopropyl)benzenethiolate(1−)]. Presumably the first event is oxidation to the known species $[Fe_4S_4(tibt)_4]^{1-}$, which is the only $[Fe_4S_4]^{3+}$ cluster as yet isolated and is of known structure (*198*). This is followed by appearance of Fe^{3+} (detected by EPR and possibly arising from Fe^{2+} that dissociated from the cluster) and another species with $g = 2.022$, a value similar to those of protein-bound $[Fe_3S_4]^{1+}$ clusters (*68*). Treatment of this solution with anhydrous $CoCl_2$ followed by the admission of air affords a species with an EPR spectrum, including eight hyperfine lines from ^{59}Co ($I = \frac{7}{2}$), described as strikingly similar to the cobalt-doped cluster above. Although the sequence of redox events is not clear, the formation of $[CoFe_3S_4]^{2+}$ in the form of cluster **70** is apparent.

A second preparative route utilizes the linear cluster $[Fe_3S_4(tibt)_4]^{3-}$ and Co(II) under anaerobic conditions and results in same product, isolated as black $(Et_4N)_2[CoFe_3S_4(tibt)_4]$ (*197*). This reaction, described as quantitative, is easily rationalized if one thiolate ligand functions as a reductant. In this case, the transformation is closely analogous to the reactions given by Eqs. (20) and (21). As yet, the cubane structure of **70** has not been verified by X-ray diffraction. Magnetization measurements indicate an $S = \frac{1}{2}$ ground state for $[CoFe_3S_4]^{2+}$. Potentials for the $[CoFe_3S_4(tibt)_4]^{2-/3-}$ and $[Fe_4S_4(tibt)_4]^{2-/3-}$ couples are -1.09 and -1.21 V, respectively, again indicating that the heterometal provides a relative stabilization of the reduced form, here $[CoFeS_4]^{1+}$. Cluster oxidation states are listed in Table V.

B. Protein Bound Clusters

With the $[Fe_3S_4] \rightarrow [Fe_4S_4]$ cluster conversion reaction (Table II) having been demonstrated, Moura *et al.* (*199*) recognized the possibility

of introducing a heterometal atom into protein-bound cluster 4. This was accomplished in 1986 by the formation of the $CoFe_3S_4$ unit in *D. gigas* Fd II. Subsequently, the clusters MFe_3S_4 with M = Zn and Cd have been formed in this protein (*100, 200*) and in *D. africanus* Fd III (*255*). Typically, these clusters are formed by incubating the dithionite-reduced protein in aqueous buffer with a large excess of an M^{2+} salt in the presence of dithiothreitol. After purification, the proteins have been inspected by Mössbauer and EPR spectroscopies, by which means ground spin states and effective oxidation states of the Fe_3S_4 portions of the clusters have been determined. Formation of protein-bound clusters is described schematically in Fig. 11. As was anticipated in Eq. (11), the protein must be reduced to the $[Fe_3S_4]^0$ state before binding of M^{2+} can occur. However, the relatively soft ion Tl^+ will bind to both oxidation states $[Fe_3S_4]^{1+/0}$ (*256*), and is the only ion thus far shown to do so. Binding of Tl^+ to $[Fe_3S_4]^{1+}$ is described as weak; it is substantially stronger with $[Fe_3S_4]^0$ inasmuch as Fe^{2+} coordination to this oxidation state is inhibited. It may be anticipated that in proteins or synthetic

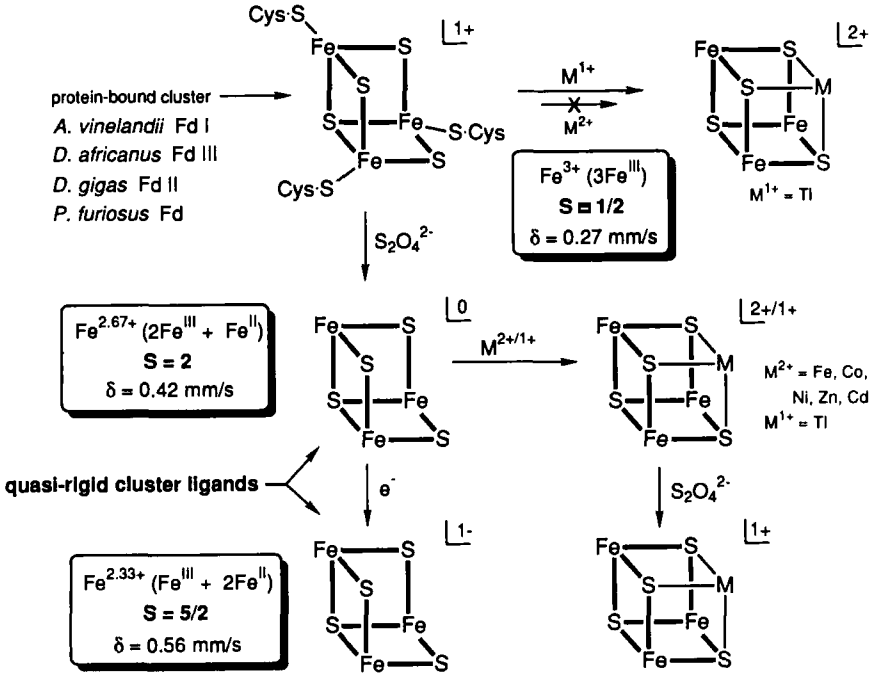

FIG. 11. Schematic depiction of protein-bound $[Fe_3S_4]$ cluster oxidation levels and the formation of heterometal $[MFe_3S_4]$ clusters by the reactions of the indicated Fd proteins with Co^{2+}, Ni^{2+}, Zn^{2+}, Cd^{2+}, and Tl^{1+} under reducing conditions (*101, 199–201, 255, 256*).

clusters, soft thiophilic metals such as Cu^+, Ag^+, and $Hg^{2+,+}$ will also bind to $[Fe_3S_4]^{1+}$.

Mössbauer parameters and oxidation and spin states for protein-bound Fe_3S_4 and MFe_3S_4 clusters are presented in Table III. It is immediately evident that the isomer shifts of $[Fe_3S_4]^{1+,0}$ clusters are practically independent of protein, and therefore are intrinsic values. The cobalt cluster was obtained in two oxidation states, while the zinc and cadmium clusters were detected in the fully reduced condition. Given these results, it is reasonable to assume that in these and other cases the $[MFe_3S_4]^{2+}$ cluster was formed first and then reduced to $[MFe_3S_4]^{1+}$ by excess dithionite (Fig. 11).

In protein-bound $[CoFe_3S_4]^{2+}$ and cluster **70**, the Fe^{3+} subsite (doublet A) and the delocalized pair (doublets B,B′) of the $[Fe_3S_4]^0$ fragment (Fig. 3) are preserved. Upon reduction, the added charge mainly reduces the Fe^{3+} subsite, such that the three iron atoms become virtually indistinguishable. In the zinc cluster the subsite with $\delta = 0.62$ mm/sec and the large quadrupole splitting (doublet A) contains Fe^{2+}, and the two smaller isomer shifts are associated with the delocalized pair. The same applies to the cadmium cluster, but details have not been published (*200*). Cluster **21**, although not heterometallic, is included in Table III because its low-spin $Fe^{II}(RNC)_3$ subsite is spin isolated from the $[Fe_3S_4]^0$ fragment and thus it behaves like Zn^{2+}. Here also the Fe^{3+} subsite and the delocalized pair are preserved. This is not the case with nickel cluster **68**, whose Mössbauer spectra can be fit by assuming delocalization over all three iron subsites. The reason for the difference in delocalization properties between $[CoFe_3S_4]^{2+}$ and $[NiFe_3S_4]^{1+}$ clusters is presently unclear.

The structure of no protein-bound MFe_3S_4 cluster has been determined by X-ray methods. However, the similarities in EPR spectra and the same ground spin state ensure that the protein-bound nickel cluster and **68** are isoelectronic, and that the nickel atom is tightly integrated into essentially isostructural cubane-type clusters. An agreeable assumption is that this structure applies to the other protein-bound clusters in Table III.

C. The Fe_3S_4 Cluster as a Ligand and Cluster Spin

Whether functioning as such in the metal-binding reaction in Fig. 11 or being built up around a metal atom in cluster self-assembly, the Fe_3S_4 fragment of an MFe_3S_4 cluster is a conceptual ligand of heterometal M. Collected in Table VI are the main structural features of single-cubane clusters with M = V, Mo, Re, and Ni. The Fe–Fe and

TABLE VI

COMPARATIVE STRUCTURAL PROPERTIES OF MFe_3S_4 (M = V, Mo, Re, Ni) SYNTHETIC SINGLE CUBANES AND PROTEIN-BOUND $[Fe_3S_4]^{1+}$ CUBOIDAL CLUSTERS[a]

Cluster	M . . . Fe	M–S	Fe . . . Fe	Fe–S	M–P	M–SR	Fe–SR	Ref.
$[VFe_3S_4Cl_3(dmpe)(MeCN)]^{1-}$ (**57**)	2.72(2)	2.32(6)	2.72(5)	2.28(2)	2.500(6)	—	—	*190*
$[MoFe_3S_4(SEt)_4(dmpe)]^{1-b}$ (**48**)	2.75(3) 2.72(1)	2.37(2) 2.37(2)	2.71(1) 2.726(8)	2.26(2) 2.27(2)	2.502(5) 2.59(3)	2.486(8) 2.566(8)	2.25(1) 2.25(2)	*177*
$[ReFe_3S_4(SEt)_4(dmpe)]^{1-b}$ (**67**)	2.79(1) 2.758(7)	2.389(6) 2.36(2)	2.72(3) 2.72(1)	2.26(3) 2.27(1)	2.413(7) 2.492(3)	2.418(1) 2.536(1)	2.254(2) 2.24(1)	*193*
$[NiFe_3S_4(SEt)_3(PPh_3)]^{2-}$ (**68**)	2.69(2)	2.262(6)	2.75(2)	2.29(2)	2.174(6)	—	2.283(6)	*195*
$[Fe_3S_4]^{1+}$ *D. gigas* Fd II[c]	—	—	2.75 2.72–2.77[d]	2.27 2.22–2.32[d]	—	—	2.24 2.16–2.30[d]	*35*
$[Fe_3S_4]^{1+}$ aconitase[e]	—	—	2.69 2.64–2.73[d]	2.30 2.25–2.35[d]	—	—	2.32 2.28–2.34[d]	*10*

[a] Mean distances (Å). The standard deviation of the mean was estimated from $\sigma \cong s = [(|\Sigma x_i^2 - nx^2|)/(n-1)]^{1/2}$.

[b] The two sets of distances refer to two independent anions.

[c] Structure solved at 1.7 Å resolution; cf. Fig. 4.

[d] Range of observed distances.

[e] Structure solved at 2.5 Å resolution.

Fe–S distances depend only slightly on M and are within the ranges of the corresponding but less accurately known distances in the protein-bound cuboidal clusters **4**. The M–S, M–Fe, and terminal Fe–SR distances are somewhat more dependent on M. A tabulation showing these same features for double-cubane structures is available (*192*). From this brief but typical comparison, we conclude that the Fe_3S_4 fragment as a tridentate ligand can accommodate metals of different sizes with only small changes in its internal dimensions.

The isomer shift data in Table III permit assignment of, or an approximation of, effective oxidation states of the cluster fragments Fe_3S_4 and M when compared against protein values as standards. Weighted mean values are used as appropriate. A formal decomposition of clusters into fragments leads to a zero-order description of charge distribution. Series (30) sets out the isomer shift/oxidation state correlation provided

$$\underset{0.27\ (Fe^{3+})}{[Fe_3S_4]^{1+}} \qquad \underset{0.42\ (Fe^{2.67+})}{[Fe_3S_4]^{0}} \qquad \underset{0.56\ (Fe^{2.33+})}{[Fe_3S_4]^{1-}} \qquad \text{mm/sec} \tag{30}$$

by presently available data; small ranges around these values are to be expected as more data become available. It is immediately evident that the shifts of all clusters with M = Fe, Co, Ni, and Zn (Set I) require that the effective oxidation levels of the iron–sulfur fragments be in the $[Fe_3S_4]^{0/1-}$ range. Thus, protein-bound $[CoFe_3S_4]^{2+}$, with $\delta_{av} = 0.41$ mm/sec, may be formalized into the indicated fragments even in the absence of knowledge of the 2+ oxidation state. Cluster **70**, with its known charge, confirms this state for the protein. A description such as $[Fe_3S_4]^{1-} + Co^{3+}$ is inconsistent with the isomer shifts as well as the tetrahedral stereochemistry of the cobalt subsite as inferred from the cluster composition. Protein-bound $[ZnFe_3S_4]^{1+}$, whose odd spin requires the indicated fragments, currently provides the only available isomer shift of the $[Fe_3S_4]^{1-}$ state. The δ value of the $[NiFe_3S_4]^{1+}$ core of **68** is biased toward, but does not reach, the value for this state. The indicated fragments are the preferred description, but this cluster, which does not preserve any subsite differentiation within the Fe_3S_4 fragment, may be more delocalized than other clusters with the Set I metals. Under the fragment formulation, the spins of clusters containing these metals can be derived from antiferromagnetic coupling of the $S = 2$ or $\frac{5}{2}$ spin of the Fe_3S_4 fragment with that of the tetrahedral M^{2+} ion. The value of $S = 1$ is predicted for $[CoFeS_4]^{1+}$; the experimental value has not been reported.

We next inquire if the same Fe_3S_4 fragment oxidation states and spin coupling apply to the early transition metal clusters in which the heterometal is in a higher oxidation state and occurs in each of the three transition series. Representative isomer shift data for clusters

with M = V, Mo, W, and Re (Set II) are included in Table III. All species have terminal thiolate ligands at the iron subsites, a requirement for internal comparison of isomer shifts. Variation of ligands at the heterometal subsites has an effect on isomer shifts that is slight compared to that of changing cluster oxidation state. Isomer shifts are decisively larger than those of the $[Fe_3S_4]^{1+}$ clusters, indicating, as for the Set I metals, the effective oxidation states $[Fe_3S_4]^{0/1-}$. Fragment formulations follow from isomer shifts, which in some cases match closely with those in series (30). Cluster spins can be rationalized in terms of antiparallel spin coupling as for the Set I cases, but with the additional assumption that d^3 and d^4 M^{z+} fragments have $S = \frac{1}{2}$ and 0, respectively. These spins can be achieved by, say, a strong trigonal distortion resulting in the order $e < a$ for orbitals of octahedral t_{2g} parentage. At the low temperatures of measurement (usually 4.2 K), only the e orbitals are populated. For example, in the $[MoFe_3S_4]^{3+}$ case the coupling is between fragments with $S = 2$ and $S = \frac{1}{2}$, resulting in the observed cluster spin $S = \frac{3}{2}$. Reduction of this core to $[MoFe_3S_4]^{2+}$ primarily affects the Fe_3S_4 fragment, and the experimental cluster spin $S = 2$ is considered to arise from coupling of $S = \frac{5}{2}$ and $\frac{1}{2}$ fragments.

In the M = Re and V cases, for which there is a limited data base of isomer shifts, the fragment formulation seems clear for $[ReFe_3S_4]^{4+}$. But for $[ReFe_3S_4]^{3+}$ the shifts do not allow, as indicated, a clear distinction between two formulations, either of which is consistent with $S = 2$. The situation with $[VFe_3S_4]^{2+}$ is similar. However, in this case, the 0/2+ formulation, under the spin-coupling model, requires a large distortion of V^{2+} (d^3, $S = \frac{1}{2}$), which may be unreasonable for a first transition series ion. The fragment formulations for clusters of known structures are entirely consistent with bond distances involving core and terminal ligand atoms (*163, 165, 176, 189–193*).

Although the fragment formulation and the spin-coupling model are simplistic and the latter lacks a theoretical foundation, they do offer an approximation to the actual charge distribution and provide a ready means of rationalizing and predicting cluster spins. For example, the unknown species $[MnFe_3S_4]^{2+/1+}$ would be expected to have spins of $S = \frac{1}{2}$ and 0, respectively. No diamagnetic MFe_3S_4 cluster has yet been prepared! Some may favor other formulations, such as $[Fe_3S_4]^{1-}$ and Mo^{4+} for $[MoFe_3S_4]^{3+}$. However, provided the heterometal does not significantly perturb fragment isomer shifts, the $[Fe_3S_4]^0 + Mo^{3+}$ formalism is preferred. Others may understandably resist the fragment concept applied to a tightly bound cluster, yet account must be taken of the effort required to obtain a theoretical electronic structural description of an open-shell cluster at the Xα calculational level (*194*).

Summarized in Table V is the scope of heterometal cluster formation

and known spin states. It is extensive and may be expected to expand considerably. We propose that the Fe_3S_4 unit be considered a *quasi-rigid cluster ligand,* whose effective oxidation state lies at or between 0 and -1 when bound to a fourth metal and whose internal structural features and electronic distribution are largely unchanged upon binding a heterometal atom (*193*). The indicated oxidation states are sufficient for binding but may not always be necessary, for as noted above $[Fe_3S_4]^{1+}$ may have latent binding affinity for the especially thiophilic (soft) metals. Also included for reference in Table III are $[Fe_3S_4]^{z+}$ clusters. Those of the types $[Fe_4S_4]^{3+/2+/1+}$ have been very thoroughly examined as synthetic analogs of biological clusters. The terminal members of the series, $[Fe_4S_4]^{4+}$ as $[Fe_4S_4(R_2dtc)_4]$ (*183, 205*) and $[Fe_4S_4]^0$ as $[Fe_4S_4(CO)_{12}]$ (*62*), have oxidation states not yet detected in native clusters. We next inquire into the biological relevance of heterometal cubane-type clusters.

D. Biological Implications

Although MFe_3S_4 clusters can be prepared in proteins (Fig. 11), no such cluster has yet been detected in a native protein. Indeed, there is as yet no clearly defined biological function of the precursor Fe_3S_4 cluster. In one case, aconitase, the Fe_3S_4 form of the enzyme is inactive but can be converted to the active form by cluster reconstitution with Fe(II) (Fig. 4). Consequently, we turn our attention to synthetic clusters.

1. Structural Models

It is uncommon that the development of a distinct area of chemistry can be traced to a single event, but this is the case with MFe_3S_4 clusters. The event was the Mo K-edge extended X-ray absorption fine structure (EXAFS) analysis of the Fe–Mo protein and Fe–Mo cofactor of nitrogenase by Hodgson and co-workers in 1978 (*206, 207*). It was concluded that molybdenum in both samples is implicated in a Mo–Fe–S cluster with similar environments of probable near-neighbor composition $MoFe_3S_3$. This work impelled development of the cluster assembly systems in Fig. 6 as well as later advancements (*165*). Subsequent Mo X-ray absorption near-edge structure (XANES) experiments ruled out tetrahedral MoS_4 and octahedral MoS_6 coordination, and pointed to the inclusion of low-Z atoms in the coordination sphere (*208*). Protein and cofactor second-derivative XANES indicated that the first coordination shells were similar but not identical and that the cofactor spectra closely resembled the edge spectra of $[MoFe_3S_4(SEt)_3Fe(cat)_3]^{3-}$ [cat is catecholate(2 $-$)] (*209*) and $[Mo_2Fe_6S_8(SEt)_6(OMe)_3]^{3-}$ (**71**) (*175, 210*).

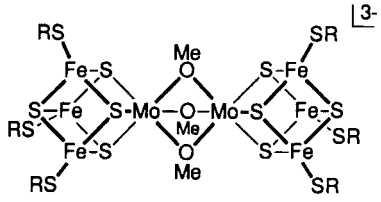

71

The preparation and properties of the Fe–Mo cofactor have been incisively summarized by Burgess (*211*), who has included an account of the X-ray absorption spectroscopic results, providing all of the concrete structural information on the native cluster. Descriptions of the Fe–V cofactor and Fe–V proteins are also available (*211, 212*). The composition of the Fe–Mo cofactor is in the range $MoFe_{6-8}S_{8-10}$. Properties of the Fe–V cofactor suggest that it is an analogous species, but this cannot be decided at present from analytical data. We confine attention to structural properties only. Average bond distances from the most recent EXAFS studies on the Fe–Mo cofactor and Fe–Mo protein (*213*), and the Fe–V protein (*214–216*), are presented in Table VII. The three species are in the semireduced oxidation state, with $S = \frac{3}{2}$, and in that sense are related to $[MoFe_3S_4]^{3+}$ and $[VFe_3S_4]^{2+}$ clusters (Table V). The sum of O + S atom numbers indicates six-coordinate molybdenum.

In formula **72**, bond distances of the Fe–Mo cofactor (italics) are compared with those of $[MoFe_3S_4Cl_3(cat)(THF)]^{2-}$ (*217*); a similar comparison between $[VFe_3S_4Cl_3(DMF)_3]^{1-}$ (**55**) (*190*) and the Fe–V protein is provided in formula **73**. Also included are Fe–Fe and Fe–S distances

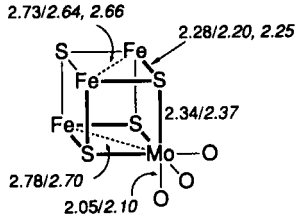

72

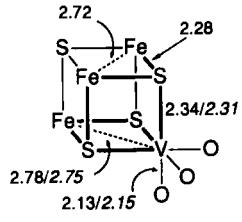

73

obtained from Fe EXAFS (*211*). In **72**, the Mo–Fe and Fe–Fe distances of the cofactor appear to be somewhat shorter, but mean values in synthetic clusters span the ranges 2.68–2.73 and 2.70–2.79 Å, respectively (*165*). The Mo—O bond length of 2.10 Å in the cofactor is in good agreement with the Mo—O(cat) distance of 2.05 Å in the synthetic cluster. When compared with the Mo—O(THF) value of 2.35 Å, the cofactor bond length is further seen to be consistent with an anionic ligand, perhaps homocitrate, which has been shown to be an endoge-

TABLE VII

THE M = Mo/V SITES IN THE Fe–Mo COFACTOR AND Fe–Mo/V PROTEINS OF NITROGENASE FROM EXAFS RESULTS

Sample	Distance (Å)			No. of atoms		
	M–S	M–Fe	M–O	S	Fe	O
Fe–Mo cofactor (as isolated)[a]	2.37(2)	2.70(2)	2.10(2)	3.1	2.6	3.1
Fe–Mo protein (semireduced)[a]	2.37(1)	2.68(1)	2.12(1)	4.5	3.5	1.7
Fe–V protein (semireduced)[b]	2.31	2.75	2.15	3(1)	3(1)	3(1)

[a] *Clostridium pasteurianum* and *A. vinelandii* nitrogenase (*213*).

[b] *Azotobacter chroococcum* nitrogenase (*214, 215*); very similar results have been obtained for the *A. vinelandii* Fe–V protein (*216*).

nous component of the cofactor (*211*). The apparent bond distance concordance in **73** is even better. Here the V—O distance involves a neutral ligand (DMF). From a Mo EXAFS intensity analysis of single crystals of the Fe–Mo protein, it has been concluded that a linear Fe–Mo–Fe arrangement is unlikely and that the Fe–Mo–Fe angle lies within the limits 50–130° (*218*). This angle in the cluster summarized by **72** is 59°, a typical value for such species, in which the $MoFe_3$ unit is a distorted tetrahedron.

All evidence sustains the conclusion that the cubane-type cluster **72** still provides the best structural model for the molybdenum site in the cofactor. This conclusion is less satisfactory for the protein-bound cofactor. It follows from the results of Table VII that the (minimum) coordination number of the molybdenum atom is the same in the free cofactor and in the protein, but the atom composition changes pursuant to protein binding. One iron and one sulfur atom appear in the molybdenum environment, indicating that a change in core structure cannot be discounted. Cluster **73** is clearly an excellent model for the vanadium site in the Fe–V protein, in which cofactor binding apparently differs to some extent from that in the Fe–Mo protein. The boldface portions of **72** and **73** imply fragments of radially averaged structural similarity to the native clusters. The cubane structure cannot be proved because the nonbonded M . . . S intracluster distance of ~4 Å is too long to be observed by EXAFS. Last, no structure such as **72** can generate second shell scattering and Fe–Fe separations near 3.7 Å deduced from the Fe EXAFS of the Fe–Mo cofactor (*211*). The native cluster has a more elaborate structure, as required by its composition.

2. *Linked Cubane Clusters*

There is no shortage of models, all synthetically unfulfilled, for the Fe–Mo cofactor (*164, 165*). One of these, containing the $MoFe_7S_6$ noncubane polyhedron and originating in this laboratory (*163, 219*), could account for the long-range Fe–Fe scattering observed by EXAFS. In the quest for the synthesis of the Fe–Mo cofactor, clusters within the core compositional limits have been difficult to achieve. The species $[MoFe_6S_6(CO)_{16}]^{2-}$ (*185*), which does not contain a heterometal cubane unit, is the closest approximation to the composition. Although it is a possible precursor to a model, it is not one.

Given the considerable thermodynamic stabilities of Fe_4S_4 and $MoFe_3S_4$ clusters as judged from their rapid, high-yield formation in assembly systems, a rational cofactor structure concept follows. That structure may consist of a linked combination of these two cubane-type units. The highly significant crystallographic work of Bolin *et al.* (*220*) on the Fe–Mo protein of *C. pasteurianum* places the two cofactor clusters 70 Å from each other, thereby eliminating as directly pertinent to the nitrogenase problem any unit containing two molybdenum atoms and substrate reductions based on binuclear activation by molybdenum. Nonetheless, the problem at hand requires, at the outset, learning how to link clusters of these types, whether the same or different. One method, employing subsite-differentiated clusters and affording the singly bridged double cubanes **23**–**25**, is outlined in Fig. 2. The double cubane $[(Fe_4S_4Cl_3)_2S]^{4-}$ has been isolated and the Fe–S–Fe bridge was proved by an X-ray structure determination (*53*). Very recently, Coucouvanis and co-workers (*221–223*) demonstrated means of linking two $MoFe_3S_4$ clusters. The reactions given by Eq. (31) lead to the doubly bridged clusters **74** and **75**. Unlike the double cubane, **46**, the bridges connect the same metal atom. In **74**, the bridges are unsymmetrical, especially at the molybdenum atom where Mo—S = 2.60 and 2.69 Å. The mean Fe—S bridge distance (2.20 Å) is shorter than the average of core Fe—S distances [2.27(3) Å], presumably because of the lesser bridging multiplicity in the former bond. In contrast, the mean Mo—S bridge distance (2.65 Å) is substantially longer than the average of core Mo—S distances [2.35(2) Å]. A somewhat related feature is the long terminal Mo—S distance of 2.60 Å found in the single cubane $[MoFe_3S_4(S\text{-}p\text{-}C_6H_4Cl)_4(cat)]^{3-}$ (**48**) (*224*). In **74** and **75**, Fe—S—Fe = 98–99° [5° less than in $[(Fe_4S_4Cl_3)_2S]^{4-}$], and Mo—X—Mo = 137° and 158°, respectively. With limited data, it would appear that these double cubanes are constructed with bridges of unexceptional bond distances and Mo—X—Mo angles that vary as required for structural stability.

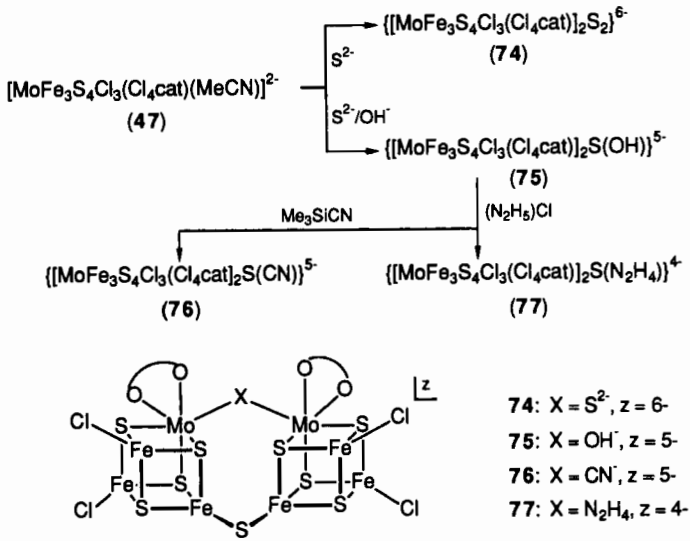

In the reactions given by Eq. (32), the Mo—(OH)—Mo bridge is cleaved and the potentially reducible substrates cyanide and hydrazine are inserted between two units capable of one-electron reduction. A low-resolution X-ray study is said to support structure **77** (*222*). No substrate transformations have yet been reported. Coucouvanis (*223*) has hypothesized a pathway for the reduction of dinitrogen in which the substrate is bridged between molybdenum and iron subsites of different cubanes in an otherwise singly bridged (Mo–S–Fe) double cubane of the type $MoFe_3S_4$–S–Fe_4S_4. Isolation of such a cluster has been mentioned but structural proof is lacking (*221*).

E. Nonbiological $M'M_3S_4$ Clusters

The existence of the cuboidal M_3S_4 unit **31** (Table IV) raises the possibility of $M_3S_4 \rightarrow M'M_3S_4$ cluster conversion reactions when **31** is in a suitable oxidation state. The Mo_3S_4 core **78** is available in a variety of clusters and is potentially susceptible to closure to cubanes. A rather extensive group of clusters with the cubane-type $M'M_3S_4$ cores (M = Mo, W, and Cr) in fact has been synthesized, all since 1981; these clusters are collected in Table VIII. The large majority have been characterized by X-ray structural determinations. Representative structures are depicted in Fig. 12. Only the species with M = Cr were *not* synthesized by a cluster conversion reaction. These clusters are termed "nonbiological" inasmuch as neither the M_3S_4 portion nor the $M'M_3S_4$ core has been found in a natural molecule.

TABLE VIII

HETEROMETALLIC $M'M_3S_4$ CUBANE-TYPE CLUSTERS

Cluster	Ref.
$[M'Mo_3S_4]$	
Group I	
$[Fe^{II}Mo_3S_4(OH_2)_{10}]^{4+}$	*225, 226*
$[Fe^{II}Mo_3S_4(NH_3)_9(OH_2)]^{4+}$	*225*
$[Ni^{II}Mo_3S_4(OH_2)_{10}]^{4+}$ (**80**)	*227, 228*
$[Ni^{II}Mo_3S_4(nta)_2(Hnta)Cl]^{5-}$ (**81**)	*227*
$[Sn^{IV}Mo_3S_4(OH_2)_x]^{6+}$	*229*
$[Sn^{IV}Mo_3S_4(Hnta)_3Cl_3]^{3-}$	*229*
$[Sn^{IV}(Mo_3S_4(OH_2)_9)_2]^{8+}$ (**82**)	*229*
$[Mo(Mo_3S_4(OH_2)_9)_2]^{8+}$	*230*
$[Hg(Mo_3S_4(OH_2)_9)_2]^{8+}$	*231*
$[Sb(Mo_3S_4(OH_2)_9)_2]^{8+}$	*254*
$[Co^{II}_2(Mo_3S_4(OH_2)_9)_2]^{8+}$	*231*
$[Cu^{I}_2(Mo_3S_4(OH_2)_9)_2]^{8+}$ (**83**)	*232*
Group II	
$[Sn^{IV}Mo_3S_4(S_2PEt_2)_6]$ (**84**)	*233*
$[WMo_3S_4(S_2PEt_2)_6]$	*234*
$[Cu^{I}Mo_3S_4(dtp)_3I(Cl_3CO_2)(MeCN)]$	*235*
$[Cu^{I}Mo_3S_4(dtp)_3I(OAc)L]$ (L = DMF, H_2O) (**85**)	*236*
$[Sb^{III}Mo_3S_4(dtp)_4Cl_3L]$ (L = EtOH, oxazole)	*237*
$[M'WS_4]$	
$[Cu^{I}W_3S_4(dtp)_3I(OAc)(py)]$	*238*
$[M'Fe_3S_4]$	
$[Cp_4VFe_3S_4]$	*239*
$[Cp_4NbFe_3S_4]$	*239*
$[M'Cr_3S_4]$	
$[Cp_3Fe(O_2C\text{-}t\text{-}Bu)Cr_3S_4]$ (**86**)	*240*
$[Cp_3Fe(SPh)Cr_3S_4]$ (**87**)	*241*
$[Cp_3Co(CO)Cr_3S_4]$, $[(MeCp)_3Co(CO)Cr_3S_4]$	*242, 243*

Because of differences in preparation, it is convenient to subdivide $M'Mo_3S_4$ clusters into two groups, as indicated in Table VIII. All clusters in Group I are prepared by the core conversion reaction, Eq. (33),

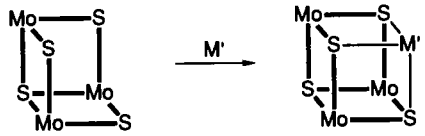

78 **79**

(M = Fe, Co, Ni, Cu, Mo, Hg, Sn, Sb) (33)

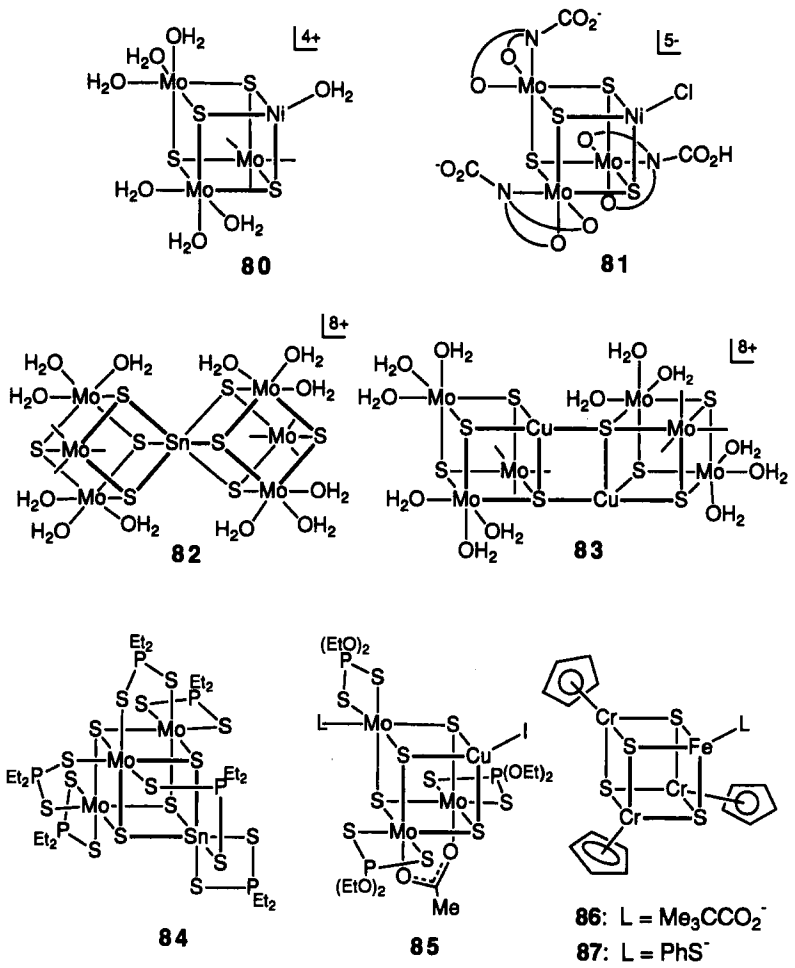

FIG. 12. Schematic structures of the $M'M_3S_4$ cubane-type clusters **80–87** (Table VIII).

in which the boldface portion of product cluster **79** emphasizes the ligand nature of **78**. In an elegantly simple experiment reported in 1986, Shibahara *et al.* (*225*) performed the redox reaction (a) given by Eq. (34) (M′ = Fe) in aqueous acid solution. This reaction not only afforded the indicated product but has been generalized for the preparation of the aqua clusters shown in Eq. (34).

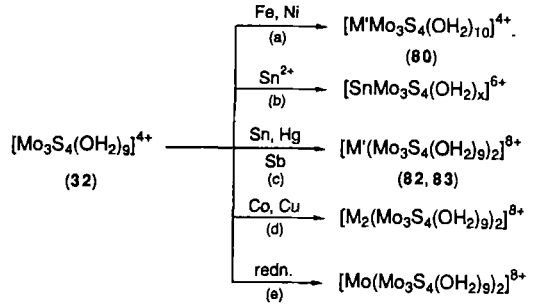

(34)

In this experiment, iron wire was placed in a 2 *M* HCl solution of **32**; a color change from green to red-purple ensued in a few hours. The product aqua ion was separated by cation exchange. Treatment of the reaction mixture with concentrated ammonia led to the formation of $[FeMo_3S_4(NH_3)_9(OH_2)]^{4+}$, which was isolated as the chloride salt. An analogous reaction afforded the $NiMo_3S_4$ cluster **80**, which was readily converted to the chelated cluster **81** with nitrilotriacetate(3 −) (NTA). The structures of these species confirm the cubane cores, tetrahedral M′ subsites, and six-coordinate molybdenum subsites; the latter is an invariant feature of the clusters in Table VIII. Reaction (b) in Eq. (34) gives the tin cluster; it has not been isolated and the exact number of aqua ligands is not known. With the metals in reactions (c) and (d) in Eq. (34) double cubanes are obtained. Clusters containing tin, antimony, or mercury are bridged by a six-coordinate metal atom as in **82**, whereas the copper and cobalt clusters are bridged by two M′—S bonds involving distorted tetrahedral heterometal subsites as in **83**. In reaction (e) in Eq. (34), cuboidal **32** is fragmented by reduction and the product cluster, whose structure is analogous to **82**, is obtained in low (15%) yield.

The processes involved in reactions (a)–(d) in Eq. (34), excluding that with copper and possibly mercury, are satisfactorily interpreted in terms of a two-electron reduction of **32** by the M′ reactant (*227*). This results in formation of the $[Mo_3S_4]^{2+}$ core, which, because of the reduced oxidation state ($Mo^{3.33+}$) and consequent attenuated electrophilic demand of the molybdenum atoms, is a much more effective ligand. In an equivalent reaction, cluster **80** has been obtained by the reduction of **32** with $NaBH_4$ in the presence of $NiCl_2$ in aqueous acid solution (*228*). Tetrahedral stereochemistry at the copper subsites in **83** implies Cu(I) and a one-electron reduction of **32**, a plausible situation given the affinity of Cu(I) for sulfur ligands. In the case of M′ = Hg, Shibahara *et al.* (*231*) conclude that the Hg—S bonds are too long to indicate

oxidation to Hg(II), but bond distances were not given. On the basis of E_0 values, mercury, of all metals M′ in Eq. (34), is the most difficult to oxidize in acid solution. Shibahara has summarized his work in this field (*257*).

Among Group II clusters, the approximately octahedral coordination at the tin subsite of **84** implies Sn(IV) and a two-electron oxidation of Sn(II) in Eq. (35). The presence of Cu(I) is quite obvious in clusters typified by **85**, whose copper subsite is tetrahedrally coordinated. The product cluster of Eq. (36) is isostructural with **84** and the $[WMo_3S_4]^{6+}$

$$Sn(S_2PEt_2)_2 + Mo_3S_4(S_2PEt_2)_4 \rightarrow SnMo_3S_4(S_2PEt_2)_6 \quad (35)$$

$$Mo_3S_4(S_2PEt_2)_4 + (Et_2P(S))_2S_2 + W(CO)_3(MeCN)_3 \rightarrow WMo_3S_4(S_2PEt_2)_6 + 3CO + 3MeCN \quad (36)$$

core is generated with two oxidizing equivalents from the ligand disulfide. Although the preferred formulation in terms of W(IV) and $[Mo_3S_4]^{2+}$ (*234*) may be meaningful, this compound points out the difficulty in deducing simple charge distributions in this class of compounds. Inasmuch as molybdenum does not provide a Mössbauer nucleus, charge distributions will have to be deduced from the isomer shifts of the heterometal (when applicable) and ^{95}Mo chemical shifts (when observable). Either method will require a data base for interpretations of cluster properties. It remains to be seen if other techniques such as XANES or X-ray photoelectron spectroscopy can be applied to these clusters, whose polarizable sulfide ligands can be expected to attenuate differences arising from changes in metal oxidation state.

From the array of $M'Mo_3S_4$ clusters in Table VIII and their means of formation, it is evident that two features in particular contribute to stability: (1) the oxidation state of the Mo_3S_4 fragment and (2) the intrinsic affinity of heterometal M′ for anionic sulfur ligands. Overall, Eqs. (37) and (38) (aqua ligands omitted) (*226, 228*), whereby hetero-

$$2[FeMo_3S_4]^{4+} + O_2 + 4H^+ \rightarrow 2[Mo_3S_4]^{4+} + 2Fe^{2+} + 2H_2O \quad (37)$$

$$[NiMo_3S_4]^{4+} + 2Fe^{III} \rightarrow [Mo_3S_4]^{4+} + Ni^{2+} + 2Fe^{2+} \quad (38)$$

metal cores are disrupted by oxidation, underscore the necessity for a reduced Mo_3S_4 fragment as a ligand to Fe(II) and Ni(II). The $[Mo_3S_4]^{3+,2+}$ states have not been demonstrated for the aqua ion but have been detected electrochemically in $[Mo_3S_4(ida)_3]^{3-,4-}$ [ida is imidodiacetate(2−)] (*115*). When reactions are carried out without an exogenous reductant as in scheme (34), a requirement equivalent to feature (1) mentioned above is that the M′ reactant be a sufficient reductant. Standard potentials for the two-electron reductants in Eq. (34) occur in

the range −0.44 (Fe) to +0.15 V (Sn^{2+}). With Cu (+0.52 V) as a reactant, a one-electron reduction suffices. It would appear that a substantial number of other clusters should be accessible by the methods of this scheme or by the addition of a reductant in the presence of **32** and an M′ source. It remains to be seen if $[W_3S_4(OH_2)_9]^{4+}$ can be reduced to a level that will support cluster formation. In the cuboidal series of ions on p. 28, the ease of reducibility is expected to decrease in proceeding to the right. No reductant is necessary for the formation of the $[CuMo_3S_4]^{5+}$ cores in clusters such as **85**, which are formed directly from $[Mo_3S_4(dtp)_4(OH_2)]$ and a Cu(I) source. Given the existence of cuboidal species such as $[Mo_2MS_4(edt)_2(PPh_3)]^{1-}$ (M = Cu, Ag) (*244, 245*), it would appear that heterotrimetallic clusters are within easy reach.

The final set of heterometal clusters in Table VIII contains the $M'Cr_3S_4$ core unit; these clusters have been prepared by Pasynskii and co-workers. The synthetic methods for these compounds utilize the common starting material $[Cp_2Cr_2(\mu\text{-}St\text{-}Bu)_2(\mu\text{-}S)]$ and proceed by oxidative decarbonylation of M′ carbonyl precursors under thermal or photolytic conditions. The steps in the formation of the clusters are decidedly obscure. Clusters **86** and **87** are of potential interest in the manipulation of one labile subsite in molecules whose three other subsites are irreversibly blocked.

F. Prospectus

It has now been 20 years since the Fe_4S_4 cubane-type structure was proved by protein crystallography, in a landmark contribution by Sieker, Adman, and Jensen (*246*), and since the first synthetic analog of the native cluster was prepared (*247*). In the intervening period, the compositions and structures of only two other native iron–sulfur clusters, of the types Fe_2S_2 and Fe_3S_4 and in that order, have yielded to experimentation. One need only contemplate the P-clusters and cofactors of nitrogenase (*22, 211, 220, 248*) and the H-clusters of hydrogenase (*21*) to recognize that there remain formidable challenges in protein-bound cluster structural, electronic, and reactivity characterization and in the synthesis of meaningful analogs of these clusters. What role, if any, Fe_3S_4 and MFe_3S_4 clusters will play in a fuller exposition of iron–sulfur biochemistry remains to be learned. What is evident is that one cluster affords the other in a protein and in the laboratory, but we must progress further before knowing if nature executes cluster conversion and regards heterometal cubanes as salutary to any biological function. In the context of inorganic clusters, these are the most

rapidly growing type. Only lack of ingenuity will prevent the synthesis of MFe_3S_4 clusters containing nearly all metals and metalloids. That this report has concentrated mainly on synthesis and structure is one indication that, with the exception of $[VFe_3S_4]^{2+}$ and $[MoFe_3S_4]^{3+}$ clusters, the understanding of electronic structures and reactivities at all metal subsites is presently quite elementary. Harris (*249*) has presented a useful survey of cubane-type clusters and qualitative core bonding models. Nonetheless, developments in iron–sulfur chemistry and biochemistry have proceeded apace. It is desired that their treatment here vindicates the title of this article.

ACKNOWLEDGMENTS

It is a personal privilege of high order to contribute to this volume, which honors the scientific works of Helmut Beinert. His collective contributions to iron–sulfur biochemistry over three decades, well known to veteran investigators in the field, stand second to none. For those who have been attracted only recently to the subject, examination of the work of Beinert and his colleagues on the aconitase problem will reveal a modern chemical/biochemical classic.

The research of the author in iron–sulfur and heterometal cluster chemistry has, since its inception (*247*), been supported by the National Institutes of Health and the National Science Foundation. I thank C. K. Ryder for preparation of figures and formulas and S. C. Lee for useful discussions.

REFERENCES

1. Berg, J. M., and Holm, R. H., *in* "Iron-Sulfur Proteins" (T. G. Spiro, ed.), Chap. 1. Wiley (Interscience), New York, 1982.
2. Adman, E. T., Sieker, L. C., and Jensen, L. H., *J. Biol. Chem.* **248,** 3987 (1973); Adman, E. T., Sieker, L. C., and Jensen, L. H., *J. Biol. Chem.* **251,** 3806 (1976).
3. Carter, C. W., Jr., Kraut, J., Freer, S. T., Xuong, N., Alden, R. A., and Bartsch, R. G., *J. Biol. Chem.* **249,** 4212 (1974).
4. Carter, C. W., Jr., Kraut, J., Freer, S. T., and Alden, R. A., *J. Biol. Chem.* **249,** 6339 (1974).
5. Lim, L. W., Shamala, N., Mathews, F. S., Steenkamp, D. J., Hamlin, R., and Xuong, N., *J. Biol. Chem.* **261,** 15140 (1986).
6. Stout, G. H., Turley, S., Sieker, L. C., and Jensen, L. H., *Proc. Natl. Acad. Sci. U.S.A.* **85,** 1020 (1988).
7. Stout, C. D., *J. Biol. Chem.* **263,** 9256 (1988); Stout, C. D., *J. Mol. Biol.* **205,** 545 (1989).
8. Fukuyama, K., Nagahara, Y., Tsukihara, T., Katsube, Y., Hase, T., and Matsubara, H., *J. Mol. Biol.* **199,** 183 (1988).
9. Fukuyama, K., Matsubara, H., Tsukihara, T., and Katsube, Y., *J. Mol. Biol.* **210,** 383 (1989).

10. Robbins, A. H., and Stout, C. D., *Proc. Natl. Acad. Sci. U.S.A.* **86,** 3639 (1989); Robbins, A. H., and Stout, C. D., *Proteins* **5,** 289 (1989).
11. Martin, A. E., Burgess, B. K., Stout, C. D., Cash, V. L., Dean, D. R., Jensen, G. M., and Stephens, P. J., *Proc. Natl. Acad. Sci. U.S.A.* **87,** 598 (1990).
12. Carney, M. J., Papaefthymiou, G. C., Spartalian, K., Frankel, R. B., and Holm, R. H., *J. Am. Chem. Soc.* **110,** 6084 (1988); and references therein.
13. Carney, M. J., Papaefthymiou, G. C., Whitener, M. A., Spartalian, K., Frankel, R. B., and Holm, R. H., *Inorg. Chem.* **27,** 346 (1988).
14. Carney, M. J., Papaefthymiou, G. C., Frankel, R. B., and Holm, R. H., *Inorg. Chem.* **28,** 1497 (1989).
15. Yu, S., Papaefthymiou, G. C., and Holm, R. H., *Inorg. Chem.* **30,** 3476 (1991); and references therein.
16. Simon, W., Wilk, A., Krebs, B., and Henkel, G., *Angew. Chem., Int. Ed. Engl.* **26,** 1009 (1987).
17. Barbaro, P., Bencini, A., Bertini, I., Briganti, F., and Midollini, S., *J. Am. Chem. Soc.* **112,** 7238 (1990).
18. Backes, G., Mino, Y., Loehr, T. M., Meyer, T. E., Cusanovich, M. A., Sweeney, W. V., Adman, E. T., and Sanders-Loehr, J., *J. Am. Chem. Soc.* **113,** 2055 (1991).
19. Beinert, H., and Kennedy, M. C., *Eur. J. Biochem.* **186,** 5 (1989).
20. Beinert, H., *FASEB J.* **4,** 2483 (1990).
21. Adams, M. W. W., *Biochim. Biophys. Acta* **1020,** 115 (1990).
22. Holm, R. H., Ciurli, S., and Weigel, J. A., *Prog. Inorg. Chem.* **38,** 1 (1990).
23. Lindahl, P. A., and Kovacs, J. A., *J. Cluster Sci.* **1,** 29 (1990).
24. Bruschi, M., and Guerlesquin, F., *FEMS Microbiol. Rev.* **54,** 155 (1988).
25. Conover, R. C., Kowal, A. T., Fu, W., Park, J.-B., Aono, S., Adams, M. W. W., and Johnson, M. K., *J. Biol. Chem.* **265,** 8533 (1990).
26. Okawara, N., Ogata, M., Yagi, T., Wakabayashi, S., and Matsubara, H., *J. Biochem. (Tokyo)* **104,** 196 (1988).
27. Ogata, M., Kondo, S., Okawara, N., and Yagi, T., *J. Biochem. (Tokyo)* **103,** 121 (1988).
28. Bovier-Lapierre, G., Bruschi, M., Bonicel, J., and Hatchikian, E. C., *Biochim. Biophys. Acta* **913,** 20 (1987).
29. Armstrong, F. A., George, S. J., Cammack, R., Hatchikian, E. C., and Thomson, A. J., *Biochem. J.* **264,** 265 (1989).
30. George, S. J., Armstrong, F. A., Hatchikian, E. C., and Thomson, A. J., *Biochem. J.* **264,** 275 (1989).
31. Kerscher, L., Nowitzki, S., and Oesterhelt, D., *Eur. J. Biochem.* **128,** 223 (1982).
32. Minami, Y., Wakabayashi, S., Wada, K., Matsubara, H., Kerscher, L., and Oesterhelt, D., *J. Biochem. (Tokyo)* **97,** 745 (1983).
33. Wakabayashi, S., Fujimoto, N., Wada, K., Matsubara, H., Kerscher, L., and Oesterhelt, D., *FEBS Lett.* **162,** 21 (1983).
34. O'Keefe, D. P., Gibson, K. J., Emptage, M. H., Lenstra, R., Romesser, J. A., Litle, P. J., and Omer, C. A., *Biochemistry* **30,** 447 (1991).
35. Kissinger, C. R., Adman, E. T., Sieker, L. C., and Jensen, L. H., *J. Am. Chem. Soc.* **110,** 8721 (1988).
36. Kissinger, C. R., Sieker, L. C., Adman, E. T., and Jensen, L. H., *J. Mol. Biol.* **219,** 693 (1991).
37. Plank, D. W., and Howard, J. B., *J. Biol. Chem.* **263,** 8184 (1988).
38. Werst, M. M., Kennedy, M. C., Beinert, H., and Hoffman, B. M., *Biochemistry* **29,** 10526 (1990).

39. Kennedy, M. C., Kent, T. A., Emptage, M. H., Merkle, H., Beinert, H., and Münck, E., *J. Biol. Chem.* **259,** 14463 (1984).
40. Plank, D. W., Kennedy, M. C., Beinert, H., and Howard, J. B., *J. Biol. Chem.* **264,** 20385 (1989).
41. Hagen, K. S., Watson, A. D., and Holm, R. H., *J. Am. Chem. Soc.* **105,** 3905 (1983).
42. Stack, T. D. P., Weigel, J. A., and Holm, R. H., *Inorg. Chem.* **29,** 3745 (1990).
43. Stack, T. D. P., and Holm, R. H., *J. Am. Chem. Soc.* **110,** 2484 (1988).
44. Ciurli, S., and Holm, R. H., *Inorg. Chem.* **28,** 1685 (1989).
45. Whitener, M. A., Peng, G., and Holm, R. H., *Inorg. Chem.* **30,** 2411 (1991).
46. Wong, G. B., Bobrik, M. A., and Holm, R. H., *Inorg. Chem.* **17,** 578 (1978).
47. Wiegel, J. A., and Holm, R. H., *J. Am. Chem. Soc.* **113,** 4184 (1991).
48. Ciurli, S., Carrié, M., Weigel, J. A., Carney, M. J., Stack, T. D. P., Papaefthymiou, G. C., and Holm, R. H., *J. Am. Chem. Soc.* **112,** 2654 (1990).
49. Cleland, W. E., Holtman, D. A., Ibers, J. A., DeFotis, G. C., and Averill, B. A., *J. Am. Chem. Soc.* **105,** 6021 (1983).
50. Weigel, J. A., Holm, R. H., Surerus, K. K., and Münck, E., *J. Am. Chem. Soc.* **111,** 9246 (1989).
51. Weigel, J. A., Srivastava, K. K. P., Day, E. P., Münck, E., and Holm, R. H., *J. Am. Chem. Soc.* **112,** 8015 (1990).
52. Stack, T. D. P., Carney, M. J., and Holm, R. H., *J. Am. Chem. Soc.* **111,** 1670 (1989).
53. Challen, P. R., Koo, S.-M., Dunham, W. R., and Coucouvanis, D., *J. Am. Chem. Soc.* **112,** 2455 (1990).
54. Liu, H. Y., Scharbert, B., Holm, R. H., *J. Am. Chem. Soc.* **113,** 9529 (1991).
55. Reynolds, J. G., and Holm, R. H., *Inorg. Chem.* **20,** 1873 (1981).
56. Conover, R. C., Park, J.-B., Adams, M. W. W., and Johnson, M. K., *J. Am. Chem. Soc.* **113,** 2791 (1991).
57. Kanatzidis, M. G., Baenziger, N. C., Coucouvanis, D., Simopoulos, A., and Kostikas, A., *J. Am. Chem. Soc.* **106,** 4500 (1984).
58. Kanatzidis, M. G., Coucouvanis, D., Simopoulos, A., Kostikas, A., and Papaefthymiou, V., *J. Am. Chem. Soc.* **107,** 4925 (1985).
59. Saak, W., and Pohl, S., *Z. Naturforsch., B: Chem. Sci.* **43B,** 813 (1988).
60. Pohl, S., and Bierbach, U., *Z. Naturforsch., B: Chem. Sci.* **46B,** 68 (1991).
61. Weigel, J. A., and Holm, R. H., unpublished results (1991).
62. Nelson, L. L., Lo, F. Y.-K., Rae, A. D., and Dahl, L. F., *J. Organomet. Chem.* **225,** 309 (1982).
63. Tsukihara, T., Fukuyama, K., Nakamura, M., Katsube, Y., Tanaka, N., Kakudo, M., Wada, K., Hase, T., and Matsubara, H., *J. Biochem (Tokyo)* **90,** 1763 (1981).
64. Sussman, J. L., Brown, J. H., and Shoham, M., *in* "Iron-Sulfur Protein Research" (H. Matsubara, Y. Katsube, and K. Wada, eds.), p. 68. Japan Sci. Soc. Press, Tokyo/ Springer-Verlag, Berlin, 1987.
65. Tsukihara, T., Fukuyama, K., Mizushima, M., Harioka, T., Kusunoki, M., Katsube, Y., Hase, T., and Matsubara, H., *J. Mol. Biol.* **216,** 399 (1990).
66. Rypniewski, W. R., Breiter, D. R., Benning, M. M., Wesenberg, G., Oh, B.-H., Markley, J. L., Rayment, I., and Holden, H. M., *Biochemistry* **30,** 4126 (1991).
67. Armstrong, W. H., *in* "Metal Clusters in Proteins" (L. Que, Jr., ed.), ACS Symp. Ser. No. 372, Chap. 1. American Chemical Society. Washington, D.C., 1988.
68. Beinert, H., and Thomson, A. J., *Arch. Biochem. Biophys.* **222,** 333 (1983).
69. Park, J.-B., Fan, C., Hoffman, B. M., and Adams, M. W. W., *J. Biol. Chem.* **266,** 19351 (1991).
70. Kent, T. A., Dreyer, J.-L., Kennedy, M. C., Huynh, B. H., Emptage, M. H., Beinert, H., and Münck, E., *Proc. Natl. Acad. Sci. U.S.A.* **79,** 1096 (1982).

71. Beinert, H., Emptage, M. H., Dreyer, J.-L., Scott, R. A., Hahn, J. E., Hodgson, K. O., and Thomson, A. J., *Proc. Natl. Acad. Sci. U.S.A.* **80,** 393 (1983).
72. Kennedy, M. C., Emptage, M. H., Dreyer, J.-L., and Beinert, H., *J. Biol. Chem.* **258,** 11098 (1983).
73. Emptage, M. H., Dreyer, J.-L., Kennedy, M. C., and Beinert, H., *J. Biol. Chem.* **258,** 11106 (1983).
74. Kent, T. A., Emptage, M. H., Merkle, H., Kennedy, M. C., Beinert, H., and Münck, E., *J. Biol. Chem.* **260,** 6871 (1985).
75. Kent, T. A., Moura, I., Moura, J. J. G., Lipscomb, J. D., Huynh, B. H., LeGall, J., Xavier, A. V., and Münck, E., *FEBS Lett.* **138,** 55 (1982).
76. Moura, J. J. G., Moura, I., Kent, T. A., Lipscomb, J. D., Huynh, B. H., LeGall, J., Xavier, A. V., and Münck, E., *J. Biol. Chem.* **257,** 6259 (1982).
77. Moura, J. J. G., LeGall, J., and Xavier, A. V., *Eur. J. Biochem.* **141,** 319 (1983).
78. Guigliarelli, B., Bertrand, P., More, C., Papavassiliou, P., Hatchikian, E. C., and Gayda, J. P., *Biochim. Biophys. Acta* **810,** 319 (1985).
79. George, S. J., Richards, A. J. M., Thomson, A. J., and Yates, M. G., *Biochem. J.* **224,** 247 (1984).
80. Bell, S. H., Dickson, D. P. E., Robinson, C. E., Cammack, R., Hall, D. O., and Rao, K. K., *FEBS Lett.* **142,** 143 (1982).
81. Nagayama, K., Ozaki, Y., Kyogoku, Y., Hase, T., and Matsubara, H., *J. Biochem. (Tokyo)* **94,** 893 (1983).
82. Thomson, A. J., Robinson, A. E., Johnson, M. K., Cammack, R., Rao, K. K., and Hall, D. O., *Biochim. Biophys. Acta* **637,** 423 (1981).
83. Johnson, M. K., Spiro, T. G., and Mortenson, L. E., *J. Biol. Chem.* **257,** 2447 (1982).
84. Nagayama, K., Imai, T., Ohmori, D., and Oshima, T., *FEBS Lett.* **169,** 79 (1984).
85. Stephens, P. J., Morgan, T. V., Devlin, F., Penner-Hahn, J. E., Hodgson, K. O., Scott, R. A., Stout, C. D., Burgess, B. K., *Proc. Natl. Acad. Sci. U.S.A.* **82,** 5661 (1985).
86. Thomson, A. J., Robinson, A. E., Johnson, M. K., Moura, J. J. G., Moura, I., Xavier, A. V., and LeGall, J., *Biochim. Biophys. Acta* **670,** 93 (1981).
87. Johnson, M. K., Morningstar, J. E., Bennett, D. E., Ackrell, B. A. C., and Kearney, E. B., *J. Biol. Chem.* **260,** 7368 (1985).
88. Morningstar, J. E., Johnson, M. K., Cecchini, G., Ackrell, B. A. C., and Kearney, E. B., *J. Biol. Chem.* **260,** 13631 (1985).
89. Johnson, M. K., Bennett, D. E., Fee, J. A., and Sweeney, W. V., *Biochim. Biophys. Acta* **911,** 81 (1987).
90. Johnson, M. K., Thomson, A. J., Richards, A. J. M., Peterson, J., Robinson, A. E., Ramsay, R. R., and Singer, T. P., *J. Biol. Chem.* **259,** 2274 (1984).
91. Day, E. P., Peterson, J., Bonvoisin, J. J., Moura, I., and Moura, J. J. G., *J. Biol. Chem.* **263,** 3684 (1988).
92. Sweeney, W. V., Rabinowitz, J. C., and Yoch, D. C., *J. Biol. Chem.* **250,** 7842 (1975).
93. Cammack, R., Rao, K. K., Hall, D. O., Moura, J. J. G., Xavier, A. V., Bruschi, M., LeGall, J., Deville, A., and Gayda, J.-P., *Biochim. Biophys. Acta* **490,** 311 (1977).
94. Ohnishi, T., Blum, H., Sato, S., Nakazawa, K., Hon-nami, K., and Oshima, T., *J. Biol. Chem.* **255,** 345 (1980).
95. Armstrong, F. A., Butt, J. N., George, S. J., Hatchikian, E. C., and Thomson, A. J., *FEBS Lett.* **259,** 15 (1989).
96. Surerus, K. K., Kennedy, M. C., Beinert, H., and Münck, E., *Proc. Natl. Acad. Sci. U.S.A.* **86,** 9846 (1989).
97. Emptage, M. H., Kent, T. A., Huynh, B. H., Rawlings, J., Orme-Johnson, W. H., and Münck, E., *J. Biol. Chem.* **255,** 1793 (1980).

98. Huynh, B. H., Moura, J. J. G., Moura, I., Kent, T. A., LeGall, J., Xavier, A. V., and Münck, E. *J. Biol. Chem.* **255,** 3242 (1980).
99. Papaefthymiou, V., Girerd, J.-J., Moura, I., Moura, J. J. G., and Münck, E., *J. Am. Chem. Soc.* **109,** 4703 (1987).
100. Girerd, J.-J., Papaefthymiou, V., Surerus, K. K., and Münck, E., *Pure Appl. Chem.* **61,** 805 (1989).
101. Surerus, K. K., Münck, E., Moura, I., Moura, J. J. G., and LeGall, J., *J. Am. Chem. Soc.* **109,** 3805 (1987).
102. This statement excludes compounds containing the $M_3S_7 = [M_3(\eta^4\text{-}\mu_2\text{-}S_2)_3(\mu_3\text{-}S)]^{4+}$ unit, examples of which were known somewhat earlier [Lee, S. C., and Holm, R. H., *Angew. Chem., Int. Ed. Engl.* **29,** 840 (1990)].
103. Vergamini, P. J., Vahrenkamp, H., and Dahl, L. F., *J. Am. Chem. Soc.* **93,** 6327 (1971).
104. Beck, W., Danzer, W., and Thiel, G., *Angew. Chem., Int. Ed. Engl.* **12,** 582 (1973).
105. Müller, A., and Reinsch, U., *Angew. Chem., Int. Ed. Engl.* **19,** 72 (1980).
106. Müller, A., Jostes, R., and Cotton, F. A., *Angew. Chem., Int. Ed. Engl.* **19,** 875 (1980).
107. Cotton, F. A., Dori, Z., Llusar, R., and Schwotzer, W., *J. Am. Chem. Soc.* **107,** 6734 (1985).
108. Kathirgamanathan, P., Martinez, M., and Sykes, A. G., *J. Chem. Soc., Chem. Commun.* **953,** 1437 (1985).
109. Martinez, M., Ooi, B.-L., and Sykes, A. G., *J. Am. Chem. Soc.* **109,** 4615 (1987).
110. Akashi, H., Shibahara, T., and Kuroya, H., *Polyhedron* **9,** 1671 (1990).
111. Ooi, B.-L., and Sykes, A. G., *Inorg. Chem.* **28,** 3799 (1989).
112. Money, J. K., Huffman, J. C., and Christou, G., *Inorg. Chem.* **27,** 507 (1988).
113. Howlader, N. C., Haight, G. P., Jr., Hambley, T. W., Lawrance, G. A., Rahmoeller, K. M., and Snow, M. R., *Aust. J. Chem.* **36,** 377 (1983).
114. Cotton, F. A., Dori, Z., Llusar, R., and Schwotzer, W., *Inorg. Chem.* **25,** 3654 (1986).
115. Shibahara, T., and Kuroya, H., *Polyhedron* **5,** 357 (1986).
116. Cotton, F. A., Llusar, R., Marler, D. O., and Schwotzer, W., *Inorg. Chim. Acta* **102,** L25 (1985).
117. Wunderlich, H., *Acta Crystallogr., Sect. C: Cryst. Struct. Commun.* **C43,** 24 (1987).
118. Keck, H., Kuchen, W., and Mathow, J., *Z. Anorg. Allg. Chem.* **537,** 123 (1986).
119. Keck, H., Kuchen, W., Mathow, J., and Wunderlich, J., *Angew. Chem., Int. Ed. Engl.* **21,** 929 (1982).
120. Halbert, T. R., McGauley, K., Pan, W.-H., Czernuszewicz, R. S., and Stiefel, E. I., *J. Am. Chem. Soc.* **106,** 1849 (1984).
121. Cotton, F. A., and Llusar, R., *Polyhedron* **9,** 1741 (1987).
122. Cotton, F. A., Kibala, P. A., Matusz, M., McCaleb, C. S., and Sandor, R. B. W., *Inorg. Chem.* **28,** 2623 (1989).
123. Cotton, F. A., Llusar, R., and Eagle, C. T., *J. Am. Chem. Soc.* **111,** 4332 (1989).
124. Saito, T., Yamamoto, N., Yamagata, T., and Imoto, H., *Chem. Lett.*, 2025 (1987).
125. Lin, X., Lin, Y., Huang, J., and Huang, J., *Kexue Tongbao* **32,** 810 (1987).
126. Lu, S., Huang, J., Lin, Y., and Huang, J., *Jiegou Huaxue* **6,** 154 (1987).
127. Zheng, U., Zhu, N., Zhan, H., and Wu, X., *Acta Crystallogr., Sect. C: Cryst. Struct. Commun.* **C45,** 1632 (1989).
128. Fedin, V. P., Sokolov, M. N., Mironov, Yu. V., Kolesov, B. A., Tkachev, S. V., and Federov, V. Ye., *Inorg. Chim. Acta* **167,** 39 (1990).

129. Huang, J. Q., Huang, J. L., Shang, M. Y., Lu, S. F., Lin, X. T., Lin, Y. H., Huang, M. D., Zhuang, H. H., and Lu, J. X., *Pure Appl. Chem.* **60,** 1185 (1988).
130. Shibahara, T., Takeuchi, A., Ohtsuji, A., Kohda, K., and Kuroya, H., *Inorg. Chim. Acta* **127,** L45 (1987).
131. Nasreldin, M., Olatunji, A., Dimmock, P. W., and Sykes, A. G., *J. Chem. Soc., Dalton Trans.*, 1765 (1990).
132. Shibahara, T., Kohda, K., Ohtsuji, A., Yasuda, K., and Kuroya, H., *J. Am. Chem. Soc.* **108,** 2757 (1986).
133. Cotton, F. A., and Llusar, R., *Inorg. Chem.* **27,** 1303 (1988).
134. Shibahara, T., and Yamasaki, M., *Inorg. Chem.* **30,** 1687 (1991).
135. Fedin, V. P., Sokolov, M. N., Geras'ko, O. A., Sheer, M., Federov, V. Ye., Mironov, A. V., Slovokhotov, Yu. L., and Strutchkov, Yu. T., *Inorg. Chim. Acta* **165,** 25 (1989).
136. Zheng, Y., Zhan, H., and Wu, X., *Acta Crystallogr., Sect. C: Cryst. Struct. Commun.* **C45,** 1424 (1989).
137. Zhan, H., Zheng, Y., Wu, X., and Lu, J., *J. Cryst. Mol. Struct.* **196,** 241 (1989).
138. Shibahara, T., Hattori, H., and Kuroya, H., *J. Am. Chem. Soc.* **106,** 2710 (1984).
139. Shibahara, T., Miyake, H., Kobayashi, K., and Kuroya, H., *Chem. Lett.*, 139 (1986).
140. Dori, Z., Cotton, F. A., Llusar, R., and Schwotzer, W., *Polyhedron* **5,** 907 (1986).
141. Shibahara, T., Miyake, H., Kobayashi, K., and Kuroya, H., *Chem. Lett.*, 139 (1986).
142. Shibahara, T., Takeuchi, A., and Kuroya, H., *Inorg. Chim. Acta* **127,** L39 (1987).
143. Shibahara, T., Takeuchi, A., Nakajima, M., and Kuroya, H., *Inorg. Chim. Acta* **143,** 147 (1988).
144. Shibahara, T., Akashi, H., Nagahata, S., Hattori, H., and Kuroya, H., *Inorg. Chem.* **28,** 362 (1989).
145. Cotton, F. A., Diebold, M. P., Dori, Z., Llusar, R., and Schwotzer, W., *J. Am. Chem. Soc.* **107,** 6735 (1985).
146. Shibahara, T., Yamada, T., Kuroya, H., Hills, E. F., Kathirgamanathan, P., and Sykes, A. G., *Inorg. Chim. Acta* **113,** L19 (1986).
147. Akashi, H., Shibahara, T., Narahara, T., Tsuru, H., and Kuroya, H., *Chem. Lett.*, 129 (1989).
148. Ooi, B.-L., Sharp, C., and Sykes, A. G., *J. Am. Chem. Soc.* **111,** 125 (1989).
149. Shibahara, T., Kuroya, H., Matsumoto, K., and Ooi, S., *J. Am. Chem. Soc.* **106,** 789 (1984); Shibahara, T., Kuroya, H., Matsumoto, K., and Ooi, S., *Inorg. Chim. Acta* **116,** L25 (1986).
150. Dimmock, P. W., McGinnis, J., Ooi, B.-L., and Sykes, A. G., *Inorg. Chem.* **29,** 1085 (1990).
151. Christou, G., Sabat, M., Ibers, J. A., and Holm, R. H., *Inorg. Chem.* **21,** 3518 (1982).
152. Strasdeit, H., Krebs, B., and Henkel, G., *Inorg. Chem.* **23,** 1816 (1984).
153. You, J.-F., Snyder, B. S., Papaefthymiou, G. C., and Holm, R. H., *J. Am. Chem. Soc.* **112,** 1067 (1990).
154. Chu, C. T.-W., and Dahl, L. F., *Inorg. Chem.* **16,** 3245 (1977).
155. Glidewell, C., Lambert, R. J., Harman, M. E., and Hursthouse, M. B., *J. Chem. Soc., Dalton Trans.*, 2685 (1990).
156. Müller, A., Schimanski, U., and Schimanski, J., *Inorg. Chim. Acta* **76,** L245 (1983).
157. Clegg, W., Garner, C. D., Nicholson, J. R., and Raithby, P. R., *Acta Crystallogr., Sect. C: Cryst. Struct. Commun.* **C39,** 1007 (1983).
158. Clegg, W., Scattergood, D., and Garner, C. D., *Acta Crystallogr., Sect. C: Cryst. Struct. Commun.* **C44,** 29 (1988).
159. Müller, A., Bögge, H., and Schimanski, U., *Inorg. Chim. Acta* **69,** 5 (1983).

160. Wolff, T. E., Berg, J. M., Warrick, C., Hodgson, K. O., Holm, R. H., and Frankel, R. B., *J. Am. Chem. Soc.* **100,** 4630 (1978).
161. Christou, G., Garner, C. D., and Mabbs, F. E., *Inorg. Chim. Acta* **28,** L189 (1978).
162. Christou, G., Garner, C. D., Mabbs, F. E., and King, T. J., *J. Chem. Soc., Chem. Commun.,* 740 (1978).
163. Holm, R. H., *Chem. Soc. Rev.* **10,** 455 (1981).
164. Averill, B. A., *Struct. Bonding* **53,** 59 (1983).
165. Holm, R. H., and Simhon, E. D., *in* "Molybdenum Enzymes" (T. G. Spiro, ed.), Chap. 2. Wiley (Interscience), New York, 1985.
166. Müller, A., Diemann, E., Jostes, R., and Bögge, H., *Angew. Chem., Int. Ed. Engl.* **20,** 934 (1981).
167. Müller, A., Krickemeyer, E., and Bögge, H., *Z. Anorg. Allg. Chem.* **554,** 61 (1987).
168. McDonald, J. W., Freisen, G. D., Rosenhein, L. D., and Newton, W. E., *Inorg. Chim. Acta* **72,** 205 (1983).
169. Zhang, Y., and Holm, R. H., *Inorg. Chem.* **27,** 3875 (1988).
170. Latroche, M., and Ibers, J. A., *Inorg. Chem.* **29,** 1503 (1990); and references therein.
171. Lee, S. C., and Holm, R. H., *J. Am. Chem. Soc.* **112,** 9654 (1990).
172. Klepp, K. O., and Bronger, W., *Z. Anorg. Allg. Chem.* **532,** 23 (1986).
173. Wolff, T. E., Berg, J. M., Hodgson, K. O., Frankel, R. B., and Holm, R. H., *J. Am. Chem. Soc.* **101,** 4140 (1979).
174. Wolff, T. E., Power, P. P., Frankel, R. B., and Holm, R. H., *J. Am. Chem. Soc.* **102,** 4694 (1980).
175. Christou, G., and Garner, C. D., *J. Chem. Soc., Dalton Trans.,* 2354 (1980).
176. Christou, G., Mascharak, P. K., Armstrong, W. H., Papaefthymiou, G. C., Frankel, R. B., and Holm, R. H., *J. Am. Chem. Soc.* **104,** 2820 (1982).
177. Zhang, Y., Bashkin, J. K., and Holm, R. H., *Inorg. Chem.* **26,** 694 (1987).
178. Kovacs, J. A., Bashkin, J. K., and Holm, R. H., *J. Am. Chem. Soc.* **107,** 1784 (1985); Kovacs, J. A., Bashkin, J. K., and Holm, R. H., *Polyhedron* **6,** 1445 (1987).
179. Anglin, R. J., Bonomi, F., and Kurtz, D. M., Jr. *Inorg. Chem.* **27,** 3434 (1988).
180. Liu, Q., Huang, L., Kang, B., Liu, C., Wang, L., and Lu, J., *Acta Chim. Sin.,* 107 (1986).
181. Liu, Q., Huang, L., Kang, B., Yang, Y., and Lu, J., *Kexue Tongbao* **32,** 898 (1987).
182. Lei, X., Huang, Z., Hong, M., Liu, Q., and Liu, H., *Jiegou Huaxue* **8,** 152 (1989).
183. Liu, Q., Huang, L., Liu, H., Lei, X., Wu, D., Kang, B., and Lu, J., *Inorg. Chem.* **29,** 4131 (1990).
184. Bose, K. S., Chmielewski, S. A., Eldredge, P. A., Sinn, E., and Averill, B. A., *J. Am. Chem. Soc.* **111,** 8953 (1989).
185. Eldredge, P. A., Bose, K. S., Barber, D. E., Bryan, R. F., Sinn, E., Rheingold, A., and Averill, B. A., *Inorg. Chem.* **30,** 2365 (1991).
186. Coucouvanis, D., Al-Ahmad, S., Salifoglou, A., Dunham, W. R., and Sands, R. H., *Angew. Chem., Int. Ed. Engl.* **27,** 1353 (1988).
187. Kovacs, J. A., and Holm, R. H., *J. Am. Chem. Soc.* **108,** 340 (1986).
188. Do, Y., Simhon, E. D., and Holm, R. H., *Inorg. Chem.* **24,** 4635 (1985).
189. Carney, M. J., Kovacs, J. K., Zhang, Y.-P., Papaefthymiou, G. C., Spartalian, K., Frankel, R. B., and Holm, R. H., *Inorg. Chem.* **26,** 719 (1987).
190. Kovacs, J. A., and Holm, R. H., *Inorg. Chem.* **26,** 702, 711 (1987).
191. Ciurli, S., Carney, M. J., Holm, R. H., and Papaefthymiou, G. C., *Inorg. Chem.* **28,** 2696 (1989).
192. Ciurli, S., Carrié, M., and Holm, R. H., *Inorg. Chem.* **29,** 3493 (1990).
193. Ciurli, S., and Holm, R. H., *Inorg. Chem.* **30,** 743 (1991).

194. Cook, M., and Karplus, M., *J. Chem. Phys.* **83,** 6344 (1985).
195. Ciurli, S., Yu, S.-B., Holm, R. H., Srivastava, K. K. P., and Münck, E., *J. Am. Chem. Soc.* **112,** 8169 (1990).
196. Gloux, J., Gloux, P., and Rius, P., *J. Am. Chem. Soc.* **108,** 3541 (1986).
197. Roth, E. K. H., Greneche, J. M., and Jordanov, J., *J. Chem. Soc., Chem. Commun.,* 105 (1991).
198. O'Sullivan, T., and Millar, M. M., *J. Am. Chem. Soc.* **107,** 4096 (1985).
199. Moura, I., Moura, J. J. G., Münck, E., Papaefthymiou, V., and LeGall, J., *J. Am. Chem. Soc.* **108,** 349 (1986).
200. Münck, E., Papaefthymiou, V., Surerus, K. K., and Girerd, J.-J., *in* "Metal Clusters in Proteins" (L. Que, Jr., ed.), ACS Symp. Ser. 372, Chap. 15. American Chemical Society, Washington, D.C., 1988.
201. Conover, R. C., Park, J.-B., Adams, M. W. W., and Johnson, M. K., *J. Am. Chem. Soc.* **112,** 4562 (1990).
202. Mascharak, P. K., Papaefthymiou, G. C., Armstrong, W. H., Foner, S., Frankel, R. B., and Holm, R. H., *Inorg. Chem.* **22,** 2851 (1983).
203. Christou, G., Garner, C. D., Miller, R. M., Johnson, C. E., and Rush, J. D., *J. Chem. Soc., Dalton Trans.,* 2363 (1980).
204. Ciurli, S., Ph.D. Thesis, Harvard University, Cambridge, Massachusetts (1990).
205. Liu, Q. T., Huang, L. R., Yang, Y., and Lu, J. X., *Kexue Tongbao* **33,** 1633 (1988).
206. Cramer, S. P., Hodgson, K. O., Gillum, W. O., and Mortenson, L. E., *J. Am. Chem. Soc.* **100,** 3398 (1978).
207. Cramer, S. P., Gillum, W. O., Hodgson, K. O., Mortenson, L. E., Stiefel, E. I., Chisnell, J. R., Brill, W. J., and Shah, V. K., *J. Am. Chem. Soc.* **100,** 3814 (1978).
208. Conradson, S. D., Burgess, B. K., Newton, W. E., Hodgson, K. O., McDonald, J. W., Rubinson, J. F., Gheller, S. F., Mortenson, L. E., Adams, M. W. W., Mascharak, P. K., Armstrong, W. H., Holm, R. H., *J. Am. Chem. Soc.* **107,** 7935 (1985).
209. Wolff, T. E., Berg, J. M., and Holm, R. H., *Inorg. Chem.* **20,** 174 (1981).
210. Huang, L., and Lin, S., *Jiegou Huaxue* **3,** 25 (1984).
211. Burgess, B. K., *Chem. Rev.* **90,** 1377 (1990).
212. Eady, R. R., *Polyhedron* **8,** 1695 (1989); Eady, R. R., *Adv. Inorg. Chem.* **36,** 77 (1991).
213. Conradson, S. D., Burgess, B. K., Newton, W. E., Mortenson, L. E., and Hodgson, K. O., *J. Am. Chem. Soc.* **109,** 7507 (1987).
214. Arber, J. M., Dobson, B. R., Eady, R. R., Stevens, P., Hasnain, S. S., Garner, C. D., and Smith, B. E., *Nature (London)* **325,** 372 (1987).
215. Arber, J. M., Dobson, B. R., Eady, R. R., Hasnain, S. S., Garner, C. D., Matsushita, T., Nomura, M., and Smith, B. E., *Biochem. J.* **258,** 733 (1989).
216. George, G. N., Coyle, C. L., Hales, B. J., and Cramer, S. P., *J. Am. Chem. Soc.* **110,** 4057 (1988).
217. Palermo, R. E., and Holm, R. H., *J. Am. Chem. Soc.* **105,** 4310 (1983).
218. Flank, A. M., Weininger, M., Mortenson, L. E., and Cramer, S. P., *J. Am. Chem. Soc.* **108,** 1050 (1986).
219. Christou, G., Hagen, K. S., and Holm, R. H., *J. Am. Chem. Soc.* **104,** 1744 (1982).
220. Bolin, J. T., Ronco, A. E., Mortenson, L. E., Morgan, T. V., Williamson, M., and Xuong, N.-H., *in* "Nitrogen Fixation: Achievements and Objectives" (R. Gresshoff, J. Stacey, and W. E. Newton, eds.), Chapman & Hall, New York, 1990.
221. Coucouvanis, D., Challen, P. R., Koo, S.-M., Davis, W. M., Butler, W., and Dunham, W. R., *Inorg. Chem.* **28,** 4183 (1989).
222. Challen, P. R., Koo, S.-M., Kim, C. G., Dunham, W. R., and Coucouvanis, D., *J. Am. Chem. Soc.* **112,** 8606 (1990).

223. Coucouvanis, D., *Acc. Chem. Res.* **24,** 1 (1991).
224. Mascharak, P. K., Armstrong, W. H., Mizobe, Y., and Holm, R. H., *J. Am. Chem. Soc.* **105,** 475 (1983).
225. Shibahara, T., Akashi, H., and Kuroya, H., *J. Am. Chem. Soc.* **108,** 1342 (1986).
226. Dimmock, P. W., and Sykes, A. G., *J. Chem. Soc., Dalton Trans.,* 3101 (1990).
227. Shibahara, T., Yamasaki, M., Akashi, H., and Katayama, T., *Inorg. Chem.* **30,** 2693 (1991).
228. Dimmock, P. W., Lamprecht, G. J., and Sykes, A. G., *J. Chem. Soc., Dalton Trans.,* 955 (1991).
229. Akashi, H., and Shibahara, T., *Inorg. Chem.* **28,** 2906 (1989).
230. Shibahara, T., Yamamoto, T., Kanadani, H., and Kuroya, H., *J. Am. Chem. Soc.* **109,** 3495 (1987).
231. Shibahara, T., Akashi, H., Yamasaki, M., and Hashimoto, K., *Chem. Lett.,* 689 (1991).
232. Shibahara, T., Akashi, H., and Kuroya, H., *J. Am. Chem. Soc.* **110,** 3313 (1988).
233. Keck, H., Kruse, A., Kuchen, W., Mootz, D., Wiskemann, R., and Wunderlich, H., *Z. Naturforsch., B: Chem. Sci.* **45B,** 461 (1990).
234. Deeg, A., Keck, H., Kruse, A., Kuchen, W., and Wunderlich, H., *Z. Naturforsch., B: Chem. Sci.* **43B,** 1541 (1988).
235. Wu, X., Zheng, Y., Zhu, N., and Lu, J., *Jiegou Huaxue* **7,** 137 (1988).
236. Wu, X., Lu, S., Zu, L., Wu, Q., and Lu, J., *Inorg. Chim. Acta* **133,** 39 (1987).
237. Lu, S., Huang, J., Lin, Y., and Huang, J., *Huaxue Xuebao* **45,** 666 (1987).
238. Zhan, J., Zheng, Y., Wu, X., and Lu, J., *Jiegou Huaxue* **7,** 157 (1988).
239. Pasynskii, A. A., Eremenko, I. L., Orazsakhatov, B., Kalinnikov, V. T., Aleksandrov, G. G., and Struchkov, Yu. T., *J. Organomet. Chem.* **216,** 211 (1981).
240. Eremenko, I. L., Pasynskii, A. A., Orazsakhatov, B., Ellert, V. M., Novotortsev, V. M., Kalinnikov, V. T., Porai-Koshits, M. A., Antsyshkina, A. S., Dikareva, L. M., Ostrikova, V. N., Struchkov, Yu. T., and Gerr, R. G., *Inorg. Chim. Acta* **73,** 225 (1983).
241. Nefedov, S. E., Pasynskii, A. A., Eremenko, I. L., Stomakhina, E. E., Yanovsky, A. I., and Struchkov, Yu. T., *J. Organomet. Chem.* **405,** 287 (1991).
242. Pasynskii, A. A., Eremenko, I. L., Orazsakhatov, B., Kalinnikov, V. T., Aleksandrov, G. G., and Struchkov, Yu. T., *J. Organomet. Chem.* **214,** 367 (1981).
243. Pasynskii, A. A., Eremenko, I. L., Katugin, A. S., Gasanov, G. Sh., Turchanova, E. A., Ellert, O. G., Struchkov, Yu. T., Shklover, V. E., Berberova, N. T., Sogomonova, A. G., and Okhlobystin, O. Yu., *J. Organomet. Chem.* **344,** 195 (1988).
244. Zhu, N., Zheng, Y., and Wu, X., *Inorg. Chem.* **29,** 2707 (1990).
245. Zhu, N., Wu, X., and Lu, J., *J. Chem. Soc., Chem. Commun.,* 235 (1991).
246. Sieker, L. C., Adman, E., and Jensen, L. H., *Nature (London)* **235,** 40 (1972).
247. Herskovitz, T., Averill, B. A., Holm, R. H., Ibers, J. A., Phillips, W. D., and Weiher, J. F., *Proc. Natl. Acad. Sci. U.S.A.* **69,** 2437 (1972).
248. Orme-Johnson, W. H., *Annu. Rev. Biophys. Biophys. Chem.* **14,** 419 (1985).
249. Harris, S., *Polyhedron* **8,** 2843 (1989).
250. Shibahara, T., Yamasaki, M., Sakane, G., Minami, K., Yabuki, T., and Ichimura, A., *Inorg. Chem.* **31,** 640 (1992).
251. Fedin, V. P., Sokolov, M. N., Geras'ko, O. A., Kolesov, B. A., Fedorov, V. Ye., Mironov, A. V., Yufit, D. S., Slovohotov, Yu. L., and Struchkov, Yu. T., *Inorg. Chim. Acta* **175,** 217 (1990).
252. Cotton, F. A., Kibala, P. A., and Miertschin, C. S., *Inorg. Chem.* **30,** 548 (1991).

253. Zheng, Y., Zhan, H., and Wu, X., *Acta Crystallogr., Sect. C: Cryst. Struct. Commun.* **C45,** 1424 (1989).
254. Shibahara, T., Hashimoto, K., Sakano, G. Abstract, Fifth International Conference on Bioinorganic Chemistry, Oxford, 1991; Shibahara, T., Hashimoto, K., and Sakano, G., *J. Inorg. Biochem.* **43,** 280 (1991).
255. Butt, J. N., Armstrong, F. A., Breton, J., George, S. J., Thomson, A. J., and Hatchikian, E. C., *J. Am. Chem. Soc.* **113,** 6663 (1991).
256. Butt, J. N., Sucheta, A., Armstrong, F. A., Breton, J., Thomson, A. J., and Hatchikian, E. C., *J. Am. Chem. Soc.* **113,** 8948 (1991).
257. Shibahara, T., *Adv. Inorg. Chem.* **37,** 143 (1991).